

Optimisation criteria of a Rankine steam cycle powered by a thorium HTR

SC van Niekerk
20808410

Dissertation submitted in fulfilment of the requirements for the degree *Master* in *Engineering* at the Potchefstroom Campus of the North-West University

Supervisor: Mr CP Kloppers
Co- Supervisor: Prof CP Storm

May 2014

ABSTRACT

HOLCIM has various cement production plants across India. These plants struggle to produce the projected amount of cement due to electricity shortages. Although coal is abundant in India, the production thereof is in short supply.

It is proposed that a thorium HTR (100 MW_t) combined with a PCU (Rankine cycle) be constructed to supply a cement production plant with the required energy. The Portland cement production process is investigated and it is found that process heat integration is not feasible.

The problem is that for the feasibility of this IPP to be assessed, a Rankine cycle needs to be adapted and optimised to suit the limitations and requirements of a 100 MW_t thorium HTR.

Advantages of the small thorium HTR (100 MW_t) include: on-site construction; a naturally safe design and low energy production costs. The reactor delivers high temperature helium (750°C) at a mass flow of 38.55 kg/s. Helium re-enters the reactor core at 250°C.

Since the location of the cement production plant is unknown, both wet and dry cooling tower options are investigated. An overall average ambient temperature of India is used as input for the cooling tower calculations.

EES software is used to construct a simulation model with the capability of optimising the Rankine cycle for maximum efficiency while accommodating various out of the norm input parameters. Various limitations are enforced by the simulation model.

Various cycle configurations are optimised (EES) and weighed against each other. The accuracy of the EES simulation model is verified using FlowNex while the optimised cycle results are verified using Excel's X-Steam macro.

It is recommended that a wet cooling tower is implemented if possible. The 85% effective heat exchanger delivers the techno-economically optimum Rankine cycle configuration. For this combination of cooling tower and heat exchanger, it is recommended that the cycle configuration consists of one de-aerator and two closed feed heaters (one specified).

After the Rankine cycle (PCU) has been designed and optimised, it is evident that the small thorium HTR (100 MW_t) can supply the HOLCIM plant with the required energy. The

optimum cycle configuration, as recommended, operates with a cycle efficiency of 42.4% while producing 39.867 MW_e. A minimum of 10 MW_e can be sold to the Indian distribution network at all times, thus generating revenue.

KEYWORDS

Cement
Dry cooling
Heat exchanger effectiveness
Helium
HOLCIM
HTR
IPP
Optimisation
Portland process
Rankine Cycle
Regenerative feed heating
Steam
Thermal efficiency
Thorium
Wet cooling

SYSTEM SPECIFICATION

Output specifications and limitations set by the small thorium HTR (100 MW_t) for its working fluid (helium):

	Variable	Value	Unit
Helium mass flow	\dot{m}_r	38.55	kg/s
Maximum HTR outlet temperature	$T_{r_{max}}$	750	°C
Minimum HTR inlet temperature	$T_{r_{min}}$	250	°C

Rankine cycle input specifications and limitation parameters as enforced by various factors:

		Variable	Value	Unit
Input specifications				
Average ambient temperature		T_{amb}	24.4	°C
Condenser inlet temperature	wct	T_1	49.4	°C
	dct		59.4	°C
Condenser temperature losses		T_R	16	°C
		TTD	3	°C
		T_{Sub}	2	°C
HX effectiveness		HX_{eff}	85	%
Limitation parameters				
HX outlet pressure		$P_{max} \leq 19$		MPa
LPT outlet steam quality		$88 \leq x_{crit} \leq 92$		%
De-aerator bleed pressure		$0.1 \leq P_{de} \leq 1$		MPa
HPT polytropic efficiency		$88 \leq \eta_{h,\infty} \leq 90$		%
LPT polytropic efficiency		$79 \leq \eta_{l,\infty} \leq 81$		%

Rankine cycle component selection is influenced by various techno-economic and other considerations:

	Included
Reheat	X
Steam turbine driven feed pumps	X
Attemperation	✓
De-aerator	✓
Closed feed heaters	✓

Optimised Rankine cycle results for the 85% heat exchanger effectiveness in combination with the wet cooling tower:

	Variable	Value	Unit
Energy Balance	E_b	0	MW
Cycle efficiency	η_R	42.38	%
Net work	W_{net}	42.376	MW
Turbine work	W_{turb}	43.382	MW
Pump work	W_{pumps}	1.006	MW
Heat input	Q_{in}	100	MW
Heat rejected	Q_{out}	57.624	MW
Total mass flow	\dot{m}_{tot}	32.99	kg/s
HP feed heater mass flow	$\dot{m}[1]$	3.416	kg/s
De-aerator mass flow	$\dot{m}[2]$	1.134	kg/s
LP feed heater mass flow	$\dot{m}[3]$	1.313	kg/s
Minimum Temperature	T_{min}	322.6	K
Maximum HPT Pressure	P_{max}	19	MPa
LPT outlet quality	x_{crit}	88.94	%
HX water inlet temperature	$T_{HX,i}$	435	K
HX water outlet temperature	T_{max}	934.8	K
Polytropic HPT efficiency	$\eta_{h,\infty}$	89.44	%
Polytropic LPT efficiency	$\eta_{l,\infty}$	80.58	%

DECLARATION

I, Steven Cronier Van Niekerk (Identity Number: 881007 5177 083), hereby declare that the work contained in this dissertation is my own work. Some of the information contained in this dissertation has been gained from various journal articles; text books etc., and has been referenced accordingly.

S.C Van Niekerk

Witness

ACKNOWLEDGEMENTS

I would like to take this opportunity to thank the following persons:

- My wife and my parents for their on-going support and patience. Thanks to them for the opportunities they provided and for making me believe that anything is possible
 - My supervisors, Mr C.P. Kloppers and Prof C.P. Storm for the guidance and support they provided as well as all the time and energy spent through the course of this study.
-

CONTENTS

Title Page.....	i
Abstract.....	ii
Key Words.....	iv
System Specification.....	v
Declaration.....	vii
Acknowledgements.....	viii
Contents.....	ix
List of Tables.....	xv
List of Figures.....	xviii
Nomenclature.....	xxii
1 Chapter 1: Introduction.....	1-1
1.1 Background.....	1-1
1.2 Problem Statement	1-2
1.3 Objective of study	1-2
1.4 Research methodology	1-3
1.5 Scope and limits of the study	1-3
1.6 Dissertation structure.....	1-4
1.7 Key aspects	1-6
2 Chapter 2: Literature Survey - Cement manufacturing.....	2-1
2.1 Introduction	2-1
2.2 Energy Consumption.....	2-3
3 Chapter 3: Literature survey - Nuclear reactor options	3-1
3.1 introduction	3-1

3.2	Nuclear fuel reserves	3-2
3.3	Generation IV Reactors.....	3-3
3.3.1	Light Water Reactors (LWR)	3-4
3.3.2	High Temperature Gas cooled Reactors (HTR).....	3-5
3.3.3	Fast Neutron Reactors (FNR).....	3-8
3.3.4	Small Nuclear Reactors	3-8
3.4	Key aspects	3-9
4	Chapter 4: Rankine cycle development.....	4-1
4.1	Introduction	4-1
4.2	Ideal Rankine cycle	4-2
4.2.1	Simple Rankine cycle with Superheat	4-2
4.2.2	Reheat	4-4
4.2.3	Regenerative feed water heating	4-7
4.3	Actual Rankine cycle.....	4-11
4.3.1	Actual vs Ideal	4-11
4.3.2	Attemperation	4-13
4.4	Limitation parameters.....	4-16
4.4.1	Heat input into the cycle (Q_{in})	4-16
4.4.2	HPT inlet pressure	4-16
4.4.3	LP turbine outlet quality (x_{crit}).....	4-17
4.4.4	Minimum cycle temperature (T_{min}).....	4-19
4.4.5	Wet Cooling Tower	4-20

4.4.6 Dry Cooling Tower	4-20
4.5 Optimisation criteria	4-20
4.6 Key aspects	4-21
5 Chapter 5: Design Considerations	5-1
5.1 Introduction	5-1
5.2 Integration	5-1
5.3 Thorium reactor: 100 MW _t	5-2
5.4 Reactor minimum temperature	5-2
5.5 Maximum cycle Temperature	5-3
5.5.1 Coal fired power stations	5-4
5.5.2 Thorium Reactor	5-6
5.6 Ambient Conditions in India	5-6
5.7 Cycle efficiency	5-7
5.8 Steam turbine driven feed pumps	5-8
5.9 De-aerator	5-8
5.10 Reheat	5-9
5.11 Key aspects	5-9
6 Chapter 6: Heat Exchanger	6-1
6.1 Introduction	6-1
6.2 Water inlet temperature	6-1
6.3 Maximum cycle temperature	6-2
6.4 Rankine cycle mass flow	6-3

6.5	Pinch Point.....	6-5
6.6	Material selection	6-8
6.6.1	Stainless Steel.....	6-8
7	Chapter 7: Simulation	7-1
7.1	Introduction	7-1
7.2	Assumptions	7-2
7.3	Input parameters.....	7-2
7.4	Optimised configurations.....	7-4
7.4.1	$HX_{eff}(\epsilon) = 80\%$	7-5
7.4.2	$HX_{eff}(\epsilon) = 85\%$	7-7
7.4.3	$HX_{eff}(\epsilon) = 87.5\%$	7-10
7.4.4	$HX_{eff}(\epsilon) = 90\%$	7-13
8	Chapter 8: Optimum cycle configuration	8-1
8.1	Introduction	8-1
8.2	$HX_{eff}(\epsilon) = 80\%$	8-1
8.2.1	Wet cooling tower	8-1
8.2.2	Dry cooling tower	8-3
8.3	$HX_{eff}(\epsilon) = 85\%$	8-5
8.3.1	Wet cooling tower	8-5
8.3.2	Dry cooling tower	8-7
8.4	$HX_{eff}(\epsilon) = 87.5\%$	8-9
8.4.1	Wet cooling tower	8-9

8.4.2 Dry cooling tower	8-11
8.5 $HX_{eff} (\epsilon) = 90\%$	8-13
8.5.1 Wet cooling tower	8-13
8.5.2 Dry cooling tower	8-16
8.6 Heat exchanger comparison	8-18
8.7 Electricity production	8-19
9 Chapter 9: Model Verification.....	9-1
9.1 Introduction	9-1
9.2 Wet cooling tower	9-2
9.2.1 $HX_{eff} (\epsilon) = 85\%$	9-2
10 Chapter 10: Conclusions And Recommendations	10-1
10.1 Background.....	10-1
10.2 Summary	10-2
10.3 Recommendations	10-5
10.3.1Wet cooling tower	10-5
10.3.2Dry cooling tower	10-6
10.4 Conclusions	10-7
10.5 Future study	10-8
11 References.....	11-1
12 Appendices.....	12-1
12.1 EES	12-1
12.1.1Simulation Model	12-1

12.1.2 Procedure	12-2
12.2 EES optimised results	12-7
12.2.1 Wet Cooling Tower	12-7
12.2.2 Dry Cooling Tower	12-9
12.3 Excel (X-Steam)	12-11
12.3.1 $HX_{eff} = 80\%$	12-11
12.3.2 $HX_{eff} = 87.5\%$	12-15
12.3.3 $HX_{eff} (\epsilon) = 90\%$	12-18
12.4 FlowNex simulation model	12-22
12.5 Influence of minimum and maximum temperatures	12-23
12.6 CD	Error! Bookmark not defined.

LIST OF TABLES

Table 1 – Electric energy distribution for cement production.....	2-5
Table 2 - Known recoverable resources of Uranium in 2011	3-2
Table 3 - Estimated resources of Thorium.....	3-3
Table 4 - Rankine cycle development Result comparison.....	4-1
Table 5 - Simple Ideal Rankine cycle input parameters	4-3
Table 6 - Simple Ideal Rankine cycle results	4-4
Table 7 - Ideal Rankine cycle with reheat input parameters.....	4-5
Table 8 - Ideal Rankine cycle with reheat results.....	4-6
Table 9 - Ideal Rankine cycle with contact feed heater input parameters	4-8
Table 10 - Ideal Rankine cycle with contact feed heater results.....	4-9
Table 11 - Ideal Rankine cycle with feed heating results	4-11
Table 12 - Actual Rankine cycle with feed heaters input parameters.....	4-11
Table 13 - Actual Rankine cycle with feed heaters results.....	4-13
Table 14 - Ideal vs. Actual Rankine with feed heaters RESULT comparison	4-13
Table 15 - Actual Rankine cycle Attenuation input parameters.....	4-14
Table 16 - Actual Rankine with Attenuation Results	4-15
Table 17 - Energy losses from coal burner to working fluid	5-5
Table 18 – Indian average ambient temperature	5-7
Table 19 - Heat exchanger, 85% effectiveness	6-3
Table 20 - Optimising model inputs; Wet cooling tower	7-2

Table 21 - Optimising model inputs; Dry cooling tower	7-3
Table 22 - $HX_{eff} = 80\%$; wct; Optimum cycle configuration results	8-2
Table 23 – $HX_{eff} = 80\%$; wct; Optimum bleed points	8-3
Table 24 - $HX_{eff} = 80\%$; dct; Optimum cycle configuration results	8-4
Table 25 – $HX_{eff} = 80\%$; dct; Optimum bleed points	8-4
Table 26 - $HX_{eff} = 85\%$; wct; Optimum cycle configuration results	8-6
Table 27 - $HX_{eff} = 85\%$; wct; Optimum bleed points	8-6
Table 28 - $HX_{eff} = 85\%$; dct; Optimum cycle configuration results	8-8
Table 29 – $HX_{eff} = 85\%$; dct; Optimum bleed points	8-8
Table 30 - $HX_{eff} = 87.5\%$; wct; Optimum cycle configuration results	8-10
Table 31 – $HX_{eff} = 87.5\%$; wct; Optimum bleed points	8-10
Table 32 - $HX_{eff} = 87.5\%$; dct; Optimum cycle configuration results	8-12
Table 33 – $HX_{eff} = 87.5\%$; dct; Optimum bleed points	8-12
Table 34 - $HX_{eff} = 90\%$; wct; Optimum cycle configuration results	8-14
Table 35 - $HX_{eff} = 90\%$; wct; Optimum bleed points	8-15
Table 36 - $HX_{eff} = 90\%$; dct; Optimum cycle configuration results	8-17
Table 37 – $HX_{eff} = 90\%$; dct; Optimum bleed points	8-17
Table 38 – Optimum cycle configurations; Electric energy produced	8-19
Table 39 - $HX_{eff} = 85\%$; wct; Enthalpy verification; EES - FlowNex	9-3
Table 40 - $HX_{eff} = 85\%$; wct; Parameter verification; EES - FlowNex	9-4
Table 41 - $HX_{eff} = 85\%$; wct; OPTIMUM verification; EES - Excel	9-5
Table 42 – $HX_{eff} = 85\%$; wct; EES versus Excel	9-8

Table 43 - Reactor specifications	10-2
Table 44 - Heat exchanger; Rankine working fluid.....	10-2
Table 45 – Optimised cycle configurations; Wet cooling tower; Summary	10-5
Table 46 – Optimised cycle configurations; Dry cooling tower; Summary	10-6
Table 47 – Optimum cycle configurations; Electric energy produced	10-7
Table 48 - $HX_{eff} = 80\%$; wct; Optimised cycle configuration; EES results	12-11
Table 49 – $HX_{eff} = 80\%$; wct; EES versus Excel	12-14
Table 50 - $HX_{eff} = 87.5\%$; wct; Optimised cycle configuration; EES results	12-15
Table 51 – $HX_{eff} = 87.5\%$; wct; EES versus Excel.....	12-17
Table 52 - $HX_{eff} = 90\%$; wct; Optimised cycle configuration; EES results	12-18
Table 53 – $HX_{eff} = 90\%$; wct; EES versus Excel	12-21

LIST OF FIGURES

Figure 1 - Cement production process.....	2-1
Figure 2 - Energy flow for cement production	2-4
Figure 3 - HTR fuel element	3-6
Figure 4 - HTR-modular unit with steam generator	3-7
Figure 5 - Simple Rankine Flow Diagram	4-2
Figure 6 - Simple Ideal Rankine T-s Diagram	4-3
Figure 7 - Rankine with Reheat Flow Diagram	4-5
Figure 8 - Ideal Rankine with reheat T-s Diagram.....	4-6
Figure 9 – Ideal Rankine with Feed Heating Diagram.....	4-8
Figure 10 – Ideal Rankine with Contact Feed Heater T-s Diagram	4-9
Figure 11 – Ideal Rankine with Contact and Closed Feed Heaters T-s Diagram	4-10
Figure 12 – Actual Rankine with Contact and Closed Feed Heaters T-s Diagram	4-12
Figure 13 - Actual Rankine with Attenuation T-s Diagram	4-15
Figure 14 - Mass flow rate parameter	4-16
Figure 15 - Critical Point of Water.....	4-17
Figure 16 - LPT outlet steam quality vs. HPT inlet P_{\max}	4-18
Figure 17 - LPT outlet steam quality vs. Q_{out} and η_R	4-19
Figure 18 - Cycle efficiency vs. Maximum cycle temperature: η_R vs. T_{\max}	5-3
Figure 19 - Energy losses from coal flame to work working fluid.....	5-4
Figure 20 - Heat exchanger effectiveness, mass flow calculation	6-4

Figure 21 - Pinch Point T-s diagram	6-5
Figure 22 - Pinch Point T-s diagram, adjusted s_{ref}	6-6
Figure 23 - Pinch Point T-s diagram, adjusted s_{ref} ; Helium minimum Temperature	6-7
Figure 24 – Hot strength characteristics of stainless steels	6-8
Figure 25 – ASTM U-436; Maximum recommended service temperature.....	6-9
Figure 26 – ASTM U-436; Physical properties.....	6-10
Figure 27 - Optimising model inputs; Reheat.....	7-4
Figure 28 – Optimising model inputs; Regenerative feed heater specification	7-4
Figure 29 - $HX_{eff} = 80\%$; wct; η_R vs. number of closed feed heaters	7-6
Figure 30 - $HX_{eff} = 80\%$; dct; η_R vs. number of closed feed heaters	7-7
Figure 31 - $HX_{eff} = 85\%$; wct; η_R vs. number of closed feed heaters	7-8
Figure 32 - $HX_{eff} = 85\%$; dct; η_R vs. number of closed feed heaters	7-10
Figure 33 – $HX_{eff} = 87.5\%$; wct; η_R vs. number of closed feed heaters.....	7-11
Figure 34 - $HX_{eff} = 87.5\%$; dct; η_R vs. number of closed feed heaters	7-12
Figure 35 – $HX_{eff} = 90\%$; wct; η_R vs. number of closed feed heaters.....	7-14
Figure 36 - $HX_{eff} = 90\%$; dct; η_R vs. number of closed feed heaters	7-15
Figure 37 – $Hx_{eff} = 80\%$; wct; Optimum cycle configuration; T-s diagram.....	8-2
Figure 38 – $Hx_{eff} = 80\%$; dct; Optimum cycle configuration; T-s diagram	8-3
Figure 39 - $HX_{eff} = 85\%$; wct; Optimum cycle configuration; T-s diagram.....	8-5
Figure 40 – $Hx_{eff} = 85\%$; dct; Optimum cycle configuration; T-s diagram	8-7
Figure 41 – $HX_{eff} = 87.5\%$; wct; Optimum cycle configuration; T-s diagram	8-9
Figure 42 – $Hx_{eff} = 87.5\%$; dct; Optimum cycle configuration; T-s diagram	8-11

Figure 43 - $HX_{eff} = 90\%$; wct; Optimum cycle configuration; T-s diagram	8-13
Figure 44 – $Hx_{eff} = 90\%$; dct; Optimum cycle configuration; T-s diagram	8-16
Figure 45 – Optimised configurations; η_R vs. HX_{eff}	8-18
Figure 46 - $HX_{eff} = 85\%$; wct; HP closed feed heater; Verification	9-6
Figure 47 - $HX_{eff} = 85\%$; wct; De-aerator; Verification	9-6
Figure 48 - $HX_{eff} = 85\%$; wct; LP closed feed heater; Verification	9-7
Figure 49 - Parameter INPUT window	12-2
Figure 50 - Steam turbine driven feed pump INPUT window	12-3
Figure 51 - Feed heater and Reheat INPUT window	12-3
Figure 52 - Optimisation criteria vs. parameters	12-5
Figure 53 - Simulation model result OUTPUT window	12-6
Figure 54 - Simulation model Optimised fraction window.....	12-6
Figure 55 - $HX_{eff} = 80\%$; wct; Results	12-7
Figure 56 - $HX_{eff} = 85\%$; wct; Results	12-7
Figure 57 - $HX_{eff} = 87.5\%$; wct; Results	12-8
Figure 58 - $HX_{eff} = 90\%$; wct; Results	12-8
Figure 59 - $HX_{eff} = 80\%$; dct; Results	12-9
Figure 60 - $HX_{eff} = 85\%$; dct; Results	12-9
Figure 61 - $HX_{eff} = 87.5\%$; dct; Results	12-10
Figure 62 - $HX_{eff} = 90\%$; dct; Results	12-10
Figure 63 - $HX_{eff} = 80\%$; wct; De-aerator; Verification	12-12
Figure 64 - $HX_{eff} = 80\%$; wct; HP closed feed heater; Verification.....	12-13

Figure 65 - $HX_{eff} = 80\%$; wct; LP closed feed heater; Verification	12-14
Figure 66 - $HX_{eff} = 87.5\%$; wct; De-aerator; Verification	12-16
Figure 67 - $HX_{eff} = 87.5\%$; wct; HP closed feed heater; Verification	12-16
Figure 68 - $HX_{eff} = 87.5\%$; wct; LP closed feed heater; Verification	12-17
Figure 69 - $HX_{eff} = 90\%$; wct; HP closed feed heater; Verification	12-19
Figure 70 - $HX_{eff} = 90\%$; wct; De-aerator; Verification	12-20
Figure 71 - $HX_{eff} = 90\%$; wct; LP closed feed heater; Verification	12-20
Figure 72 – FlowNex Simulation model; $HX_{eff} = 85\%$; wct.....	12-22

NOMENCLATURE

Units

Enthalpy	kJ/kg	kilo-Joule per kilogram
Entropy	kJ/kg-K	kilo-Joule per kilogram Kelvin
mass flow	kg/s	kilogram per second
Pressure	MPa	Mega Pascal
Pressure	kPa	kilo-Pascal
Temperature	K	Kelvin
Temperature	°C	degrees Celsius

Energy

kWh	kilo-watt hour
MW _e	Mega Watt electric
MW _t	Mega Watt thermal

Abbreviations

c,i	cold working fluid inlet
c,o	cold working fluid outlet
dct	Dry cooling tower
FH	Feed heater
h,i	hot working fluid inlet
h.o	hot working fluid outlet
HPT	High Pressure Turbine
HTR	High Temperature Reactor (gas cooled)
HX	Heat exchanger
IPP	Independent Power Producer
IPT	Intermediate Pressure Turbine
LPT	Low Pressure Turbine
MCR	Maximum Continuous Rating
PCU	Power conversion unit
STL	Steenkampskraal Thorium Ltd.
wct	Wet cooling tower

1 CHAPTER 1: INTRODUCTION

1.1 BACKGROUND

Although India is the world's fifth-largest electricity producer they have an incredibly low per capita consumption of 778.71 kWh per annum. India has approximately 300 million people without access to electricity. The magnitude of India's electricity supply shortage became apparent in 2010 when blackouts halted manufacturing across the country, even hitting wealthy urban neighbourhoods. (Yep: 2012)

India is struggling with the coal demand at their coal fired power plants despite its abundant reserves and government spent approximately \$100 billion since 2007 to increase the electric capacity. The solution to the inability of the mines to produce enough coal would be to import it which would mean that additional finances must be acquired. The most probable solution to acquiring these finances would be to increase the price of electricity starting with the industrial sector. (Yep: 2012)

The Indian public supply of electric energy is unreliable which is why many industries chose to install independent power plants (IPP) in order to ensure the quality as well as the supply of their power requirements. IPP's supplied nearly one third of the industrial energy demand, which is far greater than the 17% of the American industry energy demand. (Remme et al: 2011)

With the IPP's supplying this amount of energy to the industrial sector, it is clear that the industries in India deemed the private supply of electricity necessary. According to Remme *et al*: 2011, the enactment of the Electricity Act 2003 in India, enabled industry owned (IPP) power plants to supply electric energy to the Indian distribution network by reducing the regulations for industrial concerns building power plants.

HOLCIM cement is one of the dominant industries affected by the electricity shortage. Large amounts of thermal energy are required to form clinkers in the kiln. This thermal energy comes from burning fossil fuels such as oils, coal, petroleum coke and natural gas. Burning these fossil fuels has environmental consequences due to the emissions of global greenhouse gasses such as CO₂.

As a leading manufacturer of construction materials, HOLCIM is aware of the impact of this production process on the environment and biodiversity. The consumption of natural resources is one of the greatest threats on biodiversity causing a decline in the quality of habitats and ecosystems being broken down. (HOLCIM: 2010)

Considering the current status of the Indian electricity sector and the carbon footprint of the cement production process, it would be wise to become independent of the Indian electricity sector. Installing non-coal IPP's for industrial manufacturing where economically viable would, in the long term, reduce the production costs of the product. It would also reduce the demand for electricity on the distribution network and the carbon footprint of the HOLCIM cement production plant. (Jacott *et al*: 2003)

Since the shortage of electricity prevents India from sustaining its rapid economic growth, the installation of non-coal IPP's would increase the economic growth by reducing the electric energy demand and in return reduce the electricity shortage.

Installing a 100 MW_t thorium HTR in combination with a PCU (Rankine cycle) is a possible solution to HOLCIM's energy shortage.

1.2 PROBLEM STATEMENT

The problem is that for the feasibility of this IPP to be assessed, a Rankine cycle needs to be adapted and optimised to suit the limitations and requirements of a 100 MW_t thorium HTR.

1.3 OBJECTIVE OF STUDY

- The purpose is to produce an optimised feasible Rankine cycle PCU model utilising the thermal energy of the thorium HTR in the most effective manner.
- A secondary outcome will be to evaluate the feasibility of IPP operation of this power supply unit. The evaluation of the balance of surplus power against the cement plant demand, whilst the thorium reactor and PCU operate at maximum continuous rating, must be possible.
- The optimised cycle design simulation must verify favourably against alternative software packages.

1.4 RESEARCH METHODOLOGY

- A literature survey is necessary to evaluate the scope of work, commencing with the Indian power supply and the feasibility of implementing an IPP.
- Thereafter a literature survey is required to evaluate the feasibility of waste heat energy utilisation and process heat integration on the Portland cement process.
- A literature survey is needed to identify the advantages and disadvantages of various nuclear reactor types versus the Thorium HTR, with special reference to the important process parameters such as minimum/maximum temperature limits.
- Thereafter suitable software packages will have to be evaluated to perform the required simulations and optimisation of the Rankine cycle. Packages such as EES, FlowNex and Excel X-Steam will be considered. Since verification on a practical plant or model is not possible, the most suitable package will be used for optimisation of the Rankine cycle and another for verification.
- Various Rankine cycle designs are to be developed to enable evaluation of reheat, feed heating configurations, etc. This will form the crux of the Rankine cycle design.
- Also, Rankine cycle optimisation criteria should be defined such as maximum net work, thermal efficiency, dryness fraction against cycle pressures, etc.
- Model of the various configurations are to be compared relative to the above criteria.
- Conclusions are drawn and recommendations are made according to the obtained results.

1.5 SCOPE AND LIMITS OF THE STUDY

- This dissertation is focused on the design and optimisation of the thermal cycle as a whole and will therefore not include the detailed design of heat exchangers; steam turbines or any other components.

- Possible material selection for the heat exchanger will be done to support the viability of the unusually high heat exchanger outlet temperature.
- Pump, turbine and mechanical efficiencies, as well as heat exchanger effectiveness and pressure losses are incorporated into the design to simulate reality more accurately.
- PCU design will be simulated using Engineering Equation Solver (EES) as primary software package and the results will be verified using Flownex and Excel.
- The simulation results will be calculated using base line design values of the thorium HTR, since it is still to be constructed.
- Due to the magnitude of a computational fluid dynamics (CFD) study, it is not included.
- Proportionally, pressure losses of existing Rankine cycle plants are incorporated in this study.

1.6 DISSERTATION STRUCTURE

The structure of this dissertation can be summarised as follows.

Chapter 1: Introduction

Chapter 1 is an introduction into this dissertation. It provides background information, the problem statement, objectives, research methodology, scope and limitations as well as the dissertation structure.

Chapter 2: Literature Survey - Cement

This chapter contains a review of literature on the cement production process and the energy consumed.

Chapter 3: Literature survey - Nuclear

Various reactor technologies are researched and shortly discussed in this chapter.

Chapter 4: Rankine cycle development

The Rankine cycle is to be the PCU. Various components and additions of the Rankine cycle and the effects thereof are evaluated.

Chapter 5: Design Considerations

To design the Rankine cycle powered by a 100 MW_t thorium HTR, various techno-economic aspects and limiting parameters are considered. The practicality of the design must also be taken into account.

Chapter 6: Heat Exchanger

The interaction between the thorium HTR and the Rankine cycle is a critical design focus. The influence of the heat exchanger on the Rankine cycle is evaluated in this chapter.

Chapter 7: Simulation

Various optimised design configurations are weighed against each other to determine the optimum cycle configuration for numerous input combinations.

Chapter 8: Optimum cycle configuration

The optimum cycle configuration for each input combination, as determined in Chapter 7, is discussed in this chapter.

Chapter 9: Model Verification

FlowNex and Excel are used to verify the validity of the simulation model and the optimised results respectively.

Chapter 10: Conclusion

A conclusion is made on the feasibility of installing the Rankine cycle powered by a thorium HTR as IPP for the cement production process.

References

All the reviewed and referenced literature is listed according to the NWU Harvard referencing method in this section.

Appendices

All the simulation models, results and relevant additional documents are displayed in this section and available on the attached CD.

1.7 KEY ASPECTS

- HOLCIM cement in India suffers losses due to the unreliability of the Indian electricity supply.
 - India's economic growth is limited by the shortage in electric energy supply.
 - An IPP is to be installed to supply electric energy to the cement production process.
 - A PCU needs to be designed and optimised for the generation of electricity.
 - Any IPP can generate revenue by supplying electric energy to the Indian distribution network.
-

2 CHAPTER 2: LITERATURE SURVEY - CEMENT MANUFACTURING

2.1 INTRODUCTION

In order to investigate the utilisation of process heat, it is necessary to have an overview of the entire cement manufacturing process. Cement manufacturing consist of twelve process stages. According to HOLCIM: 2012, using Figure 1 as reference, these twelve stages can be described as follows:

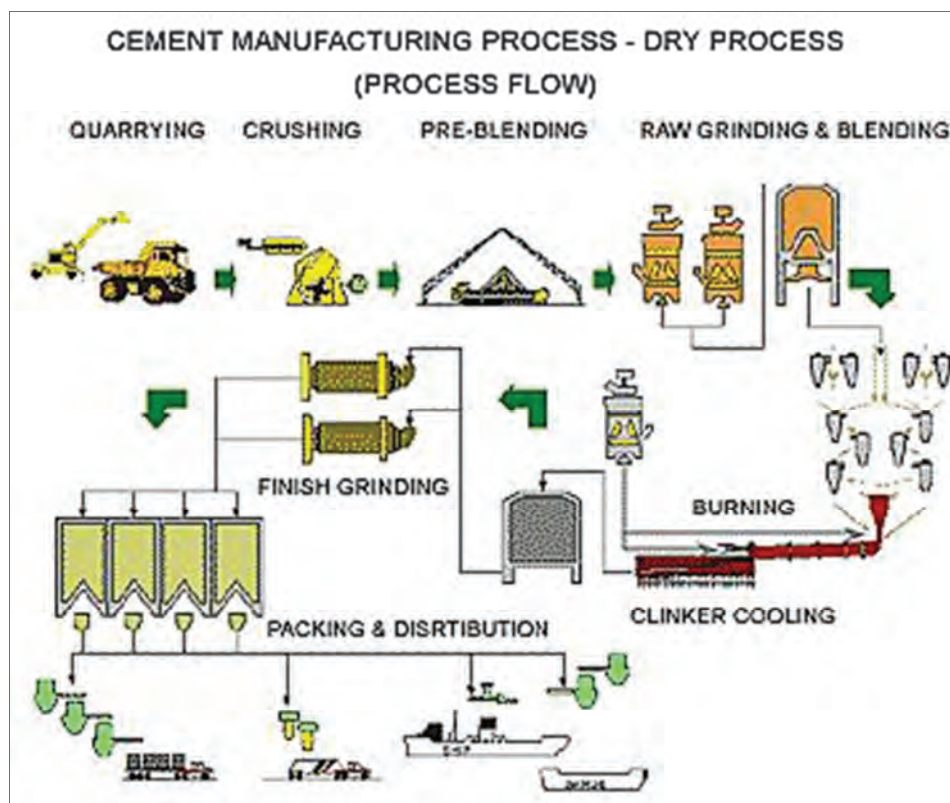


Figure 1 - Cement production process

(CEMEX: 2011)

School of Mechanical and Nuclear Engineering

1. Quarry – Drilling and blasting techniques are used to extract limestone, marl, clays and other necessary materials from a quarry.
2. Crusher – Mechanical crushers are used to reduce the size of the quarried material. Drying of raw material may be necessary to reduce the amount of water that enters the kiln.
3. Conveyer – Raw material is transported to the cement plant where it enters a mixing bed.
4. Mixing bed – Crushed limestone and clays are mixed using a stack and reclaim process.
5. Raw mill – Raw materials are milled and dried until fine enough to be carried by air.
6. Filter bag – Filters particles from the kiln exhaust for the use thereof in drying processes.
7. Preheater – Preheats the raw material before it enters the kiln as to improve energy efficiency since material is 20 to 40% calcined at kiln entry. Raw material is rapidly heated to approximately 1000°C.
8. Kiln – Material is heated in the rotating kiln which is angled at approximately 3 - 4° by transferring heat from fuel burning. Raw material is heated to 1450°C and forms calcium silicate crystals (cement clinkers).
9. Cooler – Ambient air is used to rapidly cool the cement clinkers. Air is fed into the kiln as combustion air.
10. Clinker silo – Clinkers are stored or transported in preparation for grinding.
11. Cement mill – Cement clinkers are ground together, gypsum and other materials may be added to form cement.
12. Logistics – Packing and transportation of the final cement product.

Now that the cement production process is outlined, it is important, for the design and optimisation of the Rankine cycle, to determine the impact of the energy requirements throughout this process.

2.2 ENERGY CONSUMPTION

The cement production sector consumed 18700 MWh in 2004 which is approximately 0.02% of the total world energy consumption per annum. Approximately 1.5 ton raw material produce 1 ton of finished cement during which 110 kWh electric energy is consumed. (Jankovic et al: 2004)

Since a sizeable amount of energy is used in the production of cement, it is important to focus on the reduction of energy consumed. Between 50 and 60 percent of the total production cost of cement is accounted for in energy consumption. Thermal energy costs form approximately one quarter of the energy required in the cement production process. Thermal energy is mainly used in the kilns for the clinker forming process while the electric energy is used for the cement grinding process. (Madloul *et al*: 2011).

Due to the great amount of energy required to produce 1 ton of cement, the small 100 MW_t nuclear reactor will be implemented as an electric energy source. The burning of fuel is still necessary for the forming of clinkers in the kiln as temperatures of up to 1450°C are required to produce clinkers.

The flow chart in Figure 2 shows that the cement production process requires both electric and thermal energy throughout. The PCU design can therefore focus on each of the stages in the flow chart that require either thermal or electric energy. By using the non-coal IPP to supply energy where necessary throughout the cement production process, public energy usage can greatly be decreased, if not eliminated.

The amount of electric energy required by these stages is called auxiliary power. The main design focus of the PCU will be on the total auxiliary power required throughout the various stages.

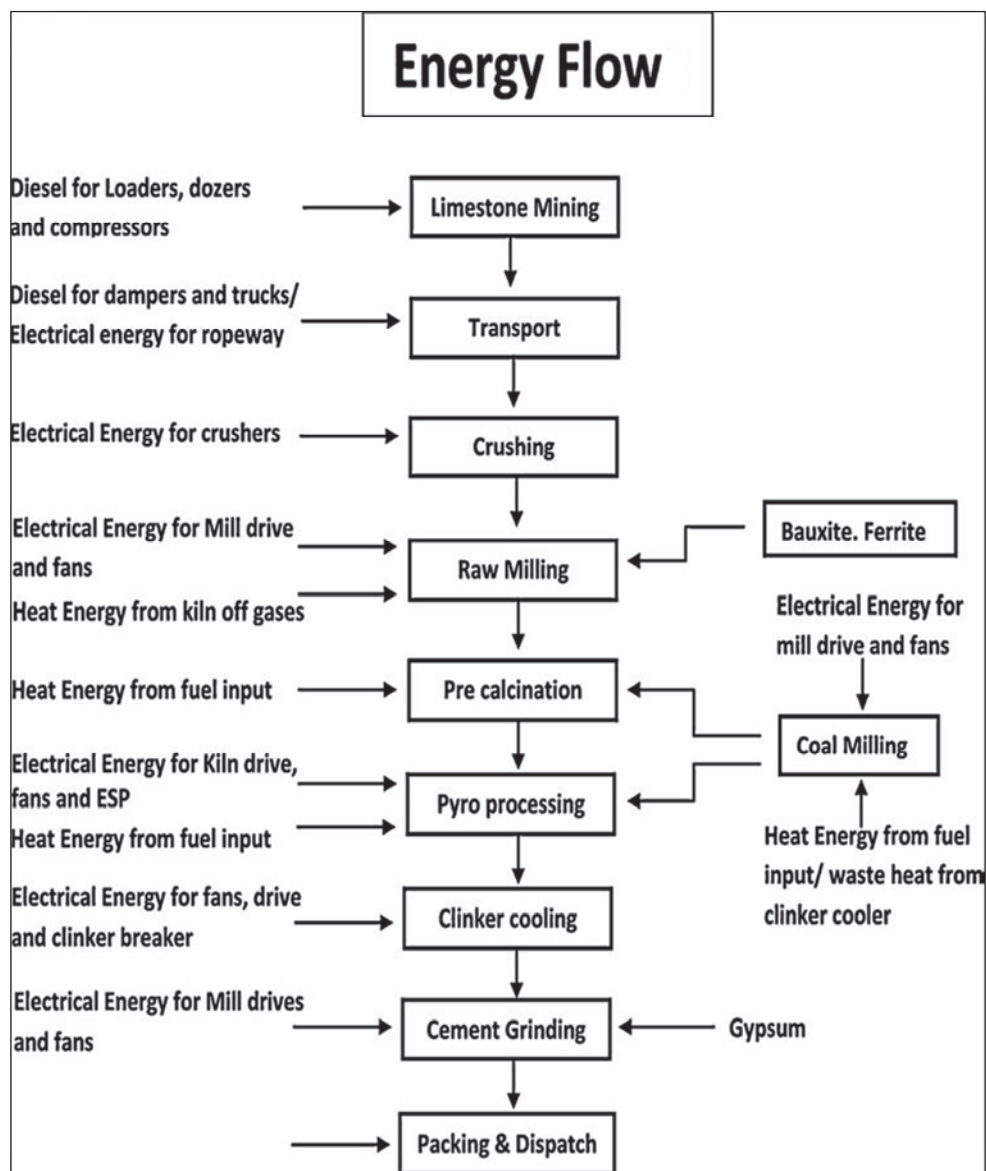


Figure 2 - Energy flow for cement production

According to Jankovic *et al*, the clinker grinding in the cement mill consumes approximately 44kWh of the 110 kWh auxiliary power required to produce 1 ton of cement.

Table 1 – Electric energy distribution for cement production

Section / Equipment	Electrical energy consumption (kWh / ton of cement)	% Energy Consumption
Mines, crusher and stacking	2.2	2.0
Reclaimer, Raw meal grinding and transport	26.4	24.0
Kiln feed, kiln and cooler	32.2	29.3
Coal mill	7.4	6.7
Cement grinding and transport	33.8	30.7
Packing	2.2	2.0
Lighting, pumps and services	5.8	5.3
Total	110	100

Table 1 show that the cement grinding and transport (conveyers) consume more than 30% of the total electric energy consumption of cement production, with the kiln and cooler at just below 30%. Raw meal grinding and transport used 24% of the electrical energy. The remaining 16% can be described as auxiliary power required.

According to Mulder (2012), the HOLCIM cement production plant consumes approximately 26 MW_e when operating at maximum capacity. According to Jankovic *et al*, the HOLCIM plant will produce approximately 235 tons of cement per hour.

3 CHAPTER 3: LITERATURE SURVEY - NUCLEAR REACTOR OPTIONS

3.1 INTRODUCTION

Coal generation cannot be used due to the lack of coal supply in India. Few generation methods, other than smaller nuclear reactors, are capable of supplying a cement production plant with adequate energy. Such reactors would be capable of supplying energy to the cement production plant without increasing the load on the coal industry.

Nuclear disasters cause great stress, chaos and destruction, clearly illustrated by the accidents at Chernobyl (1973) and Fukushima (2011). The destruction caused by the nuclear plant malfunction in Chernobyl caused a dramatic increase in reactor safety to follow in the next generation of reactors. Inherent or passive safety systems are the current ideal for reactor safety features. According to Ali (2011), inherent or passive safety features can be described as safety features that require no active controls or operational intervention to avoid accidents in the event of malfunction. These features rely on gravity, natural convection or high temperature resistance as safety measures. Inherent or passive safety therefore reduces the probability of an accident by eliminating the human factor in reactor safety.

Reactors of up to 300 MW_e are classified as 'small' reactors by the IAEA (International Atomic Energy Agency). There are three main small reactors being pursued namely: LWR's (Light Water Reactors), FNR's (Fast neutron reactors) and graphite-moderated HTR's. Advantages of small reactors include greater simplicity in design, reduced citing costs and a high level of inherent or passive safety. Many safety features in large reactors were found unnecessary in small reactors by a special committee convened by the American Nuclear Society in 2010. (WNA: 2012)

3.2 NUCLEAR FUEL RESERVES

Uranium is currently the only fuel supplied for nuclear reactors. Existing reactors such as CANDU and some advanced reactor designs are however capable of utilising thorium as fuel on a substantial scale. The advanced reactor designs include the STL thorium HTR small nuclear reactor. (WNA: 2012 [2])

In order to evaluate the viability of utilising a small nuclear reactor to supply the required thermal and electric energy to the cement production plant, it is necessary to examine the fuel reserves of India. Uranium and thorium reserves will therefore be evaluated.

Table 2 - Known recoverable resources of Uranium in 2011

Country	Uranium	
	[ton]	[%]
Australia	1 661 000	31
Kazakhstan	629 000	12
Russia	487 200	9
Canada	468 700	9
Niger	421 000	8
South Africa	279 100	5
Brazil	276 700	5
Namibia	261 000	5
USA	207 400	4
China	166 100	3
Ukraine	119 600	2
Uzbekistan	96 200	2
Mongolia	55 700	1
Jordan	33 800	1
Other countries	164 000	3
World Total	5 327 200	100

(WNA: 2012 [2])

Table 2 shows the known recoverable resources of uranium for various countries across the world. Although vast reserves of uranium can be found around the world, India has so little uranium that their contribution is not worth mentioning. This proves that India has less than one percent of the worlds' uranium reserves.

When the worlds' thorium reserves are inspected, the situation is reversed. According to WNA: 2013, India has the largest reserve of thorium resources in the world with 846 000 tons of thorium at 16% of the worlds' total reserves.

Table 3 - Estimated resources of Thorium

Country	Thorium	
	[ton]	[%]
India	846 000	16
Turkey	744 000	14
Brazil	606 000	11
Australia	521 000	10
USA	434 000	8
Egypt	380 000	7
Norway	320 000	6
Venezuela	300 000	6
Canada	172 000	3
Russia	155 000	3
South Africa	148 000	3
China	100 000	2
Greenland	86 000	2
Finland	60 000	1
Sweden	50 000	1
Kazakhstan	50 000	1
Other countries	413 000	8
World Total	5 385 000	100

(WNA: 2013)

As India has very little uranium reserves while their thorium reserves are vast, it is apparent that a thorium fuelled reactor would be more viable for operation in India.

3.3 GENERATION IV REACTORS

The most important risks with nuclear reactors include nuclear proliferation, nuclear waste and overall safety. Generation IV reactors are designed to reduce all of these risks. These reactors are inherently safer (passive safety features) than the previous generations. They are highly economical, proliferation resistant and will produce minimal waste.

The Generation IV International Forum was established in 2000. Its research and development consortium has 11 members and their four main objectives are as follows:

- Advance nuclear reactor safety.
- Address nuclear non-proliferation and physical protection issues.
- Competitive economics.
- Minimise waste and optimise natural resource utilisation.

(ELDER & ALLEN: 2009)

3.3.1 LIGHT WATER REACTORS (LWR)

Light water reactors are thermal reactors meaning that fission occurs when a neutron with a thermal energy level is absorbed by the fuel. For a neutron to reach a thermal energy level it must be moderated. Moderation occurs when a neutron loses energy due to a series of collisions with the moderator. (Lamarsh, 137: 2001)

Light water reactors use less than 5% enriched ^{235}U fuel and has a refuelling interval of less than 6 years. Ordinary water is used both as moderator and coolant in these reactors. (WNA: 2012)

There are two types of light water reactors: a pressurised water reactor (PWR) and a boiling water reactor (BWR).

3.3.1.1 PRESSURIZED WATER REACTOR

Water acting as moderator and coolant enters the pressure vessel at approximately 290°C, flows down the outside of the core acting as a reflector and enters the core at the bottom. The moderator then flows upward acting as a coolant and exits the core at approximately 325°C. The moderator is under high pressure (15MPa) which prevents it from changing to steam. A steam generator is then utilised to produce steam which in turn feeds the turbine. (Lamarsh, 137: 2001).

3.3.1.2 BOILING WATER REACTOR

This type of reactor does not make use of steam generators to produce the steam that feeds the turbines, but rather allows the water to boil under pressure (7MPa) in the reactor core. This process is classified as a direct cycle, since the water acting as moderator and coolant also feeds the turbine. It flows upward through the core, exiting in the form of steam at approximately 290°C. The water in this cycle becomes radioactive over time. (Lamarsh, 144 - 147: 2001)

3.3.2 HIGH TEMPERATURE GAS COOLED REACTORS (HTR)

Except for fast neutron reactors, these reactors use graphite as moderation material and either Helium, carbon dioxide or nitrogen as primary coolant (WNA: 2012).

Gas cooled reactors have a high thermal efficiency and produce steam at approximately 540°C and 14MPa, while operating at an overall efficiency of about 40%. This efficiency is as high as the most efficient fossil fuel plants available today. An advantage of using Helium as a coolant rather than CO₂ is that it does not absorb neutrons. It is an inert-gas and can therefore not become radioactive. (Lamarsh, 160 - 163: 2001)

Since graphite is used as moderator in gas cooled HTR's, the neutrons lose less energy than in light water reactor collisions due to the greater mass of the carbon. The average travelling distance of a thermal neutron before being absorbed is called the diffusion length. The diffusion length in a reactor using graphite as a moderator is more than 20 times that of a light water reactor. (Lamarsh, 254: 2001).

Some HTR's use a mixture of thorium and highly enriched uranium as fuel. These reactors breed by relying on the moderated neutrons in the thermal energy level to be absorbed by the thorium. When the thorium (²³²Th) absorbs a neutron, it decays to ²³³U which is highly fissionable and releases more neutrons than ²³⁵U. (Lamarsh, 189 – 190: 2001)

3.3.2.1 HTR - MODULE

Spherical fuel elements with a diameter of 60 mm are used as the fuel source for the HTR – module. These spherical fuel elements can be seen in Figure 3. The fuel elements are inserted at the top of the reactor core and gradually migrate downwards due to gravity. After removal, these elements will be inspected for physical integrity and burn-up. (Steinwarz, 47: 1987)

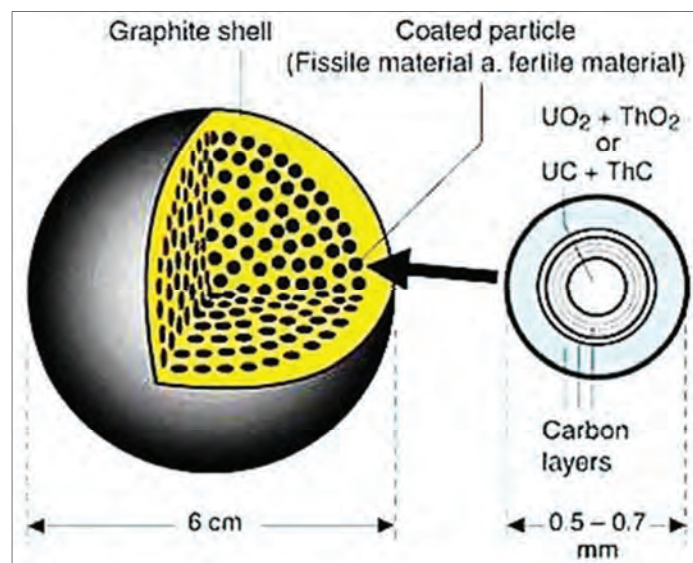


Figure 3 - HTR fuel element

(Kugeler: 2009)

HTR fuel elements consist of a graphite shell, a graphite matrix and coated particles (Figure 3). These coated particles contain the fuel ($\text{UO}_2 + \text{ThO}_2$) while the graphite surrounding these coated particles act as moderator.

According to Steinwarz (47: 1987) the HTR-module has a mean power density of 3.0 MW/m^3 with the reactor core containing 360 000 spherical fuel elements. Each spherical fuel element has 7.9% enrichment and spends approximately 1000 days inside the reactor core.

The HTR makes use of helium as coolant. The helium flows through the reactor core, absorbs the heat from the fuel elements and transfers the heat to the heat exchanger (steam generator). Using helium has various advantages, of which the main advantage is that it is a stable perfect gas and can therefore not absorb neutrons. Helium is therefore chemically inert and is not being activated except for trace amounts of tritium-gas produced due to

impurities. The neutron population in the reactor core will thus not be diminished by the coolant as in the case of water coolants.

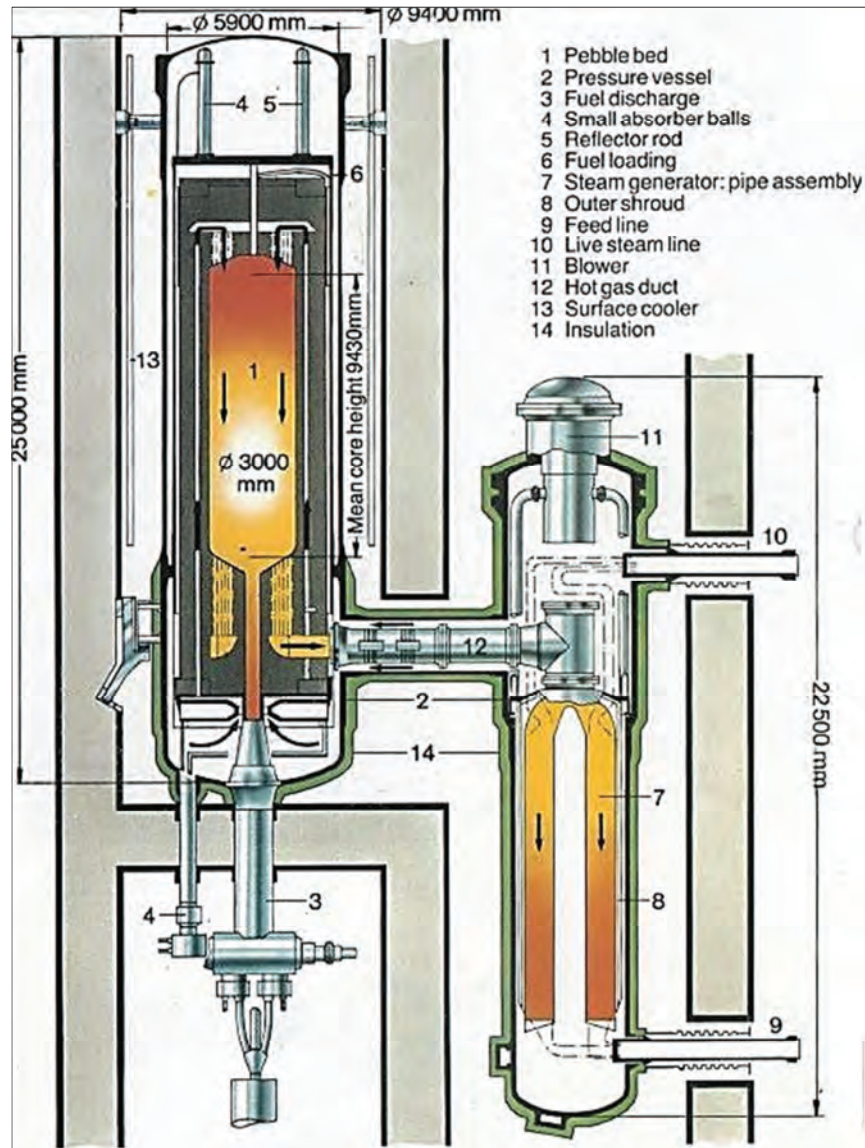


Figure 4 - HTR-modular unit with steam generator

(Steinwarz, 47: 1987)

Further advantages include the increased specific heat consumption of helium (5.19 kJ/kg-K) compared to that of water (2.354 kJ/kg-K) at 923.15 K and 6 MPa. Helium is a more superior heat transfer medium than water. A lesser mass flow is required, therefore reducing the physical size of the heat exchanger (steam generator).

Figure 4 illustrates the HTR-module to show the flow of helium (arrows) from entering the reactor core at 250°C, flowing downward and exiting at 750°C. The helium then continues through the hot gas duct to the steam generator (counter flow) where it transfers thermal energy to generate steam. During this process the helium is cooled to 250°C and can be re-used as coolant through the reactor core. (Steinwarz, 48: 1987)

3.3.3 FAST NEUTRON REACTORS (FNR)

Fast neutron reactors do not use a moderator to slow the neutrons but rely on higher energy fission. The designs of these reactors are simpler and smaller than LWR's. Higher energy fission leads to better fuel performance and a longer refuelling interval of up to 20 years. The coolant used in these reactors is liquid metal such as sodium, lead or lead-bismuth. These liquid metals have a high thermal conductivity and boiling point. The fuel is enriched to 15-20% in most cases. (Anon: 2012)

3.3.4 SMALL NUCLEAR REACTORS

Small reactors are defined by the International Atomic Energy Agency (IAEA) as reactors delivering less than 300 MW_e. Demand for these small reactors is increasing due to the various advantages thereof. (Anon: 2012)

Small reactors' construction has a reduced capital cost requirement, thus catering for smaller economies. They are ideal for remote sites and can operate independently (own PCU) or as modules in a larger complex (one PCU powered by multiple reactors). (Anon: 2012).

Due to the reduced physical size of these reactor units, the possibility of on-site construction is increased. On-site construction reduces transmission losses and eliminates the dependence on the distribution network.

Small reactor units are ideal for the proposed application. The reactor unit can be constructed on-site; 26 MW_e is required for the cement production process and revenue can be generated by selling additional energy to the Indian distribution network.

3.4 KEY ASPECTS

- Electricity shortage in India is the cause of the reduction in the rate of cement production.
 - Coal, although abundant, is in short supply.
 - India has little uranium resources while thorium is abundant.
 - A small nuclear reactor will be ideal for supplying the cement production process with thermal and electric energy where necessary.
 - The small nuclear reactor should be thorium fuelled.
 - Chapter 1 identifies the possibility of generating additional revenue by supplying any auxiliary electric energy to the Indian distribution network.
-

4 CHAPTER 4: RANKINE CYCLE DEVELOPMENT

4.1 INTRODUCTION

In order to generate electricity a PCU is required. The thermal energy produced by the thorium reactor will supply the PCU with the necessary heat input.

The Rankine cycle is used by most coal and nuclear power stations for electricity generation. The simple Rankine cycle consist of four basic components:

- Pump - Increases working fluid pressure
- Heat exchanger - Increases working fluid temperature
- Turbine - Converts thermal- to mechanical energy
- Condenser - Extracts latent energy from working fluid

Overall cycle efficiency can be increased by employing various components and alternative designs. Concepts such as attemperation do not increase cycle efficiency but rather allows for increased control capability.

Table 4 shows the relevant results pertaining to the Rankine cycle development. Detailed Rankine cycle development is discussed throughout this chapter.

Table 4 - Rankine cycle development Result comparison

	Unit	Ideal				Actual	
		Superheat Only	Reheat	Contact Feed heater	Feed heaters		Attemperation
E_{Balance}	kW	0	0	0	0	0	0
η_{Carnot}	%	61.24	61.24	61.24	61.24	61.24	61.24
η_{Rankine}	%	42.91	44.54	47.35	48.65	42.02	41.92
ω_{Turbine}	kJ/kg	1395	1701	-	-	-	-
W_{Turbine}	kW	-	1701	1570	1505	1305	1305

4.2 IDEAL RANKINE CYCLE

4.2.1 SIMPLE RANKINE CYCLE WITH SUPERHEAT

In the simple Rankine cycle (Figure 5), water is heated under pressure using a heat exchanger, after which it passes through a combination of turbines. Since the pressure drops radically through the turbines, the water is mostly steam at the LPT outlet despite the immense decrease in temperature. The working fluid is then condensed to liquid and again pumped to the heat exchanger.

The work delivered by the turbine is limited by the upper creep temperature of the heat exchanger tubes and the lower quality limit of the steam at the LPT outlet. Droplets form at the LPT outlet as the steam wetness increases. The turbine blades will wear excessively at a too low dryness factor (increased wetness).

The easiest way to overcome the water quality limit is to superheat the water before the turbine inlet. This causes the entropy and, therefore, the quality of the steam at the LPT outlet to increase. (ELDER & ALLEN: 2009)

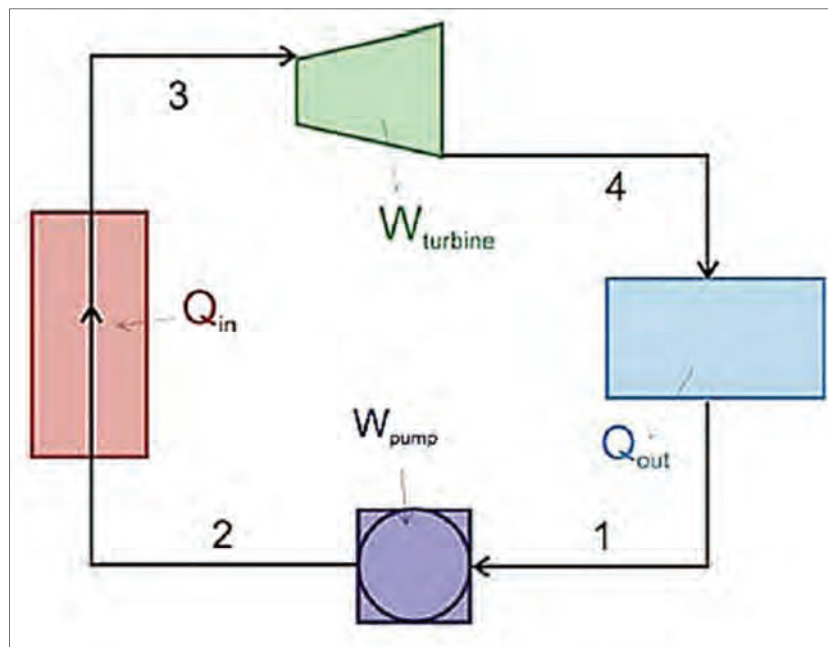


Figure 5 - Simple Rankine Flow Diagram

(ELDER & ALLEN: 2009).

The parameters for the simple ideal Rankine cycle construction are shown in Table 5.

Table 5 - Simple Ideal Rankine cycle input parameters

	Value	Unit	Description
P_{\max}	16	MPa	Maximum pressure at high pressure turbine inlet
T_{\max}	535	°C	Maximum temperature of heat exchanger tube outlet
T_{\min}	40	°C	Limited by ambient conditions
\dot{m}	1	-	Comparison done by using specific work

Figure 6 shows the T-s graph for a simple ideal Rankine cycle with superheated saturated vapour. Configuration for a simple Rankine cycle consists of a pump, heat exchanger, turbine combinations and a condenser.

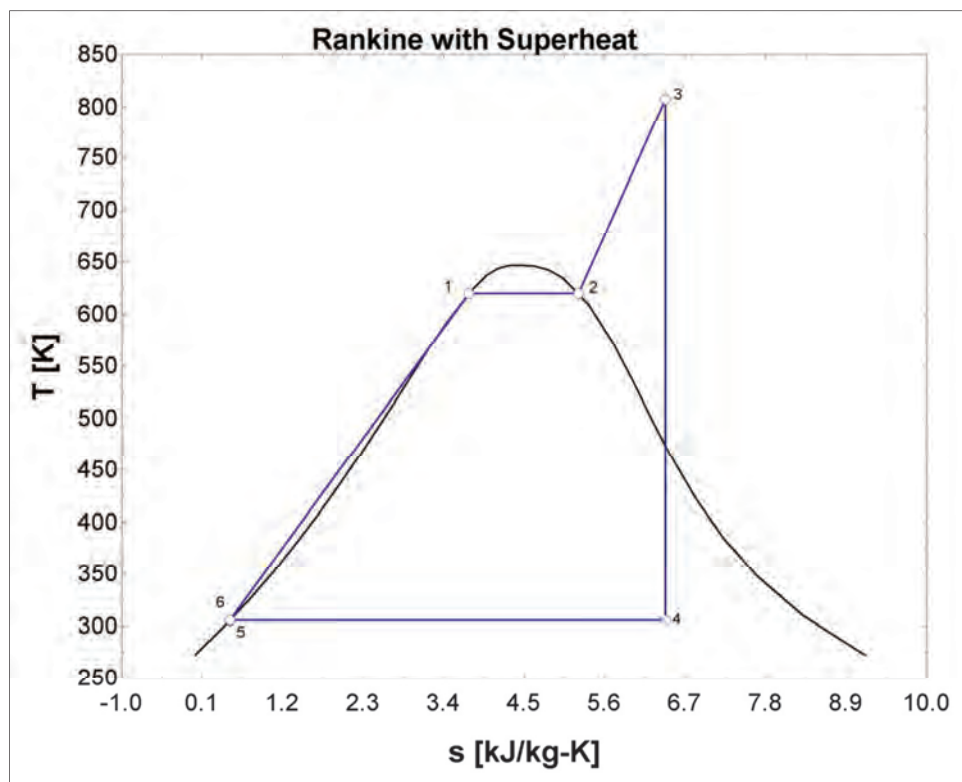


Figure 6 - Simple Ideal Rankine T-s Diagram

Table 6 is constructed to evaluate the effect of various components added to the Rankine cycle as discussed in this chapter. Carnot efficiency is the maximum efficiency available for the specific cycle and can be calculated as follows (temperature in Kelvin):

$$\eta_{Carnot} = \frac{T_{max} - T_{min}}{T_{max}} \quad (1)$$

The Carnot efficiency cannot be achieved in practice, since it is theoretical thermal maximum. The calculations do not incorporate the heat input required by the Rankine cycle or the amount of energy rejected through the condenser. The Carnot efficiency can therefore be seen as theoretical upper limit for Rankine cycle efficiency calculations. The law of Carnot states that the maximum cycle efficiency is proportional to the temperature difference. The Carnot efficiency remains constant for the same temperature difference ($T_{max} - T_{min}$)

Table 6 - Simple Ideal Rankine cycle results

	Value	Unit	Description
$E_{Balance}$	0	kW	Check to determine the accuracy of model simulation
η_{Carnot}	61.24	%	Maximum available cycle efficiency (Law of Carnot)
$\eta_{Rankine}$	42.91	%	Rankine cycle efficiency
$\omega_{Turbine}$	1395	kJ/kg	Specific work delivered by the turbines

4.2.2 REHEAT

Modifications can be made to improve the efficiency of the basic Rankine cycle. A reheating stage can be introduced (Figure 7), which increases the quality of the steam. The efficiency of the cycle is increased due to an increase in the overall ΔT . (ELDER & ALLEN: 2009)

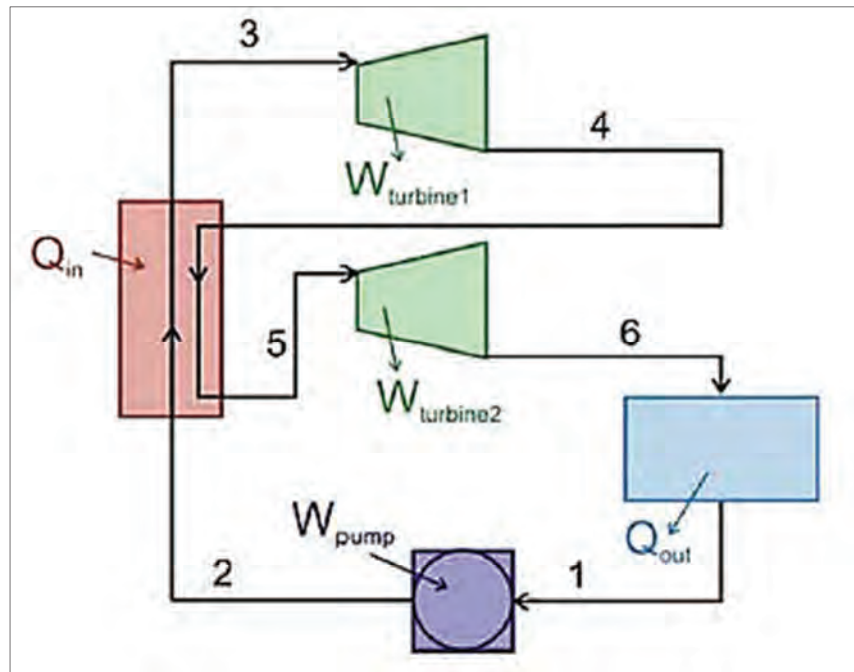


Figure 7 - Rankine with Reheat Flow Diagram

(ELDER & ALLEN: 2009).

Input parameters for the ideal Rankine cycle with reheat is shown in Table 7. To accurately compare the results of the various Rankine cycle configurations it is important that the input parameters remain constant.

Table 7 - Ideal Rankine cycle with reheat input parameters

	Value	Unit	Description
P_{\max}	16	MPa	Maximum pressure at high pressure turbine inlet
T_{\max}	535	°C	Maximum temperature of heat exchanger tube outlet
T_{\min}	40	°C	Limited by ambient conditions
\dot{m}	1	-	Comparison done by using specific work

Figure 8 shows the T-s diagram of the Rankine cycle with reheat (points 4 to 5). Reheating in the Rankine cycle increases the net work and the thermal efficiency of the cycle for the same ΔT .

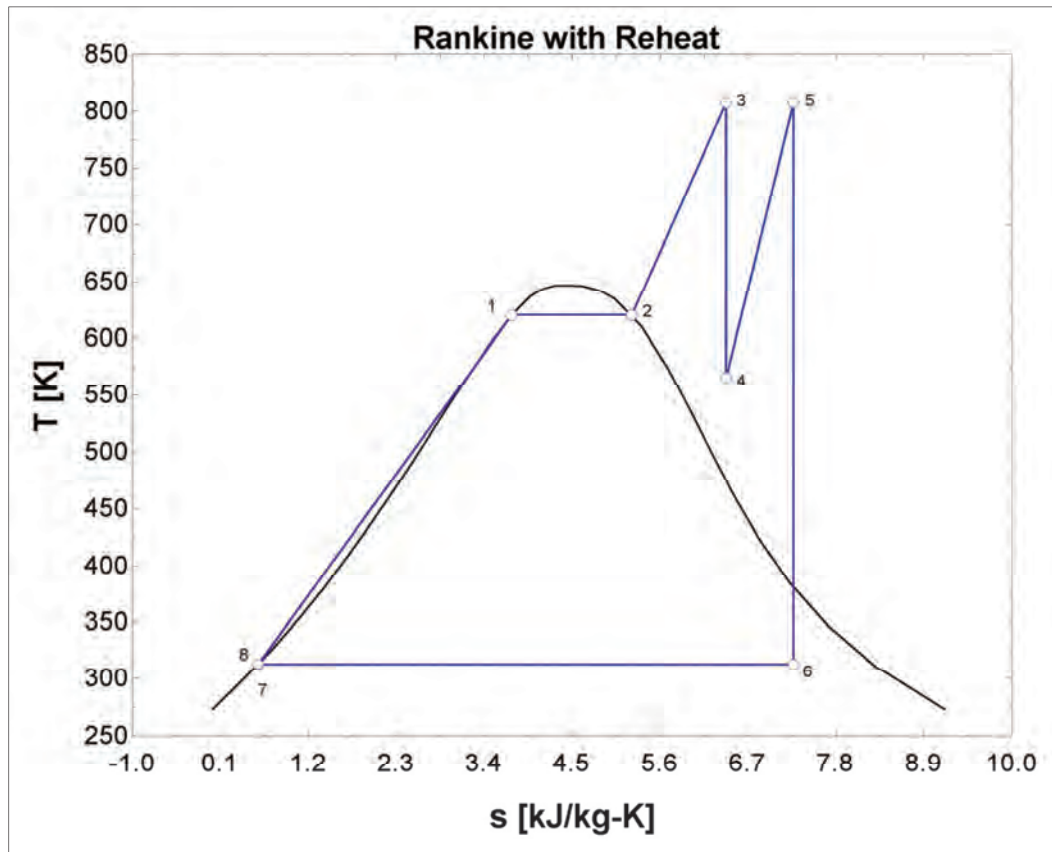


Figure 8 - Ideal Rankine with reheat T-s Diagram

Since the energy in and out in the simulation model balances (Table 8), the construction thereof is correct. The Carnot efficiency has not changed by introducing reheat into the Rankine cycle configuration, as the design parameters or ΔT remained constant. Reheating the steam after exiting the HPT, increases the work delivered and therefore cycle efficiency.

Table 8 - Ideal Rankine cycle with reheat results

	Value	Unit	Description
E_{Balance}	0	kW	Check to determine the accuracy of model simulation
η_{Carnot}	61.24	%	Maximum available cycle efficiency (Law of Carnot)
η_{Rankine}	44.54	%	Rankine cycle efficiency
ω_{Turbine}	1701	kJ/kg	Specific work delivered by the turbines
W_{Turbine}	1701	kW	At a mass flow rate of 1 kg/s for comparison purposes

W_{Turbine} is added to Table 8 to illustrate the effect of feed heating in the section below.

4.2.3 REGENERATIVE FEED WATER HEATING

The cycle efficiency can also be increased by introducing regenerative feed water heating utilising bled steam from the turbine. Contact (de-aerating) and closed feed heaters can be implemented to reduce the heat input needed by the cycle. Consequently the turbine is deprived of the bled steam mass flow, thus reducing the net work of the cycle. With the implementation of a de-aerator, the feed water pumping requires two stages to prevent feed water entering the turbine in reverse flow. (ELDER & ALLEN: 2009)

The bled steam is used to heat the feed water from the extraction pump discharge (low pressure pumping stage) prior to the suction of the main feed pump (high pressure pumping stage). This reduces the amount of thermal energy required to increase the feed water temperature to the maximum heat exchanger outlet temperature. (ELDER & ALLEN: 2009)

Closed feed heaters use heat exchangers to only increase the working fluid temperature. Multiple pumping stages are then not required, since the condensed bled steam (distillate) is flashed to a lower pressure and re-introduced into either the de-aerator or the condenser. The bled steam or distillate of a closed feed heater is never in contact with the higher pressure feed water, thus not requiring additional pumping stages.

These configurations have the additional benefit of consequently reducing the energy rejected via the condenser to the heat sink (T_{\min}), resulting in a higher cycle efficiency (First law). With the correct application of regenerative feed heaters, the minimum inlet temperature of the interface heat exchanger can thus be specified.

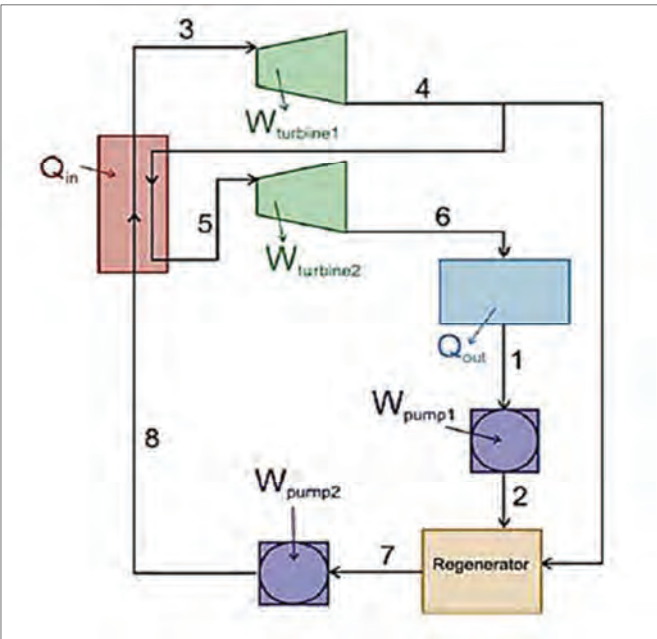


Figure 9 – Ideal Rankine with Feed Heating Diagram

(ELDER & ALLEN: 2009).

The input parameters and limitations for this configuration remain constant (Table 9), for comparison purposes.

Table 9 - Ideal Rankine cycle with contact feed heater input parameters

	Value	Unit	Description
P_{\max}	16	MPa	Maximum pressure at high pressure turbine inlet
T_{\max}	535	°C	Maximum temperature of heat exchanger tube outlet
T_{\min}	40	°C	Limited by ambient conditions
\dot{m}	1	-	Comparison done by using specific work

After the working fluid is partially expanded through the IPT (from 5 – 6), a fraction of steam is bled from the turbine and fed into the de-aerator. This is done to heat the water from the extraction pump discharge (9) to the main feed pump suction (10), thus reducing the energy necessary to heat the working fluid to the interface heat exchanger outlet (3) temperature.

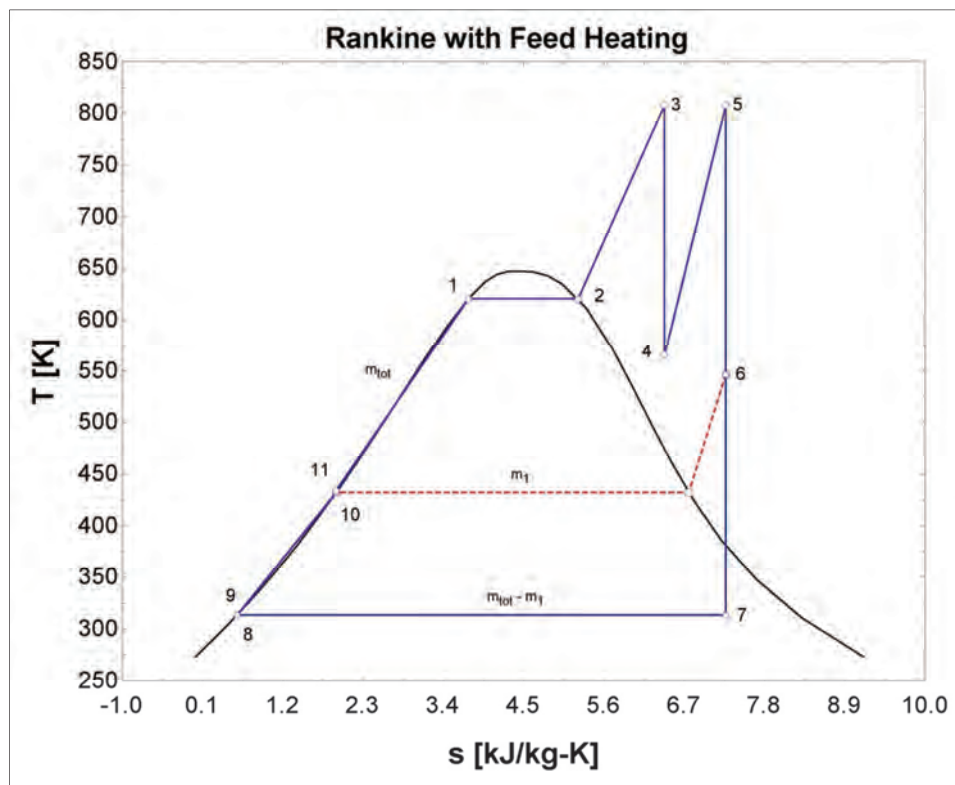


Figure 10 – Ideal Rankine with Contact Feed Heater T-s Diagram

Table 10 clearly illustrates that the efficiency has increased. This increase is attributed to the significant decrease in heat input required by the Rankine cycle (q_{in}). Although the Δh of the turbines remain unchanged, the work delivered by the turbines is reduced. The mass flow through the turbines is reduced in order to decrease the necessary heat input.

Table 10 - Ideal Rankine cycle with contact feed heater results

	Value	Unit	Description
$E_{Balance}$	0	kW	Check to determine the accuracy of model simulation
η_{Carnot}	61.24	%	Maximum available cycle efficiency (Law of Carnot)
$\eta_{Rankine}$	47.35	%	Rankine cycle efficiency
$W_{Turbine}$	1570	kW	At a mass flow rate of 1 kg/s for comparison purposes

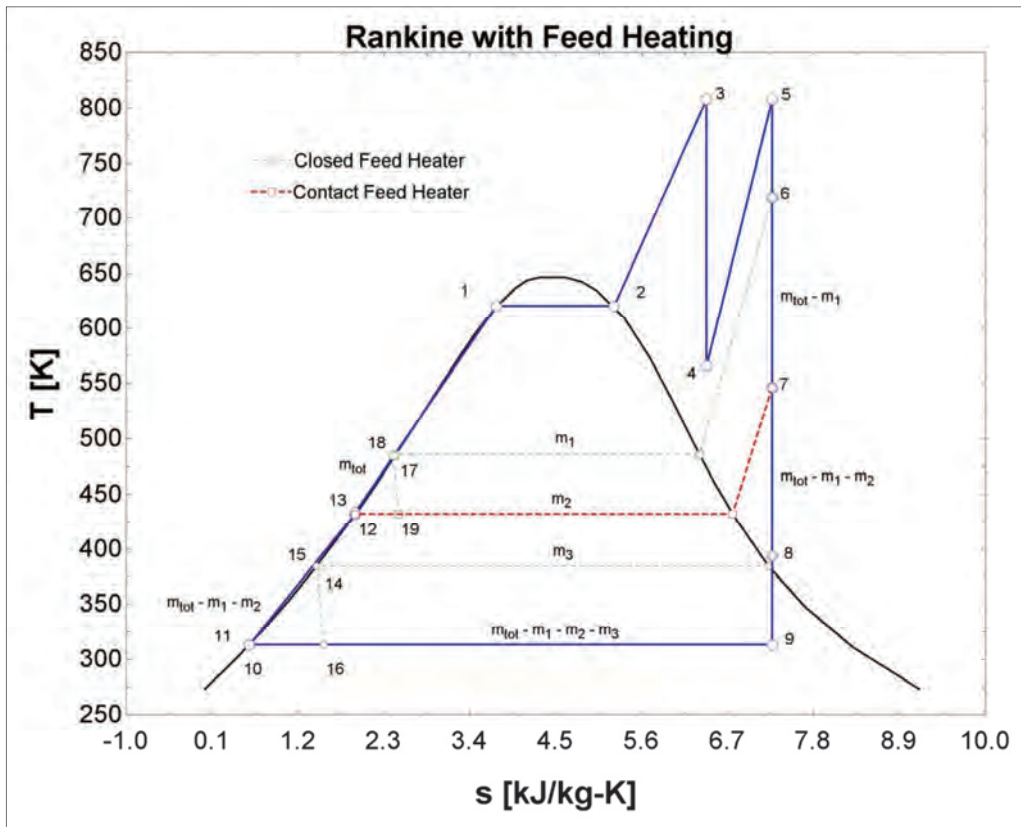


Figure 11 – Ideal Rankine with Contact and Closed Feed Heaters T-s Diagram

Figure 11 illustrates a Rankine cycle on a T-s diagram with two closed feed heaters and one contact feed heater. Point 18 on this figure indicates the minimum inlet temperature of the heat exchanger water side at approximately 475 K (200°C). This minimum temperature limit can be altered by adjusting the bleed point (6) pressure. Steam bled from the IPT at point 6 is used to heat the water from the main feed pump discharge (13) to point 18. Instead of mixing with the main line, the bled steam is flashed down and mixed in the de-aerator (19). The bled steam from point 14 is flashed down into the condenser.

Through the addition of more contact or closed feed heaters (Figure 11), the cycle efficiency can be increased even further. The efficiency of this ideal Rankine cycle is high, due to the absence of pressure drops and component efficiencies. Increasing the amount of feed heaters increases the cycle efficiency (Table 11). It is not only the amount of feed heaters that contribute to this increase but also the type and configuration thereof.

Table 11 - Ideal Rankine cycle with feed heating results

	Value	Unit	Description
E_{Balance}	0	kW	Check to determine the accuracy of model simulation
η_{Carnot}	61.24	%	Maximum available cycle efficiency (Law of Carnot)
η_{Rankine}	48.65	%	Rankine cycle efficiency
ω_{Turbine}	1701	kJ/kg	Specific work delivered by the turbines
W_{Turbine}	1505	kW	At a mass flow rate of 1 kg/s for comparison purposes

4.3 ACTUAL RANKINE CYCLE

4.3.1 ACTUAL VS IDEAL

Actual Rankine cycle design includes pressure drops through the interface heat exchanger; pressure losses through the control-valves; isentropic pump and turbine efficiencies less than 100%. There is a relation between polytropic and isentropic efficiency, where the isentropic efficiency of each stage can be calculated to the overall polytropic efficiency of the combined stages. Polytropic turbine efficiencies are thus calculated as an output for selected isentropic stage efficiencies. These losses greatly reduce the cycle efficiency and work delivered by the turbine.

The effect of introducing the various components into the Rankine cycle configuration has already been illustrated in the previous section of this chapter. Contact and closed feed heaters will therefore be incorporated in this configuration for proper comparison to the results in Table 11.

Table 12 - Actual Rankine cycle with feed heaters input parameters

	Value	Unit	Description
P_{max}	16	MPa	Maximum pressure at high pressure turbine inlet
T_{max}	535	°C	Maximum temperature of heat exchanger tube outlet
T_{min}	40	°C	Limited by ambient conditions
\dot{m}	1	-	Comparison done by using specific work

To objectively compare the ideal and actual Rankine cycle results, it is necessary to implement the same input parameters (Table 12) into the actual Rankine cycle simulation model.

Due to the pressure losses through the heat exchanger, it is necessary for the pumps to do more work to achieve the specified pressure at the HPT inlet. Polytropic efficiencies are incorporated causing an entropy gain through the various pumps. These entropy gains cannot be seen on the T-s diagram (Figure 12) due to the scale and the relatively small amount of work done by the pumps.

Similarly, there will be an entropy increase through the turbine expansion as a result of the isentropic efficiencies that are introduced. The quality of the steam is increased as a result, which is advantageous for the low pressure turbine. An entropy gain through the turbines is clearly visible on the T-s diagram.

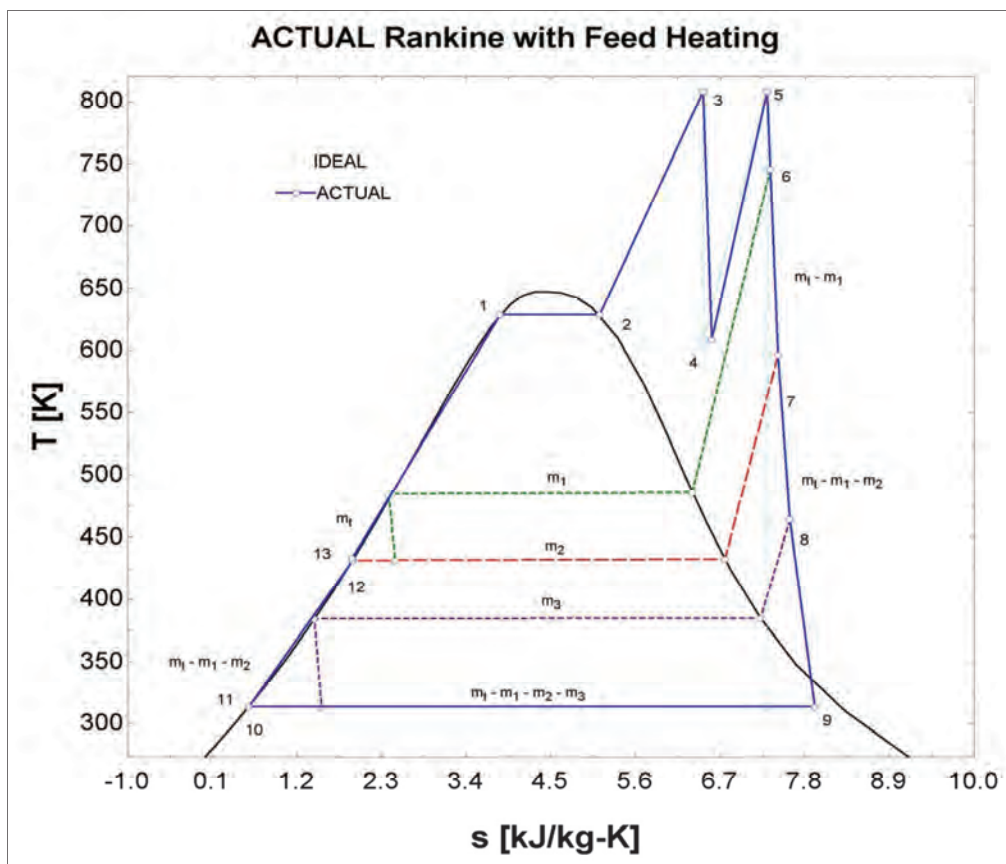


Figure 12 – Actual Rankine with Contact and Closed Feed Heaters T-s Diagram

The Carnot efficiency has remained unchanged. This isentropic efficiency ($\eta_t < 1$) of the turbine has a negative influence on the specific work and cycle efficiency.

Table 13 - Actual Rankine cycle with feed heaters results

	Value	Unit	Description
E_{Balance}	0	kJ/kg	Check to determine the accuracy of model simulation
η_{Carnot}	61.24	%	Maximum available cycle efficiency (Law of Carnot)
η_{Rankine}	42.02	%	Rankine cycle efficiency
W_{Turbine}	1277	kW	At a mass flow rate of 1 kg/s for comparison purposes

Table 14 shows similar Rankine cycle configurations for ideal and actual scenarios. Not only is the actual cycle efficiency more than 5% less than that of the ideal cycle, but the work delivered by the turbines is approximately 17% less.

Table 14 - Ideal vs. Actual Rankine with feed heaters RESULT comparison

	Unit	Ideal	Actual
E_{Balance}	kJ/kg	0	0
η_{Carnot}	%	61.24	61.24
η_{Rankine}	%	47.35	42.02
ω_{Turbine}	kJ/kg	1701	1466
W_{Turbine}	kW	1570	1305

For control purposes further additions on the practical cycle are necessary.

4.3.2 ATTEMPERATION

Steam temperature (T_{max}) control at the HPT inlet or heat exchanger outlet is of great importance. The law of Carnot states that the maximum efficiency available for a cycle is in directly related to the difference between the maximum and minimum temperatures of the cycle. The lower cycle temperature (heat sink) is established by the ambient conditions and cooling tower type.

Fluctuation in the interface heat exchanger outlet temperature (T_{\max}) cannot be tolerated, since it would have a negative effect on the turbine blade corrosion. Although an increase in the designed maximum temperature would increase the cycle efficiency, the creep temperature limit of the super heater tubes in the heat exchanger would then be exceeded. Should the designed maximum temperature decrease, the cycle efficiency would also decrease. More importantly, the steam quality at the low pressure turbine outlet would decrease as well, causing corrosion on the turbine blades.

Table 15 shows the inputs for a Rankine cycle with attemperation. Superheating the steam to 15°C above the maximum design temperature (T_{\max}), will deliberately be incorporated in the control system. High pressure feed water from the main feed pump discharge is sprayed into the steam at the heat exchanger super heater inlets, in order to sensitise the control of T_{\max} .

Table 15 - Actual Rankine cycle Attemperation input parameters

	Value	Unit	Description
P_{\max}	16	MPa	Maximum pressure at high pressure turbine inlet
T_{\max}	535	$^{\circ}\text{C}$	Maximum temperature of heat exchanger tube outlet
T_{\min}	40	$^{\circ}\text{C}$	Limited by ambient conditions
\dot{m}	1	-	Comparison done by using specific work
ΔT_{att}	15	$^{\circ}\text{C}$	Superheating for control implementing attemperation

Figure 13 shows the T-s graph of an actual Rankine cycle with attemperation. Note the arrows at the top of the graph indicating the points at the HPT inlet and the IPT inlet. The top most points are indicators of the 15°C superheating done by the heat exchanger (823.15K) while the points below represent the respective turbine inlet temperatures at 808.15K.

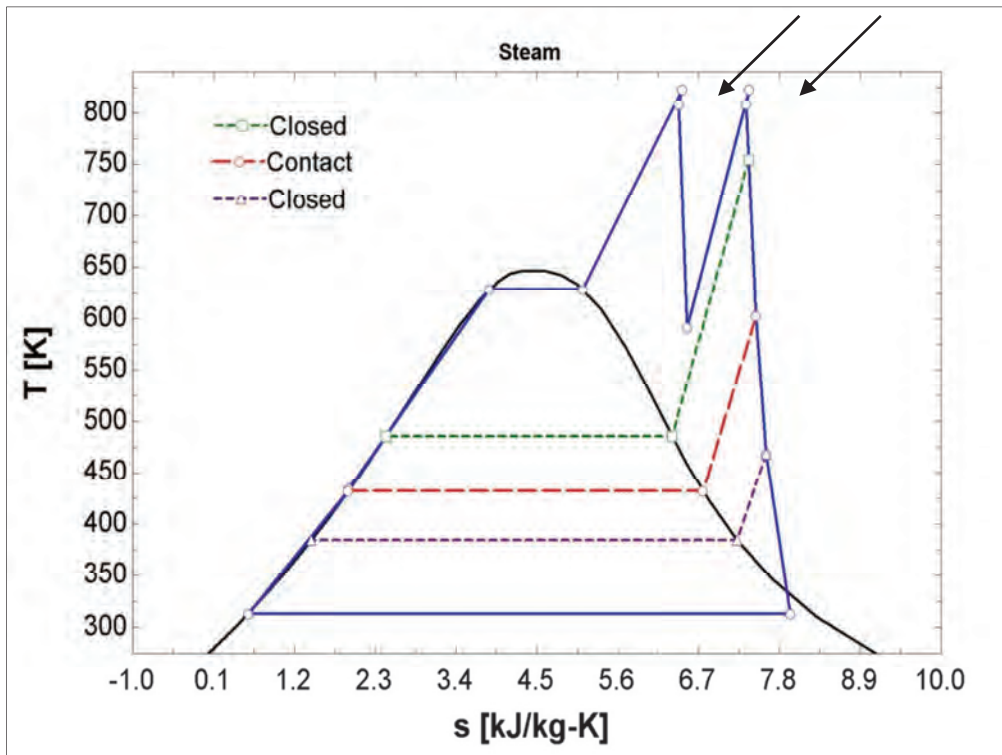


Figure 13 - Actual Rankine with Attemperation T-s Diagram

Cycle efficiency decreased with 0.1% (from 42.02% to 41.92%) when attemperation is added to the cycle design (Table 16). Work delivered by the turbines is unchanged since attemperation has no effect on the mass flow rate through the turbines. The loss in efficiency is acceptable in exchange for sensitive control of the maximum cycle temperatures. Although attemperation has no advantage on the results, it is clear that it is a necessary technique for temperature control and essential to the design.

Table 16 - Actual Rankine with Attemperation Results

	Value	Unit	Description
E_{Balance}	0	kJ/kg	Check to determine the accuracy of model simulation
η_{Carnot}	61.24	%	Maximum available cycle efficiency (Law of Carnot)
η_{Rankine}	41.92	%	Rankine cycle efficiency
ω_{Turbine}	1466	kJ/kg	Specific work delivered by the turbines
W_{Turbine}	1305	kW	At a mass flow rate of 1 kg/s for comparison purposes

4.4 LIMITATION PARAMETERS

4.4.1 HEAT INPUT INTO THE CYCLE (Q_{IN})

Some of the limitations of the Rankine steam cycle development are enforced by the thorium HTR, such as the upper and lower temperature limits of the heat exchanger at 750°C and 250°C respectively. If the heat exchanger has to operate at these temperatures, the mass flow rate of the Rankine steam cycle is determined by the mass flow rate of the helium from the reactor. Figure 14 shows a mass flow calculation for water feed flow for the fixed flow rate of helium and the ΔT at the heat exchanger water side. This sample calculation is done for ideal conditions. Heat exchanger effectiveness is not taken into account for this example.

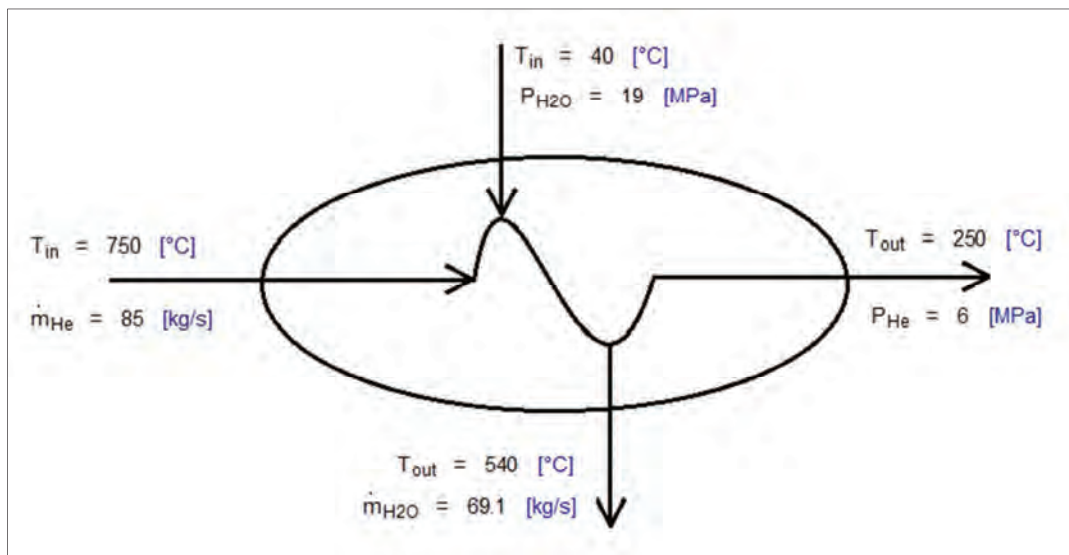


Figure 14 - Mass flow rate parameter

A mass energy balance produced a mass flow rate of 69.1 kg/s for water.

4.4.2 HPT INLET PRESSURE

Maximum cycle pressure is limited to below 22.06 MPa due to the critical point of water. Figure 15 shows a T-s diagram of water which illustrates the critical point of water at 22.06 MPa and 647.1 K.

For a cycle pressure greater than 22.06 MPa the cycle will no longer be sub-critical but supercritical. The working fluid of the cycle (water) will therefore immediately change from liquid to vapour in the heat exchanger.

Accounting for pressure losses through the heat exchanger and to still have a reasonable buffer below the critical point, the maximum pressure at the heat exchanger outlet is selected to be 19 MPa.

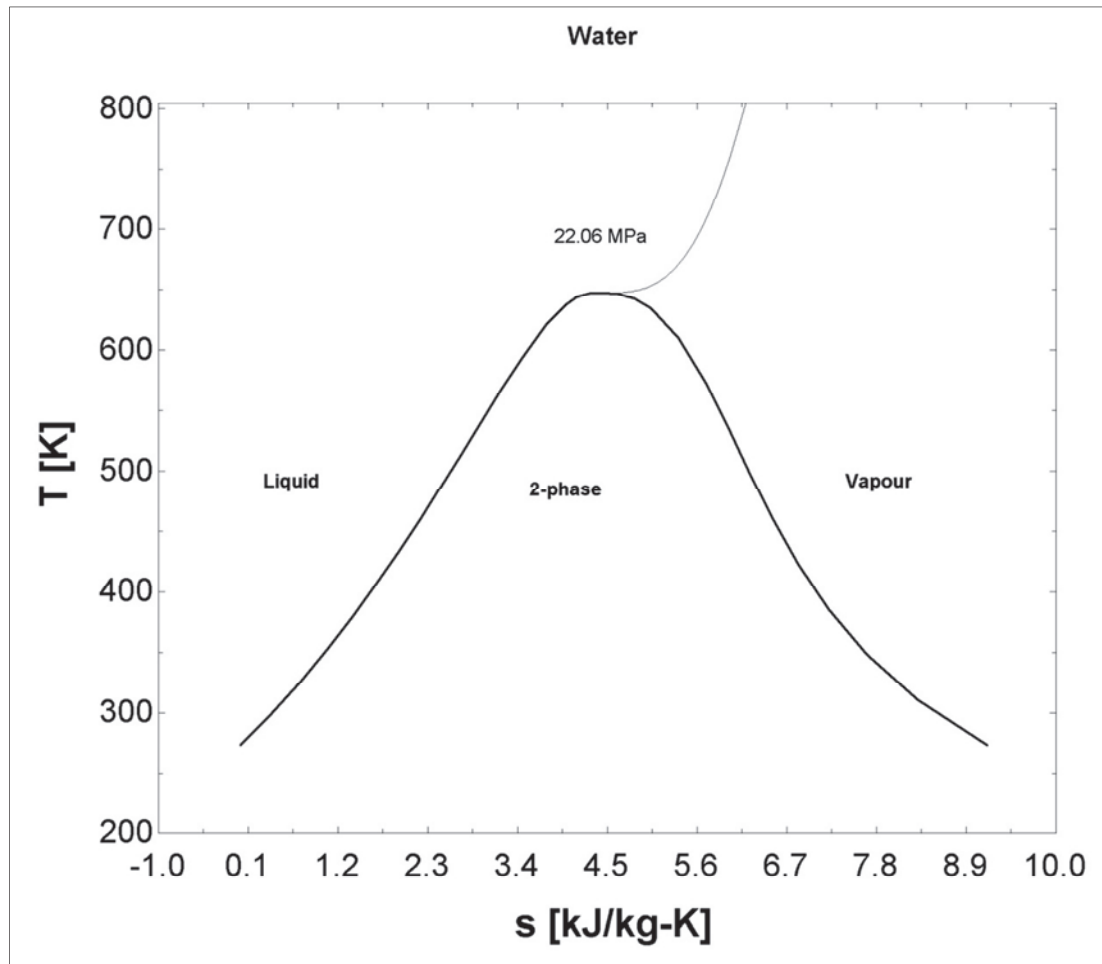


Figure 15 - Critical Point of Water

4.4.3 LP TURBINE OUTLET QUALITY (X_{CRIT})

Quality of the steam at the LPT outlet is significant for cycle efficiency and blade reliability considerations. Steam quality higher than one, would cause more thermal energy to be rejected through the condenser. Less energy would therefore be utilised through the expansion process of the turbines, resulting in a reduction in cycle efficiency and work delivered by the turbines.

A steam quality of less than 88% at the LPT outlet is taken as the lower limit for dryness fraction from present existing steam turbines. A dryness fraction less than 88% is considered unacceptable for turbine blade reliability, although it would emanate in higher cycle efficiency. All other parameters kept constant, a higher dryness fraction will be proportional to a lower cycle pressure and vice versa.

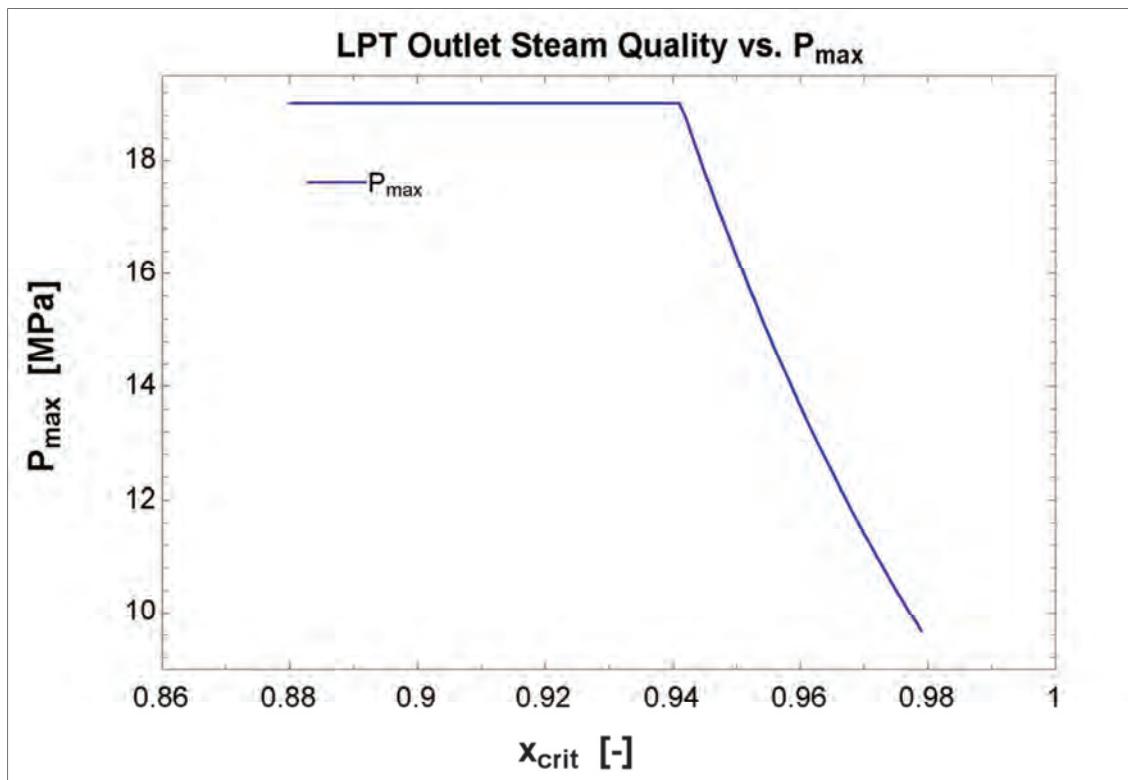


Figure 16 - LPT outlet steam quality vs. HPT inlet P_{max}

Figure 16 illustrates the maximum pressure of 19 MPa as previously explained and the minimum dryness fraction of 88%. Figure 16 also indicates that for this design the minimum dryness fraction is 94%, due to the maximum pressure being limited at 19 MPa.

Figure 17 illustrates the change in heat rejected through the condenser (Q_{out}) with increasing dryness fraction of the LPT steam outlet. The Rankine cycle efficiency is overlaid on this graph. Figure 17 is constructed for a Rankine cycle with reheat, feed heaters and

attenuation (Figure 13). From this graph it is clear that the efficiency is decreased as the heat rejected through the condenser is increased.

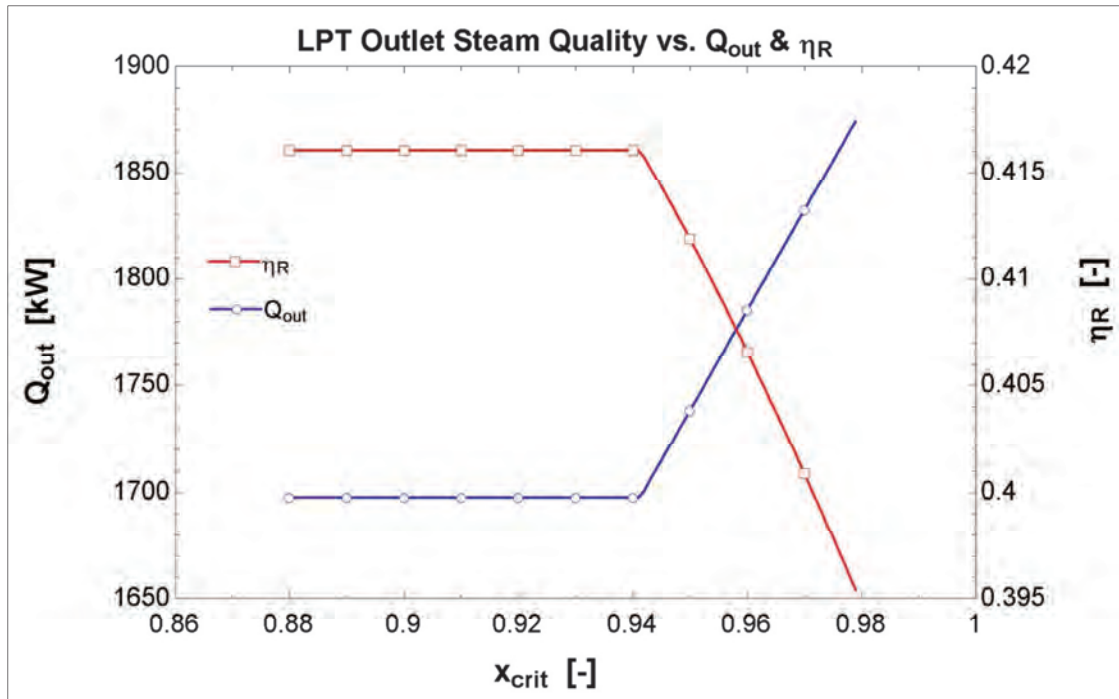


Figure 17 - LPT outlet steam quality vs. Q_{out} and η_R

The highest possible efficiency coincides with the lowest achievable LPT dryness fraction (94%), which is determined by the maximum cycle pressure (19 MPa).

4.4.4 MINIMUM CYCLE TEMPERATURE (T_{MIN})

Upon inspection of the law of Carnot, displayed in equation (1), the cycle efficiency is proportional to the temperature difference between the maximum and minimum cycle temperatures. The minimum cycle temperature influences the cycle efficiency, even more than the maximum cycle temperature. For mathematical proof that the influence of the minimum temperature is greater than that of the maximum temperature, refer to Appendix 12.5.

The minimum cycle temperature is dependent upon the ambient conditions of the construction location as well as various temperature losses through the condenser and cooling towers.

In order to pump the working fluid to a higher pressure, it is necessary for the working fluid to at least be a saturated liquid preferably sub-cooled. It is therefore necessary to extract the latent energy from the working fluid after it exits the LPT. Since the Rankine working fluid is expensive demineralised water, this latent energy is extracted through a condenser.

The condenser is essentially a closed heat exchanger (cooler); the latent energy is absorbed in the non-Rankine fluid (cooling water) flowing through the condenser. To cool the non-Rankine fluid (cooling water), a cooling tower is implemented.

4.4.5 WET COOLING TOWER

Normal water is used to cool the Rankine working fluid through the condenser. Wet cooling towers utilise a contact heat exchanger (ambient air in direct contact with water droplets) to cool the non-Rankine fluid (cooling water) returning from the condenser.

4.4.6 DRY COOLING TOWER

Dry cooling towers, spray condensers and the direct air cooling method all utilise closed heat exchangers in the cooling tower. Due to the closed heat exchanger being implemented, demineralised water can be used through the condenser and the cooling tower, since there is no loss by means of evaporation. This is done to minimise corrosion and build-up in the pipes.

4.5 OPTIMISATION CRITERIA

This dissertation's main focus is designing and optimising a PCU for a thorium HTR. The reactor supplies 100 MW_t to the PCU and the cement plant requires 26 MW_e from the PCU.

The two criteria considered as priority in this Rankine cycle design is net work and cycle efficiency. To comply with the electrical energy demand, 26 MW_e must be delivered by the cycle after conversion efficiency losses are taken into account.

It is not ideal to change the load of the reactor and it is even more impractical to change the parameters of the Rankine cycle. Due to the opportunity to generate additional revenue by supplying auxiliary energy to the Indian distribution network, the reactor can constantly operate at its maximum continuous rating. For constant heat input into the Rankine cycle,

the higher the efficiency the greater the electric energy output and revenue. Since the production of nuclear energy is low cost energy (high capital cost), it would be profitable to generate revenue by supplying energy to the Indian network.

For the purpose of generating low cost energy, the main optimisation criterion is cycle efficiency, provided that the maximum efficiency is such that the required electrical output from the PCU is achieved. Cycle efficiency is the relation between the net work delivered by the cycle (W_{net}) and the heat input into the Rankine cycle (Q_{in}).

$$\eta_R = \frac{W_{net}}{Q_{in}} \quad (2)$$

With the reactor operating at maximum continuous rating, the energy supplied to the PCU by the HTR will remain constant. Maximum cycle efficiency will be in directly proportional to the maximum net work delivered by the cycle.

4.6 KEY ASPECTS

- The Ideal Rankine cycle produces the most work at the highest efficiency. However, the Ideal cycle is impractical.
- Actual cycle considerations significantly decrease net work and cycle efficiency.
- Additions to the complexity of the cycle such as reheat; various feed heaters and attemperation, respectively increase work output; cycle efficiency, control and cost.
- Limitations such as minimum cycle temperature; maximum cycle pressure and LPT outlet steam quality need to be incorporated in the Rankine cycle design.
- Wet and dry cooling towers will be compared by simulation for the removal of energy to the heat sink.
- Cycle efficiency and therefore net work is to be maximised by means of optimising parameters such as cycle pressure, dryness fraction and regenerative feed heating combinations.

5 CHAPTER 5: DESIGN CONSIDERATIONS

5.1 INTRODUCTION

Rankine cycle is the most commonly used PCU. All coal fired power stations in South Africa make use of the Rankine cycle to convert thermal energy to kinetic energy. It is also used as a PCU for nuclear and gas applications.

It is important that the maximum cycle temperature of the Rankine cycle remain constant. Attenuation is implemented at coal power stations for the purpose of controlling the maximum cycle temperature. As the Law of Carnot states, the maximum cycle efficiency is proportional to the cycle temperature difference.

Since a small nuclear reactor (thorium; 100 MW_t) is the proposed solution for HOLCIM cement in India, a Rankine cycle will be best suited as PCU. The thorium reactor delivers 100 MW_t to the PCU using helium as working fluid. According to Geschwindt *et al.* (2011), although the reactor delivers helium at 700°C and more, steam produced by the steam generator is at 566 °C and 16.7 MPa.

According to Lior (1997), the increase in efficiency by raising the maximum temperature is not constrained by the ability of the energy source. It is however constrained by the ability of engineering materials and devices to withstand higher temperatures. The past century has delivered much progress to increase the top temperature of working fluids. Better materials and devices such as turbine blade cooling, have been implemented. (LIOR: 1997)

5.2 INTEGRATION

Cement production is a refined process, as it recycles most of the waste heat. After the clinkers are produced, it is necessary to be cooled at a certain rate using ambient air. Air leaving the cooler is fed into the kiln as preheated air for the burning of fossil fuel.

Flue gas from the kiln is fed to the pre-heater where it is used to preheat the raw material before it enters the kiln. Waste heat is also implemented in the drying of raw material.

The Rankine cycle will therefore be powered, only by the thorium reactor and only electric energy will be supplied to the cement production plant.

5.3 THORIUM REACTOR: 100 MW_t

Since revenue can be generated by supplying the Indian network with electricity, the reactor will continually be operating at maximum continuous rating. If the cement plant requires less energy than produced by the reactor and PCU combination, any excess energy can be sold to the Indian distribution network.

To avoid thermal shocks inside the reactor core, a minimum helium inlet temperature of 250°C is required. Acting as coolant (working fluid) through the reactor core, the helium is heated from 250°C to 750°C.

Mass flow rate of the helium is such that 100 MW_t is available to the PCU. The helium flows through the heat exchanger transferring heat to the working fluid (water) of the Rankine cycle. Through the heat exchanger the helium is cooled from 750°C to 250°C.

5.4 REACTOR MINIMUM TEMPERATURE

The temperature of the helium exiting the heat exchanger and entering the reactor core cannot be below 250 °C as to avoid thermal shocks.

If the water entering the heat exchanger (helium↔water) is at 50 °C, the maximum cycle temperature will be far less than the high temperature of the helium from the reactor. Regenerative feed heating allows the Rankine working fluid to enter the heat exchanger at a higher temperature.

This enables the helium to be cooled to 250°C and the maximum temperature of the Rankine working fluid to be increased.

5.5 MAXIMUM CYCLE TEMPERATURE

From the Carnot efficiency equation it is apparent that the maximum and minimum cycle temperatures have a significant influence on the Carnot efficiency.

$$\eta_C = 1 - \frac{T_C}{T_H} \quad (3)$$

Carnot efficiency represents the greatest cycle efficiency possible. It is however not achievable and is a theoretical maximum. The equation does show that an increase in maximum cycle temperature will increase the Carnot efficiency.

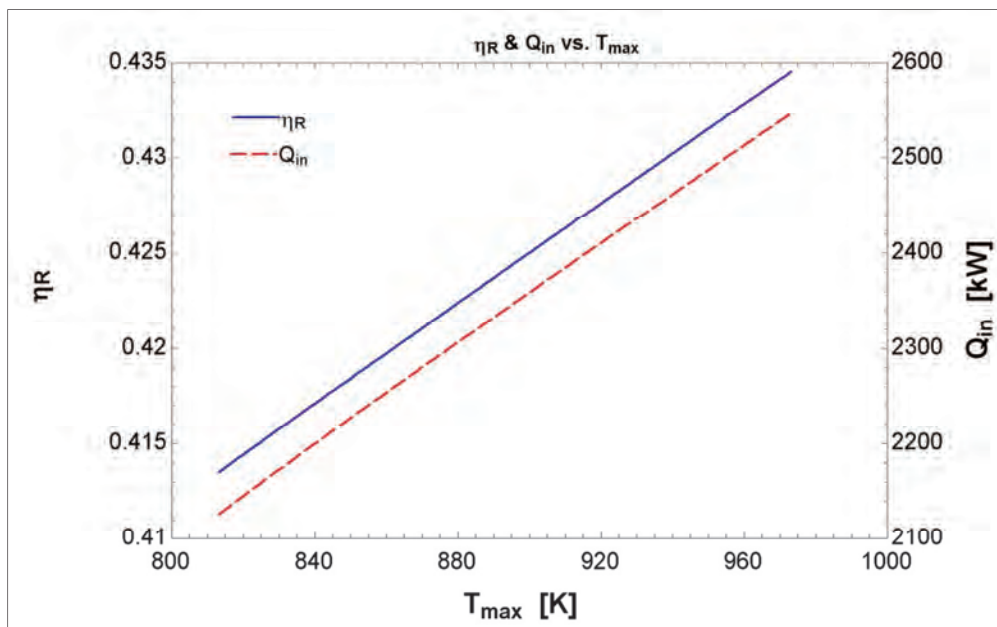


Figure 18 - Cycle efficiency vs. Maximum cycle temperature: η_R vs. T_{max}

Figure 18 shows Rankine cycle efficiency as maximum cycle temperature is increased from the 540 °C (813.15 K) to 700 °C. The heat input in to the cycle is overlaid on Figure 18 and the cycle mass flow is 1 kg/s. The Rankine cycle efficiency is increased as the maximum temperature is increased.

This increase in maximum cycle temperature increases the cycle efficiency by more than 2% even though the heat input into the cycle is also increased.

An increase in maximum cycle temperature is advantageous for cycle efficiency. The reactor produces 100 MW_t continually. With the Rankine cycle correctly designed and optimised, Q_{in} will remain constant while feed heating is used to consequently raise the maximum cycle temperature.

5.5.1 COAL FIRED POWER STATIONS

In the case of coal power stations, the maximum cycle temperature does not exceed 540°C . This temperature limit is set due to the creep temperature of the super heater tubes. The flue gas produced by a coal burner is at $1000 - 1500^\circ\text{C}$ depending on the calorific value of the coal, the air supply rate, etc.

Although the coal flame is at such a high temperature, the maximum temperature of the Rankine cycle is limited to 540°C . The flame is not in direct contact with the working fluid or the super heater tubes. Multiple temperature losses occur during the energy transfer to the working fluid.

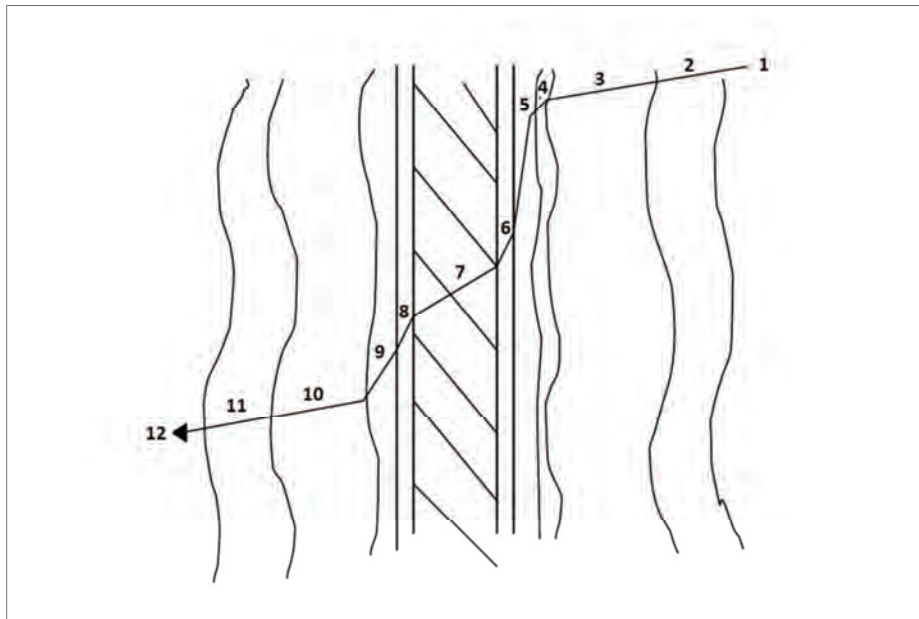


Figure 19 - Energy losses from coal flame to work working fluid

(STORM: 2013)

As the energy is transferred from the flue gas to the Rankine working fluid (water or steam), various mediums need to be passed. These mediums have different heat transfer

coefficients. As illustrated in Figure 19, the energy from the flue gas, produced by burning coal, is transferred through various mediums.

Table 17 illustrates the important temperatures at their respective mediums as the energy is transferred from the flue gas to the Rankine working fluid (water or steam). These temperatures shown represent a point near the super heater outlet.

Table 17 - Energy losses from coal burner to work working fluid

	Description	Temperature [°C]
1	Flue gas	700 - 900
2		
3		
4	Flue gas boundary layer	-
5	Clinker or bearding	-
6	Fe ₂ O ₃	-
7	Super heater tube wall	584 – 610
8	Fe ₃ O ₄	-
9	Steam boundary layer	-
10	Steam	535
11		
12		

(Storm *et al*: 2013)

The super heater outlet is chosen since the Rankine cycle upper temperature limit for a coal fired power plant is specified according to the creep limit of the super heater tube material.

With the flue gas at the outlet of the super heater tubes at 700 – 900 °C, the super heater tube wall is at 584 - 610°C. Due to the vast length of tube required in a coal fired heater and the economic considerations thereof, less expensive material is used for these tubes.

With the losses of energy transfer and the creep limit of the super heater tubes, the steam at the outlet has a maximum temperature of approximately 540 °C.

5.5.2 THORIUM REACTOR

Energy is transferred from the thorium reactor to the PCU. Since no direct flame is required, a heat exchanger can be used to transfer the energy from the helium to the Rankine working fluid. The energy through the heat exchanger does not need to overcome various mediums as the helium is in direct contact with the tubes containing the water.

Mediums that need to be included in the heat exchanger calculation, such as a steam layer, are accommodated for in the heat exchanger effectiveness.

The maximum cycle temperature is not limited (540 °C) by the creep temperature of the super heater tubes. In this case, the maximum Rankine cycle temperature is a function of the maximum temperature of the helium delivered by the thorium reactor and the effectiveness of the heat exchanger.

Sugisita *et al.* (1998) conducted a study to evaluate three closed hydrogen combustion turbine cycles. These three cycles were compared according to their thermal efficiencies. Although the Rankine cycle was determined to be the least favourable, the maximum temperature and pressure at the high pressure turbine inlet was set to 850 °C and 19.4 MPa. This shows that the turbine can handle these extreme conditions.

5.6 AMBIENT CONDITIONS IN INDIA

As discussed in section 4.4.4, the minimum cycle temperature significantly influences the cycle efficiency. This temperature is dependent on various fixed design parameters such as the ambient conditions of the construction location.

Specific ambient conditions cannot be obtained for this project as there are various possible locations for the construction of this IPP in India.

Table 18 shows the monthly and annual average temperature conditions for more than 160 cities across India, over a timespan of more than 55 years. As the reactor operate throughout the year, the annual average temperature (24.4 °C) will be used as design estimation.

Table 18 – Indian average ambient temperature

	Average Temperature [°C]	Average High Temperature [°C]	Average Low Temperature [°C]
January	18.1	24.3	11.6
February	20.1	26.4	13.4
March	23.9	30.4	17.2
April	27.4	33.7	21.0
May	29.3	35.1	23.6
June	28.8	33.5	24.3
July	27.2	30.8	23.7
August	26.7	30.2	23.4
September	26.5	30.6	22.5
October	25.1	30.3	19.8
November	21.7	27.7	15.5
December	18.8	25.0	12.3
Annual	24.4	29.8	19.1
Years	63	57	57
# Cities	191	166	166

(Adapted from www.weatherbase.com)

5.7 CYCLE EFFICIENCY

Since the liquid side of the Rankine cycle needs to be heated to a higher temperature before entering the heat exchanger, feed heaters need to be implemented. Although feed heaters reduce the net work delivered by the cycle, it increases the overall cycle efficiency. Cycle efficiency is increased due to the reduction in the required heat input into the cycle.

The equation for calculating the Rankine cycle efficiency follows:

$$\eta_R = \frac{W_{net}}{Q_{in}} \quad (4)$$

Cycle efficiency (η_R) is directly correlated to net work (W_{net}) as long as the heat input into the cycle remains constant.

As the reactor will continually be operating at its maximum continuous rating, the heat input into the cycle will remain constant at 100 MW_t . If no energy is to be wasted, the 100 MW_t needs to be transferred to the PCU.

It is critical to heat the Rankine feed water to the heat exchanger inlet temperature as determined by the heat exchanger effectiveness and helium temperatures. Optimising the cycle to maximise cycle efficiency will automatically maximise net work delivered by the cycle and vice versa.

5.8 STEAM TURBINE DRIVEN FEED PUMPS

Steam turbine driven feed pumps have the advantage of increasing the overall PCU efficiency. Driving feed pumps with steam turbines instead of with electricity, eliminates generator; transformer and other losses for the feed pumps.

Low pressure steam is bled from the turbines and expanded through the turbine driving a feed pump, usually a single shaft setup. The construction and gains for this application is not economically viable due to the small nature of the thorium reactor and the low mass flow of the Rankine cycle.

5.9 DE-AERATOR

The main function of the de-aerator is to increase the temperature of the Rankine feed water. During the expansion of the high temperature steam through the turbines, gasses are formed. The secondary function of the de-aerator is to remove any gas build-up from the steam.

Due to the de-aerator being a contact feed heater, it is necessary for it to be followed by a feed pump on the liquid side of the Rankine cycle. The amount of de-aerators present in a Rankine cycle determines the amount of feed pumps required in the Rankine cycle configuration.

It is important to weigh the implementation of the amount of de-aerators against the techno-economic considerations thereof. The implementation of more than one de-aerator is not techno-economic.

5.10 REHEAT

The influence of incorporating reheat into the design is evaluated in Table 4. Reheat causes the cycle efficiency to increase by approximately 1.5%. This is a significant increase and will produce an increased net work of approximately 1.5 MW for this application.

Construction of reheat is large and expensive. The inclusion of reheat into this Rankine cycle design is not feasible.

5.11 KEY ASPECTS

- Helium is delivered from the thorium reactor at 750 °C and has to transfer energy to the PCU. Helium re-enters the reactor at a temperature of 250 °C.
 - Feed heaters will heat the Rankine working fluid to a higher temperature.
 - Due to the use of a heat exchanger, the maximum cycle temperature is not limited to the usual 540 °C.
 - Maximum cycle temperature is only limited by the temperature of the helium from the reactor.
 - Rankine mass flow is a function of heat exchanger effectiveness and the helium mass flow.
 - Cycle efficiency will be maximised. At maximum cycle efficiency, net work will also be at a maximum.
-

6 CHAPTER 6: HEAT EXCHANGER

6.1 INTRODUCTION

Rankine steam cycles are powered by thermal power plants with the maximum temperature, at the heat exchanger outlet, to be 540°C. In coal fired power plants this maximum temperature is dependant on the metallurgical temperature limit of the super heater tubes. When these tubes are heated to their metallurgical limit, the maximum steam temperature is 540°C due to losses through the various clinker- and steam layers.

Since this study does not use a burner to heat tubes containing the working fluid, the maximum steam temperature is not limited to 540°C. The maximum heat exchanger outlet temperature is limited by the combination of the HTR outlet working fluid temperature and the effectiveness of the heat exchanger (steam generator). Heat exchangers require piping systems consisting of corrosion resistant material since the working fluid is steam.

As mentioned in Chapter 1, material selection and design is not the focus of this study. Proof of concept is required since the maximum temperature limit of this Rankine steam cycle design does not fall within usual limitations.

6.2 WATER INLET TEMPERATURE

It is critical that the helium re-enters the reactor at a temperature of 250 °C or higher to avoid thermal shocks inside the reactor core. If the helium is to be cooled from 750 °C to 250 °C, the effectiveness of the heat exchanger (ε) must be used to determine the heat exchanger water inlet temperature.

$$\varepsilon = \frac{q}{q_{max}} \quad (5)$$

$$\therefore \varepsilon = \frac{h_{He,in} - h_{He,out}}{h_{He,in} - h_{H2O,in}} \quad (6)$$

(Incropera *et al.*, 687-688: 2007)

If the counter-flow heat exchanger is ideal the helium would transfer energy to the water until the working fluid temperatures coincide. It is unrealistic to have a heat exchanger with 100% effectiveness. The effectiveness of the heat exchanger will therefore be set to 80%, 85%, 87.5% and 90% respectively while the simulation model is optimised for each.

As the inlet and outlet temperatures of the heat exchanger is specified for the helium, the water side inlet temperature is dependent on the heat exchanger effectiveness. It is therefore necessary to implement feed heaters to increase the Rankine working fluid (water) temperature.

6.3 MAXIMUM CYCLE TEMPERATURE

To transfer the heat energy from the helium to the working fluid of the Rankine cycle (water or steam), a heat exchanger is required. With heat exchanger effectiveness included into the Rankine cycle design, the maximum cycle temperature cannot be specified.

As equation (6) for the helium side is derived from equation (5), the following equation can be derived for the water side of the heat exchanger.

$$\varepsilon = \frac{h_{H_2O,out} - h_{H_2O,in}}{h_{He,in} - h_{H_2O,in}} \quad (7)$$

(Incropera *et al.*, 687-688: 2007)

If the heat exchanger effectiveness is 100%, the water energy would be increased to the heat exchanger inlet energy of the helium. It is impractical to have a heat exchanger with 100% effectiveness. The effectiveness of the heat exchanger will be set to 80%, 85%, 87.5% and 90% respectively while the simulation model is optimised.

6.4 RANKINE CYCLE MASS FLOW

The mass flow rate of the Rankine working fluid is dependent on the energy transferred from the helium. As the thorium reactor produces 100 MW_t, using the helium as coolant, the Rankine working fluid (water or steam) needs to absorb 100 MW of energy.

Upon inspection of Table 19, T_{out,HX} and T_{in,HX} values for steam (red) is calculated with a heat exchanger effectiveness of 85% and pressures of 19 and 24.39 MPa respectively. These calculations are done using equations (6) and (7) as discussed previously in this Chapter.

Table 19 - Heat exchanger, 85% effectiveness

	Unit	Helium	Water/Steam	Description
Q_{transferred}	MW	100	100	Energy transferred through heat exchanger
P_{in}	MPa	4	24.39	Pressure into Heat exchanger
P_{out}	MPa	4	19	Pressure out of Heat exchanger
T_{in,HX}	°C	750	161.9	Temperature into Heat exchanger
T_{out,HX}	°C	250	661.7	Temperature out of Heat exchanger
<i>m</i>	kg/s	38.54	?	mass flow rate through Heat exchanger

The amount of thermal energy supplied by the reactor is continually 100 MW_t. The mass flow of the water is dependent on its enthalpy difference between the heat exchanger inlet and outlet. To ensure that the helium is cooled to 250 °C, the temperature of the water side heat exchanger inlet is calculated using the heat exchanger effectiveness, as discussed in section 6.2.

The mass flow of the Rankine cycle is determined using an energy balance calculation (Figure 20). Temperatures and pressures are specified for all inlets and outlets of the heat exchanger calculation. Helium mass flow is calculated from the 100 MW_t specification of the thorium reactor.

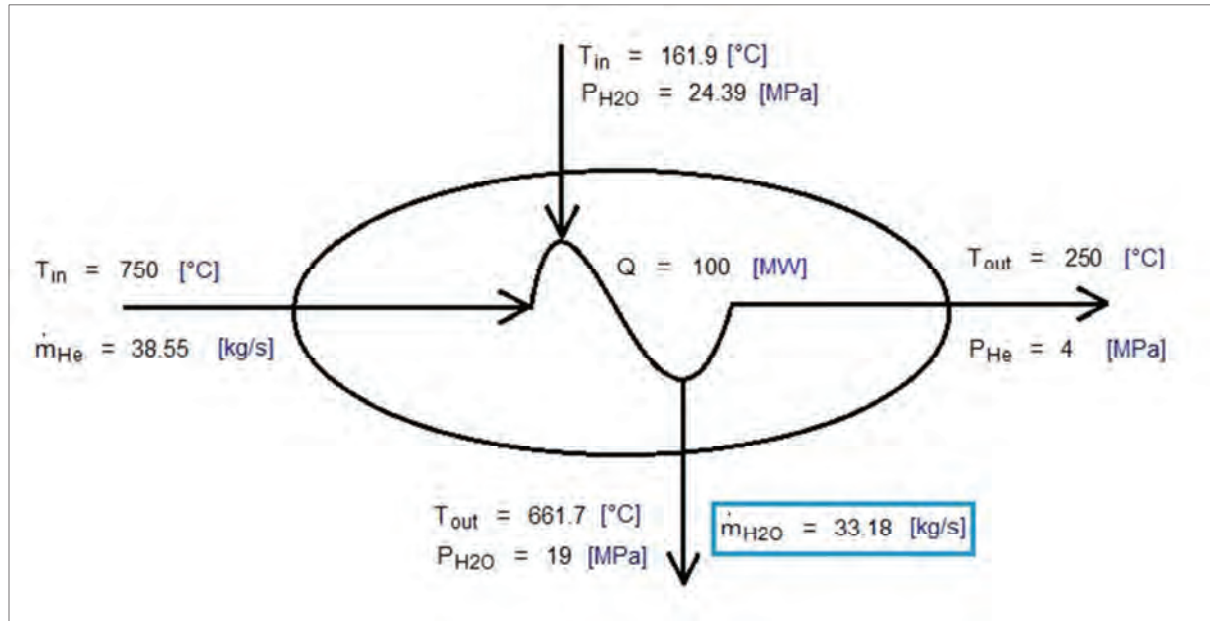


Figure 20 - Heat exchanger effectiveness, mass flow calculation

Enthalpies for each point can be determined from the specified temperature and pressure. Maximum temperature of the Rankine cycle is calculated as 661.7 °C, while the heat exchanger water inlet temperature is 161.9 °C, both at a $HX_{eff}(\varepsilon) = 85\%$.

Balancing the energy for the heat exchanger, all the energy transferred from the helium must be absorbed by the water or steam.

$$Q_{in} = Q_{out} \quad (8)$$

$$[\dot{m} \times (h_{in} - h_{out})]_{He} = [\dot{m} \times (h_{out} - h_{in})]_{Water} \quad (9)$$

Since $[\dot{m} \times (h_{in} - h_{out})]_{He} = 100 \text{ MW}_t$ the energy balance equation can be simplified and rearranged to determine the mass flow necessary to extract all the energy available.

$$\dot{m}_{Water} = \frac{100 \text{ MW}_t}{[h_{out} - h_{in}]_{Water}} \quad (10)$$

Thus calculating a mass flow rate of $\dot{m}_{H_2O} = 33.18 \text{ kg/s}$ for the Rankine cycle with a heat exchanger effectiveness of 85%.

6.5 PINCH POINT

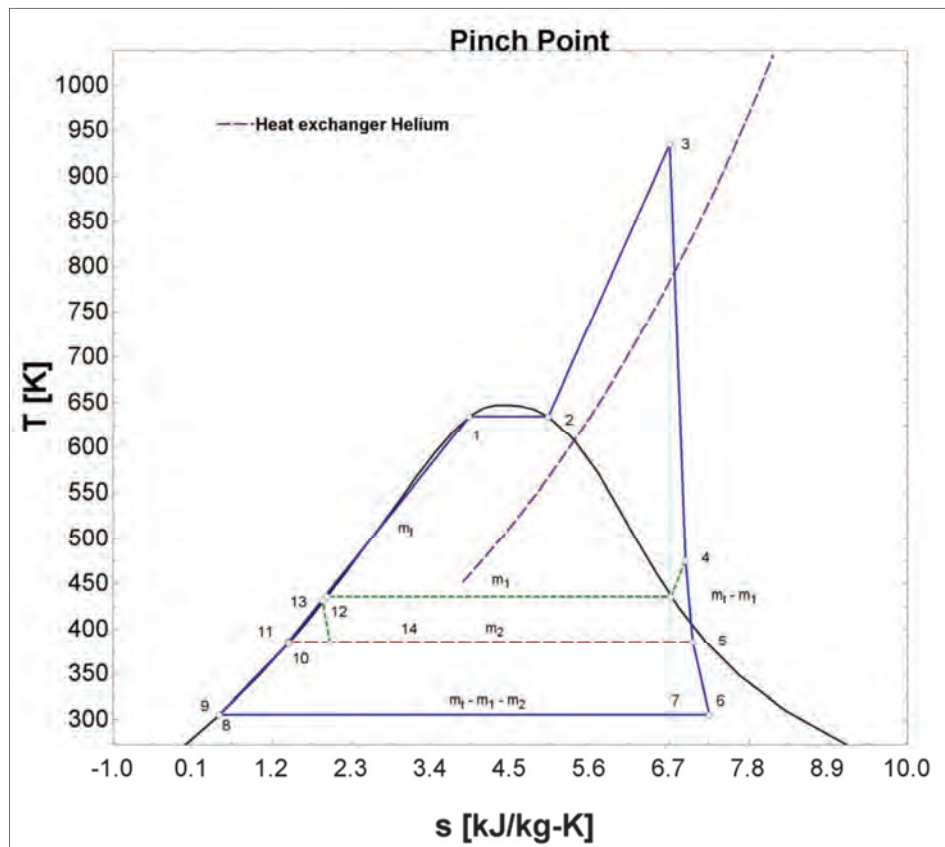


Figure 21 - Pinch Point T-s diagram

The Rankine working fluid undergoes a phase change when it is heated to maximum cycle temperature. It is necessary to identify the pinch point of water (Figure 21). Heat transfer requires that the working fluid delivering the heat, always be at a higher temperature than the cold working fluid throughout the heat exchanger.

Figure 21 shows the T-s diagram for a Rankine cycle with a maximum temperature of 700°C. One de-aerator and one closed feed heater are included into the design. To determine if the

ΔT at the pinch point is positive, the Helium side of the heat exchanger is also plotted in the diagram window.

Entropy can by definition not be measured. The concept to investigate is the change in entropy as the helium is cooled through the heat exchanger. The reference point of entropy for the helium can be adjusted accordingly.

To adjust the reference point of the entropy, 1.925 kJ/kg-K is subtracted from the entropy of helium throughout. This subtraction will have no effect on the validity of the helium entropy values as it transfers heat through the heat exchanger. Change in entropy through the heat exchanger is critical for the purpose of investigating the pinch point.

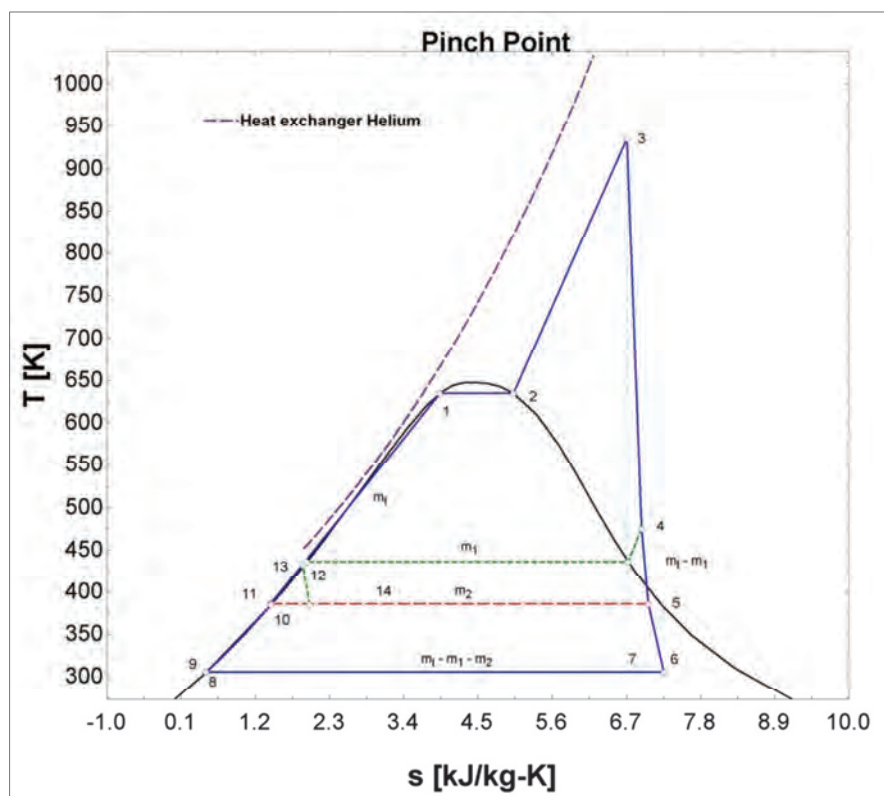


Figure 22 - Pinch Point T-s diagram, adjusted s_{ref}

Whether the factor (1.925 kJ/kg-K) is subtracted or not, the entropy change through the heat exchanger from the inlet to the outlet is $\Delta s = 4.293$ kJ/kg-K.

Adjusting the entropy reference point of helium enables the comparison of the two working fluids through the heat exchanger. It is clear from Figure 22 that the pinch point (where the graphs are closest) is between the water side inlet of the heat exchanger (point 12) and the boiling point of water (1). As the temperature of the water is increased from there, through the heat exchanger, the temperature difference between helium and water is also increased.

Figure 23 shows the helium side of the heat exchanger as it is required by the reactor. The heat exchanger outlet of the helium has a far greater temperature than that of the water side inlet. Due to this ΔT between the helium outlet and the water inlet, the heat exchanger parameters are not limited by the pinch point.

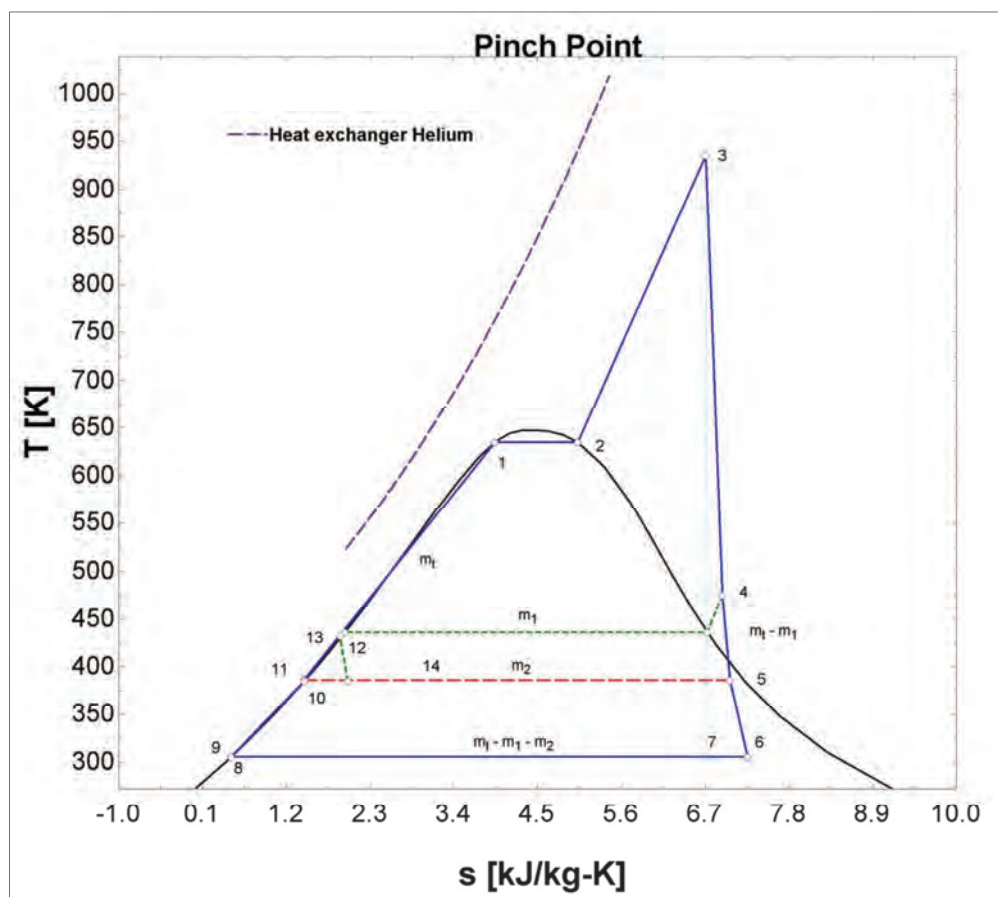


Figure 23 - Pinch Point T-s diagram, adjusted s_{ref} ; Helium minimum Temperature

6.6 MATERIAL SELECTION

6.6.1 STAINLESS STEEL

According to the Rankine steam cycle design parameters, the piping system in the heat exchanger must consist of a material that has the appropriate tensile strength at 700°C. Since the critical point of water is at a pressure of 22.06 MPa, exceeding this pressure will cause the Rankine steam cycle to be super-critical. It is therefore logical that the maximum cycle pressure must be less than 22.06 MPa at 700°C .

Figure 24 illustrates a general comparison of the hot strength characteristics between various stainless steels, low-carbon steel and semi-austenitic precipitation and transformation hardening steels.

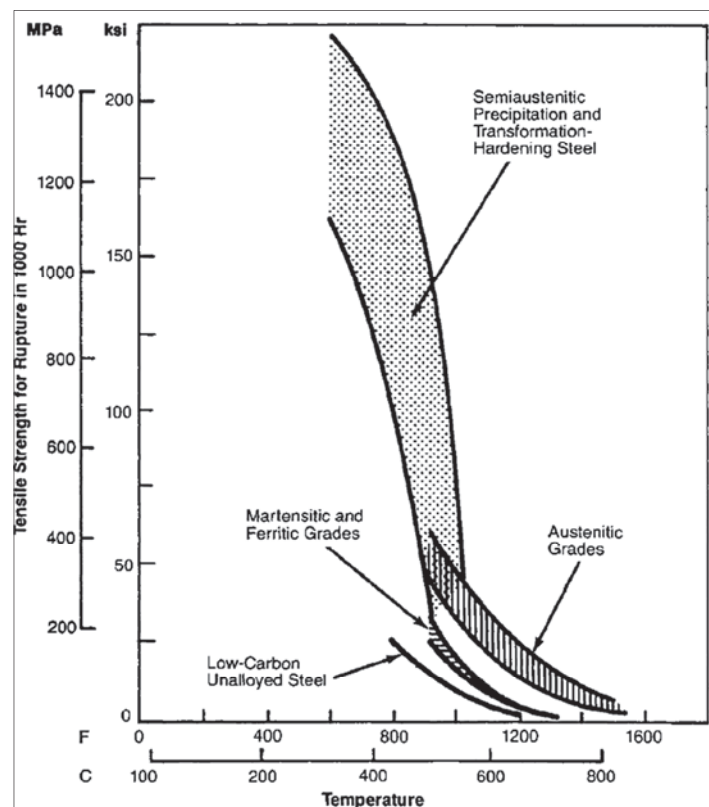


Figure 24 – Hot strength characteristics of stainless steels

(American Iron and Steel institute)

Figure 24 indicates that the stainless steels have an adequate tensile strength at 700°C. Austenitic grade stainless steel is also an option for this heat exchanger, but will be more expensive than the ferritic grade stainless steel.

ASTM U-436 is identified as a possible material for the super heater tubes of the heat exchanger at the specified parameters.

ASTM U-436 is a moly ferritic stainless steel, with an annealing temperature of 750 to 850°C. Moly ferritic stainless steels have relatively poor tensile, fatigue and toughness properties in welded areas as they are prone to grain growth in the heat affected zone of weldments. Cold or hot working is recommended for production. (SASSDA: 2013).

Maximum recommended service temperature		
Unity	Continuous (°C)	Intermittent (°C)
U-434	730	870
U-436	730	870
U-444	850	950

Figure 25 – ASTM U-436; Maximum recommended service temperature

(SASSDA, 2013)

Figure 25 shows the maximum recommended continuous service temperature for various stainless steel grades. It shows that ASTM U-436 has a maximum recommended continuous service temperature that is greater than the maximum possible Rankine cycle temperature. The maximum possible Rankine cycle temperature is less than 700°C for a heat exchanger with an effectiveness of 90%.

The physical properties of ASTM U-436 are illustrated in Figure 26.

Physical properties			
The values given below are for 20°C, unless otherwise stated.			
	U-434	U-436	U-444
Density (kg/m ³)	7 740	7 700	7 750
Modulus of Elasticity in Tension (GPa)	210		220
Modulus of Elasticity in Torsion (GPa)	65		65
Specific Heat Capacity (J/kg K)	460	440	430
Thermal conductivity at	100°C (W/m K)	26.1	26.3
	500°C (W/m K)	26.3	27.0
Electrical Resistivity (x10 ⁻⁹ Ω m)	650	580	570
Mean Coefficient of Thermal Expansion from	0 to 100°C (x10 ⁻⁶ K ⁻¹)	10.4	10.9
	0 to 300°C (x10 ⁻⁶ K ⁻¹)	11.0	11.9
	0 to 500°C (x10 ⁻⁶ K ⁻¹)	11.3	12.4
	0 to 700°C (x10 ⁻⁶ K ⁻¹)	12.1	13.4
Melting Range (°C)	1 480	1 530	1480
	1530	1 405	1 495
Magnetic	Yes	Yes	Yes

Figure 26 – ASTM U-436; Physical properties

(SASSDA, 2013)

7 CHAPTER 7: SIMULATION

7.1 INTRODUCTION

The simulation model is constructed and computes the optimum values for the independent variables when maximising cycle efficiency (APPENDIX 12.1). It is necessary to specify the required input parameters and a configuration as seen in section 12.1.2. Input parameter and additional limitations are discussed in Chapter 5.

The cycle configuration is specified by whether or not reheat is included; the amount of de-aerators, amount of closed feed heaters, the attemperation temperature difference, etc. The influence of these configuration specifications on the cycle is explained in Chapter 4.

Additions made to the simple cycle not only increase the complexity of the design but also demands additional techno-economic and feasibility considerations. Since the thorium reactor is small, the complexity and cost of constructing reheat is not feasible. The amount of feed heaters will be limited by their combined influence on the cycle efficiency.

Various amounts of feed heaters and combinations thereof will be evaluated to determine the optimum cycle configuration for maximised cycle efficiency. Maximum cycle pressure will also be optimised for maximum cycle efficiency while it is limited by the LPT outlet dryness fraction and the critical pressure of water.

Heat exchanger effectiveness has a significant influence on the configuration of the optimised cycle. The effectiveness of a heat exchanger is in correlation to the capital needed for its manufacture. Various cycle configurations will be evaluated to find the optimum cycle configuration for each previously mentioned heat exchanger effectiveness value.

Since the location of the cement production plant and the availability of water in the area is unknown, both wet and dry cooling tower simulations will be optimised for all the heat exchangers.

7.2 ASSUMPTIONS

- $T_{1(\text{wct})} = 30.4 \text{ }^{\circ}\text{C}$
- $T_{1(\text{dct})} = 40.4 \text{ }^{\circ}\text{C}$
- $88\% < \eta_{\infty, \text{HPT}} < 91\%$
- $79\% < \eta_{\infty, \text{LPT}} < 81\%$

7.3 INPUT PARAMETERS

As the limitations set by various considerations are explained in Chapter 5, the input parameters of the simulations to be computed are specified as follows.

Table 20 - Optimising model inputs; Wet cooling tower

	Variable		Input Value	Unit
PCU				
Atmospheric	Temperature	T_{atm}	297.55	K
Cooling Tower	Condenser T_{inlet}	T_1	303.55	K
	T_r	T_r	16	$^{\circ}\text{C/K}$
	T_c	T_c	3	$^{\circ}\text{C/K}$
	TTD	TTD	2	$^{\circ}\text{C/K}$
Design and components	Attemperation ΔT	ΔT_{att}	15	$^{\circ}\text{C/K}$
	Pump efficiency	η_p	0.83	-
	HPT isentropic efficiency	$\eta_{\text{hp},t}$	0.88	-
	LPT isentropic efficiency	$\eta_{\text{lp},t}$	0.79	-
Reactor				
Reactor	Maximum Temperature	$T_{r_{\text{max}}}$	1023	K
	Minimum Temperature	$T_{r_{\text{min}}}$	523.15	K
	Maximum Pressure	P_r	4	MPa
	Heat output	Q_r	100	MW
Heat Exchanger				
HX	HX effectiveness	HX_{eff}	0.85	-

In both Table 20 and Table 21, most of the inputs values remain constant. On the PCU side, only the turbine efficiencies and the condenser inlet temperature is changed.

The turbine efficiencies can be altered to ensure that the polytropic turbine efficiencies remain within realistic bounds. Due to the type of cooling tower implemented, the condenser inlet temperature (T_1) alternates between 303.55 K (wct) and 313.55 K (dct).

The heat exchanger effectiveness is changed as simulation models will be optimised for 80%, 85%, 87.5% and 90% thereof.

Table 21 - Optimising model inputs; Dry cooling tower

	Variable		Input Value	Unit
PCU				
Atmospheric	Temperature	T _{atm}	297.55	K
Cooling Tower	Condenser T _{inlet}	T ₁	313.55	K
	Tr	Tr	16	°C/K
	Tc	T _c	3	°C/K
	TTD	TTD	2	°C/K
Design and components	Attemperation ΔT	ΔT _{att}	15	°C/K
	Pump efficiency	η _p	0.83	-
	HPT isentropic efficiency	η _{hp,t}	0.88	-
	LPT isentropic efficiency	η _{lp,t}	0.79	-
Reactor				
Reactor	Maximum Temperature	Tr _{max}	1023	K
	Minimum Temperature	Tr _{min}	523.15	K
	Maximum Pressure	Pr	4	MPa
	Heat output	Q _r	100	MW
Heat Exchanger				
HX	HX effectiveness	HX _{eff}	0.85	-

In such a low mass flow Rankine cycle, techno-economic considerations prevent the implementation of reheat and steam turbine driven feed pumps. The amount of feed heaters will however be changed and optimised.

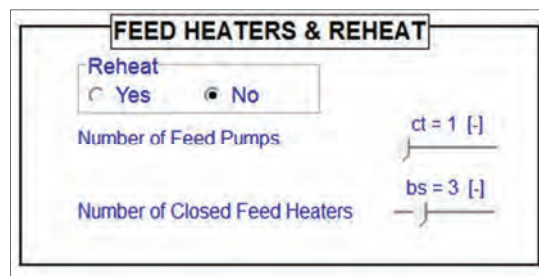


Figure 27 - Optimising model inputs; Reheat

The heat input into the cycle will remain at 100 MW since that is the thermal energy delivered by the thorium reactor. As explained in section 5.7, when cycle efficiency is maximised, the net work delivered by the cycle will also be at a maximum due to the unchanged heat input into the cycle.

In order to ensure that the heat input into the cycle remain constant, it is necessary to specify bleed point pressure for either a closed feed heater or a de-aerator. This specification is done by selecting either of the radio buttons in Figure 28. A bleed point is specified for the corresponding feed heater, resulting in the Rankine working fluid being heated to the minimum heat exchanger inlet temperature.

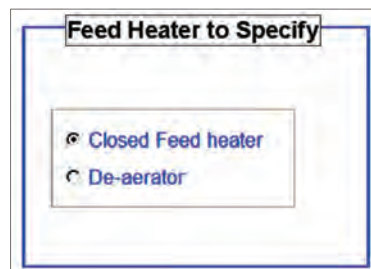


Figure 28 – Optimising model inputs; Regenerative feed heater specification

7.4 OPTIMISED CONFIGURATIONS

Implementing a dry cooling tower is usually done due to the absence of an adequate water source. Dry cooling towers have a lower efficiency than wet cooling towers and may require more upkeep.

With the average ambient temperature across India (24.4°C), the condenser working temperature for a wet cooling tower is 49.4 °C (at $P_{\text{condenser}} = 12 \text{ kPa}$). For the same ambient temperature dry cooling towers deliver a condenser working temperature of 59.4 °C (at $P_{\text{condenser}} = 19.4 \text{ kPa}$).

7.4.1 $HX_{\text{EFF}} (E) = 80\%$

Using a heat exchanger with an effectiveness of 80% the maximum and minimum temperatures of the heat exchanger on the Rankine side are determined. The minimum temperature of the Rankine side heat exchanger is used to specify the bleed point pressure of the top most feed heater.

With the heat exchanger effectiveness at 80% and the criticality of the helium to be cooled to 250 °C, the feed heater is specified to approximately 125 °C. The corresponding maximum steam temperature is 615 °C (898 K).

The optimized values of each configuration, including both wet and dry cooling tower calculations, for heat exchanger effectiveness of 80%, are available in APPENDIX 12.2.

7.4.1.1 WET COOLING TOWER

Implementing the input specifications as determined by the parameters of a wet cooling tower into the simulation model, delivers Figure 29. This figure shows the maximised cycle efficiency for each configuration as the amount of closed feed heaters is increased from one to three for both a specified closed feed heater and a specified de-aerator.

Figure 29 is an ideal representation of maximum cycle efficiency vs. the techno-economic considerations of implementing additional feed heating. The implementation of two closed feed heaters delivers a greater increase in cycle efficiency than implementing three.

Due to the constant thermal energy injection into the Rankine cycle from the thorium reactor, a similar graph to Figure 29 can be constructed for the net work delivered by the cycle.

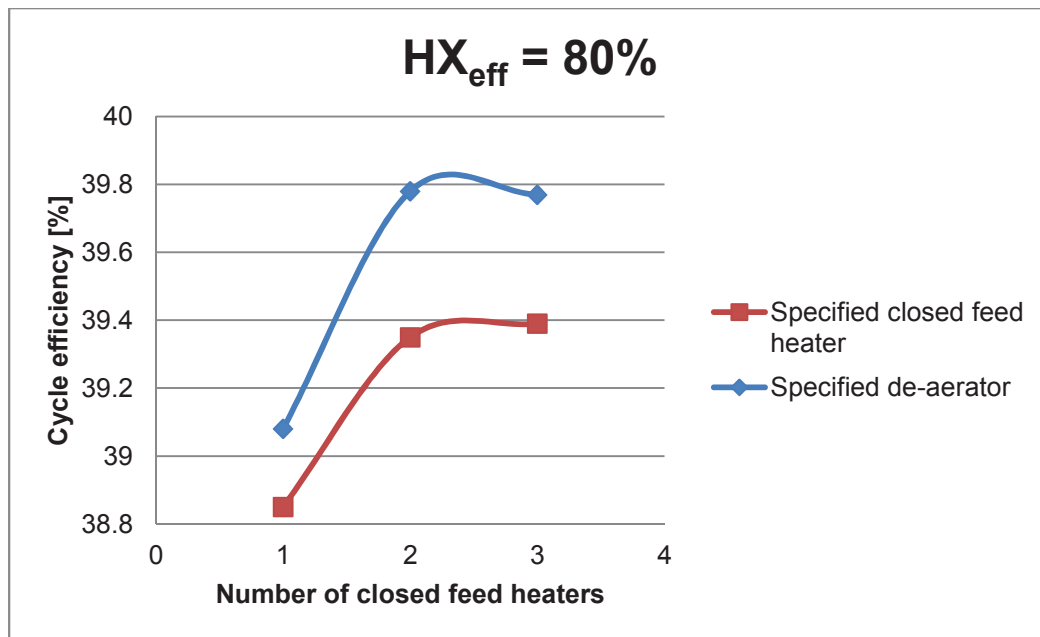


Figure 29 - HX_{eff} = 80%; wct; η_R vs. number of closed feed heaters

In Figure 29, the configurations with the specified de-aerator delivers a higher maximised cycle efficiency than its counterpart. The energy delivered to the Rankine cycle from the reactor remains constant at 100 MW_t due to the specification of a feed heater. The maximised value of the cycle efficiency and net work differ by a factor of 10⁵ continually.

By increasing the number of closed feed heaters from 1 to 2, net work delivered is increased by approximately 400 kW. Increasing the amount of closed feed heaters to three, causes less than 50 kW rise in net work for the specified closed feed heater specification.

For a heat exchanger effectiveness of 80%, the optimum configuration consists of two closed feed heaters and a specified de-aerator when accounting for techno-economic considerations.

7.4.1.2 DRY COOLING TOWER

Figure 30 is adapted from the simulation model results. These results are calculated when the parameters, as determined in Chapters 5 and 6, in combination with a dry cooling tower and a heat exchanger with an effectiveness of 80% is implemented.

Figure 30 displays the corresponding cycle efficiency as the amount of closed feed heaters is increased from one to four. In each configuration, one de-aerator is applied. Reheating and steam turbine driven feed pumps are not incorporated due to techno-economic considerations.

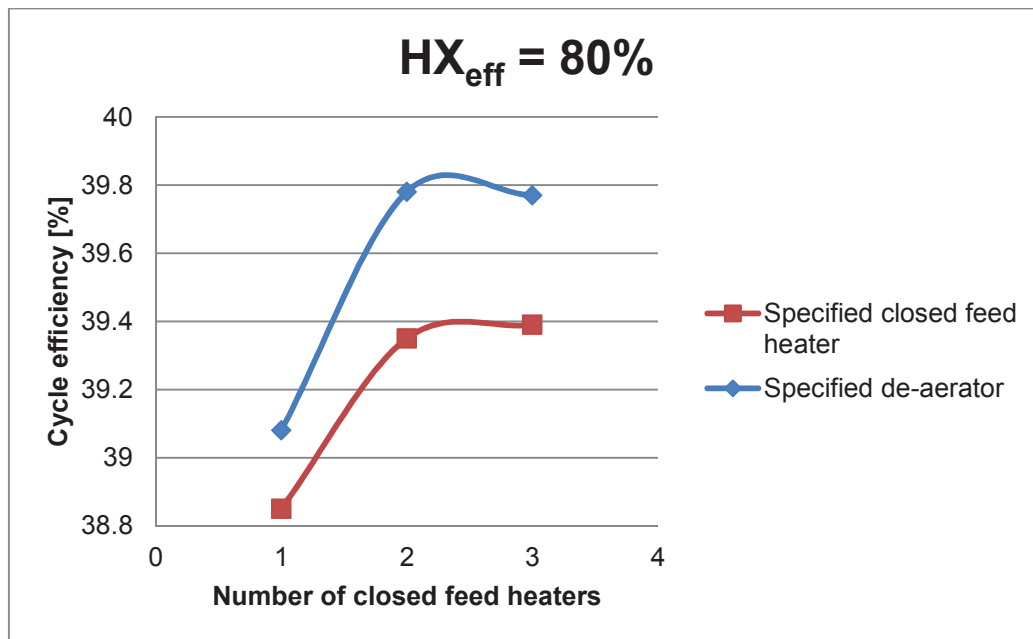


Figure 30 - $HX_{eff} = 80\%$; dct; η_R vs. number of closed feed heaters

Applying an identical thought process, as with the wet cooling tower simulation, provides the configuration with 2 closed feed heaters and a specified de-aerator as the optimum option.

7.4.2 $HX_{EFF} (E) = 85\%$

Implementation of a heat exchanger with an effectiveness of 85% increases the maximum cycle temperature to approximately 661 °C (934 K). Consequently, the temperature of the heat exchanger inlet on the Rankine side is increased to approximately 160°C.

Since the helium needs to be cooled from 750 °C to 250 °C, it is necessary that the water side inlet to the heat exchanger be specified at 160 °C. For this configuration, a feed heater

is specified, either contact or closed, at the corresponding fraction of maximum HPT inlet pressure.

7.4.2.1 WET COOLING TOWER

With higher heat exchanger effectiveness, the maximum cycle temperature is increased, causing an increase in the cycle efficiency and the net work delivered.

As previously discussed, a de-aerator or a closed feed heater needs to be implemented to raise the Rankine working fluid temperature to approximately 160 °C. Various simulation model configurations are therefore optimised for maximum cycle efficiency while complying with these demands.

Cycle efficiency is plotted in Figure 31 as the amount of closed feed heaters is increased from one to four. The red graph represents the configurations where a closed feed heater is specified, while the blue graph shows the configurations where a de-aerator is specified.

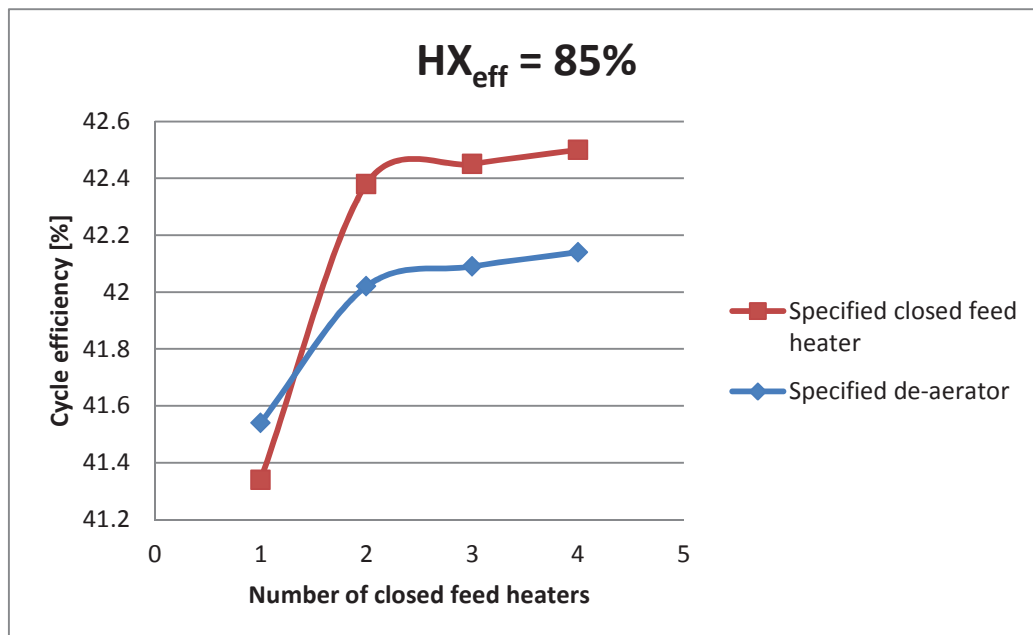


Figure 31 - HX_{eff} = 85%; wct; η_R vs. number of closed feed heaters

Increasing the amount of closed feed heaters from one to two causes the cycle efficiency of the specified closed feed heater configuration to increase by $\pm 1\%$. If only the specification of a de-aerator is inspected, this same increase in the amount of closed feed heaters will cause

a cycle efficiency increase of almost 0.5%. Further increase in the amount of closed feed heaters causes a smaller increase in cycle efficiency for both configurations.

As the heat delivered to the Rankine cycle by the thorium reactor is constantly 100 MW, the net work is still the cycle efficiency multiplied by a factor of 10^5 .

If two closed feed heaters are implemented instead of one, the net work delivered by the cycle increases by approximately 1 MW for a specified closed feed heater configuration. While the specified de-aerator configuration only causes an increase of almost 500 kW when two closed feed heaters are implemented instead of one.

If techno-economic considerations are taken into account, it is clear from Figure 31, that the optimum cycle configuration for a heat exchanger with 85% effectiveness consist of 2 closed feed heaters. The specification of a closed feed heater produces greater cycle efficiency and therefore a higher net work output.

7.4.2.2 DRY COOLING TOWER

The simulation model is used to optimise the Rankine cycle for maximum cycle efficiency. Cycle efficiency is maximised for various cycle configurations where a dry cooling tower and a heat exchanger with 85% effectiveness is implemented.

Figure 33 displays the corresponding cycle efficiency as the amount of closed feed heaters is increased from one to four. In each configuration, one de-aerator is applied and neither reheating nor steam turbine driven feed pumps are incorporated.

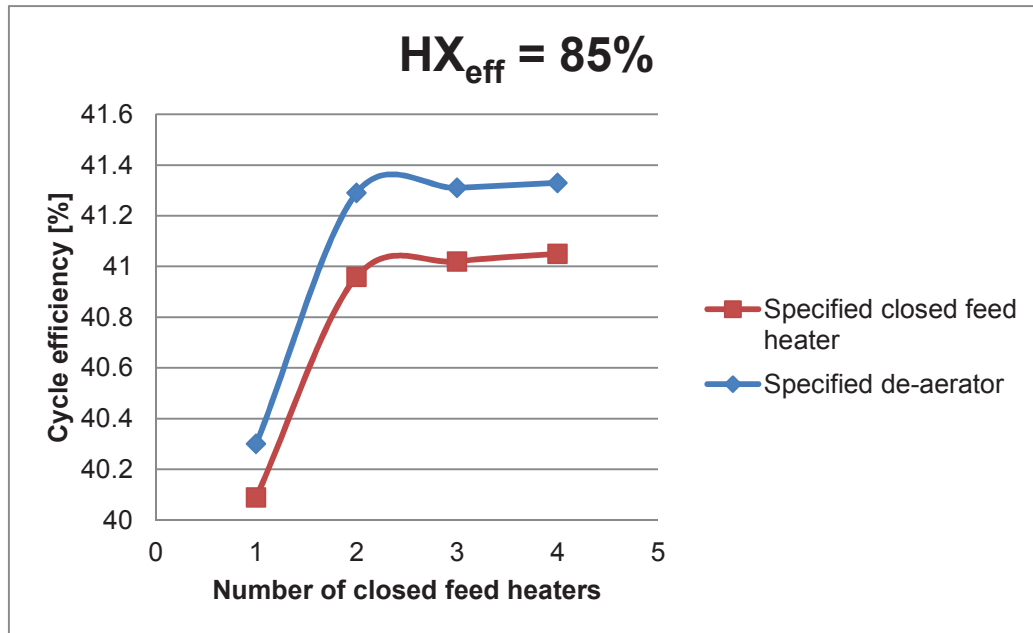


Figure 32 - $HX_{eff} = 85\%$; dct; η_R vs. number of closed feed heaters

For each configuration, the specified de-aerator delivers a higher cycle efficiency and net work than its counterpart. For this cooling tower and heat exchanger combination, two closed feed heaters and a specified de-aerator is the optimum cycle configuration.

7.4.3 $HX_{EFF} (E) = 87.5\%$

If the helium delivered by the reactor is cooled to 250°C through a heat exchanger with 87.5% effectiveness, the temperature of the heat exchanger water side inlet is calculated to be almost 175°C . The higher heat exchanger water side inlet temperature and effectiveness causes the maximum cycle temperature to increase to 678.5°C (951.6 K).

Although a heat exchanger with such high effectiveness is expensive, the implementation thereof might be justified by the increase in cycle efficiency and net work. As the cycle maximum-minimum temperature difference is increased, the cycle efficiency and net work is increased accordingly.

The optimized values of each configuration, including both wet and dry cooling tower calculations, for heat exchanger effectiveness of 87.5%, are available in APPENDIX 12.2.

7.4.3.1 WET COOLING TOWER

Figure 33 shows cycle efficiency as the amount of closed feed heaters is increased from one to four. It is necessary to specify a feed heater bleed point such that the Rankine working fluid temperature is increased to the determined heat exchanger water side inlet temperature. The specification of a closed feed heater at this point is represented by the red graph while the blue graph shows the configurations where a de-aerator is specified.

Figure 33 shows that the specification of a de-aerator produces higher cycle efficiency than the configurations where a closed feed heater is specified. From this graph, it is apparent that the implementation of two closed feed heaters is profitable with an increase in cycle efficiency of more than 1% for both configurations.

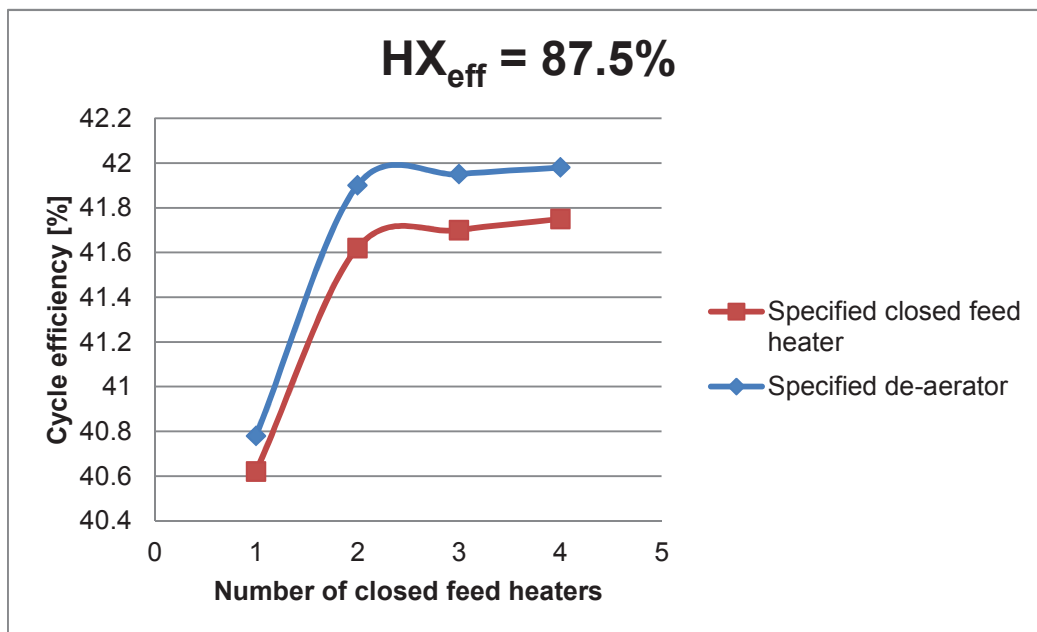


Figure 33 – HX_{eff} = 87.5%; wct; η_R vs. number of closed feed heaters

As the thorium reactor produces 100 MW_t, the heat added to the Rankine cycle remain constant. The net work delivered by the cycle is therefore maximised for each optimum cycle configuration. The net work delivered by the cycle increases by approximately 1.25 MW due to the implementation of 2 closed feed heaters instead of one.

With techno-economic considerations taken into account, for a heat exchanger with 87.5% effectiveness, the configuration consisting of 2 closed feed heaters and the de-aerator specified is the optimum configuration.

7.4.3.2 DRY COOLING TOWER

For this simulation, a dry cooling tower is used in combination with a heat exchanger with 87.5% effectiveness. The simulation model is used to maximise cycle efficiency for the various configurations.

Maximised cycle efficiency is shown in Figure 34 as the amount of closed feed heaters is increased from one to four. For each of these configurations, one de-aerator is applied.

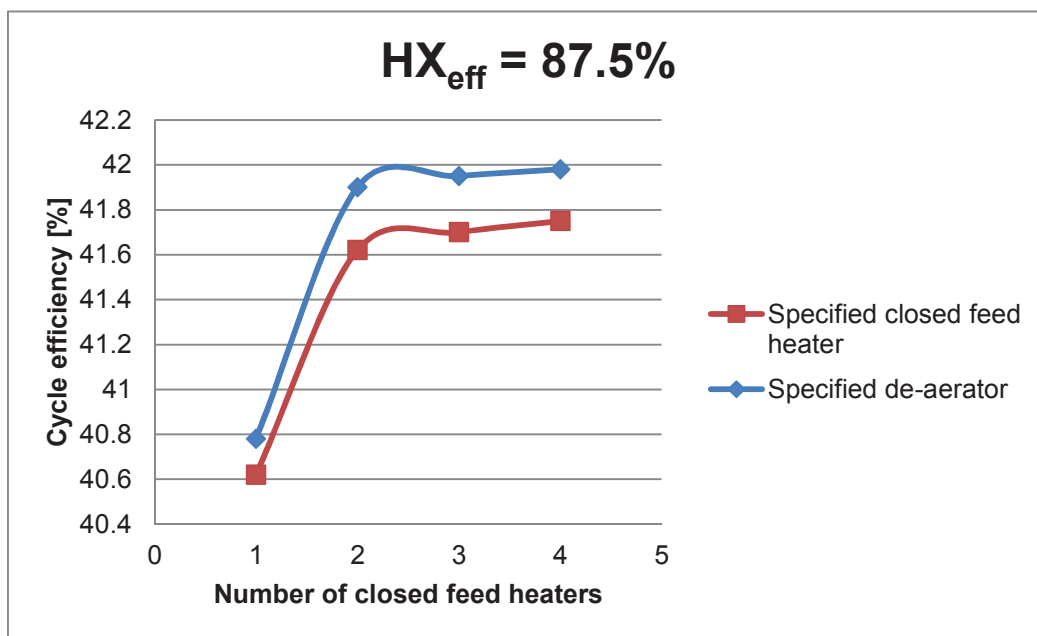


Figure 34 - HX_{eff} = 87.5%; dct; η_R vs. number of closed feed heaters

Since heat input of the cycle must remain constant at 100 MW_t , net work is maximised when cycle efficiency is maximised.

Two closed feed heaters and a specified de-aerator, is the optimum cycle configuration for this cooling tower and heat exchanger combination.

7.4.4 $HX_{EFF} (E) = 90\%$

Due to the increase in the maximum cycle temperature, the cycle efficiency will also increase as stated by the law of Carnot (equation (3)). If the heat exchanger is more effective, the temperature of the cold working fluid, required to cool the helium from 750°C to 250°C , will increase (195°C).

The increase in the water side inlet temperature in combination with the increased heat exchanger effectiveness causes the maximum cycle temperature to increase to 694.4°C (967.5 K). As discussed earlier, the increase in maximum cycle temperature will increase the cycle efficiency.

The increase in heat exchanger water side inlet temperature causes the corresponding pressure to exceed the pressure limitation set for the de-aerator bleed point. The de-aerator is unable to perform its secondary purpose of removing non-dissolved gases at the required specification point. The de-aerator cannot be specified for a heat exchanger with 90% effectiveness and it is therefore compulsory to specify a closed feed heater.

The optimized values of each configuration, including both wet and dry cooling tower calculations, for heat exchanger effectiveness of 90%, are available in APPENDIX 12.2.

Figure 35 and Figure 36 then displays the cycle efficiency as the amount of closed feed heaters is increased from one to four.

7.4.4.1 WET COOLING TOWER

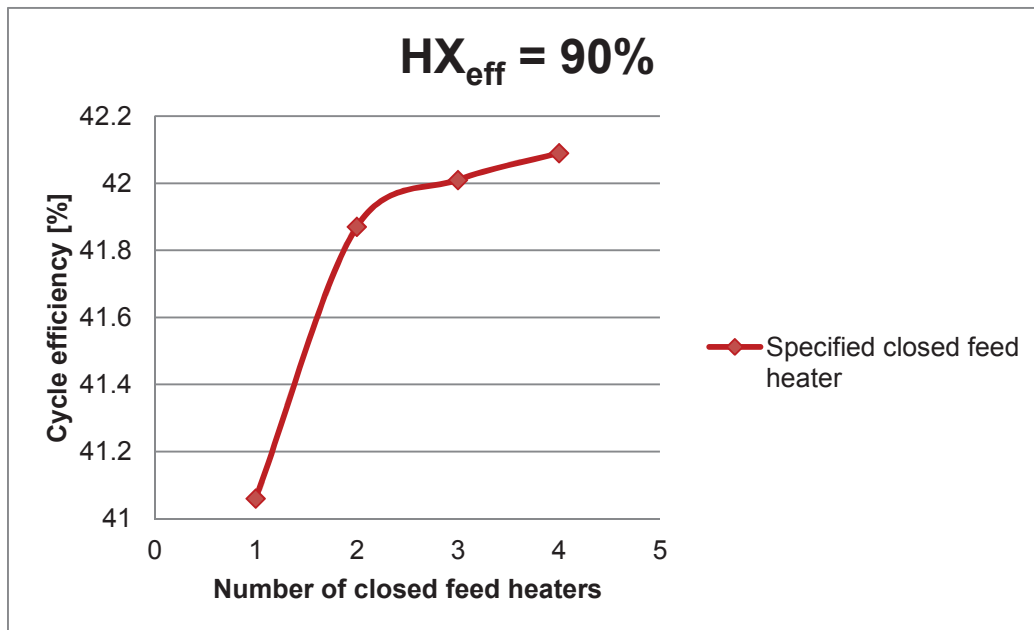


Figure 35 – $HX_{eff} = 90\%$; wct; η_R vs. number of closed feed heaters

Cycle efficiency is radically increased as the amount of closed feed heaters is increased from one to two (Figure 35). Implementation of a second closed feed heater causes an increase in cycle efficiency of approximately 1.2%. Little less than 1.2 kW output is gained by implementing a second closed feed heater.

Due to the limitations set for the de-aerator bleed point pressure ($0.1 \text{ MPa} < P_{de} < 1 \text{ MPa}$), there is a cycle efficiency drop for the configuration with 3 closed feed heaters. Both the configurations consisting of two and four closed feed heaters are optimised to deliver higher cycle efficiencies than the configuration consisting of 3 closed feed heaters.

When techno-economic considerations are taken into account for a heat exchanger with 90% effectiveness, the cycle configuration consisting of 2 closed feed heaters is the optimum configuration.

7.4.4.2 DRY COOLING TOWER

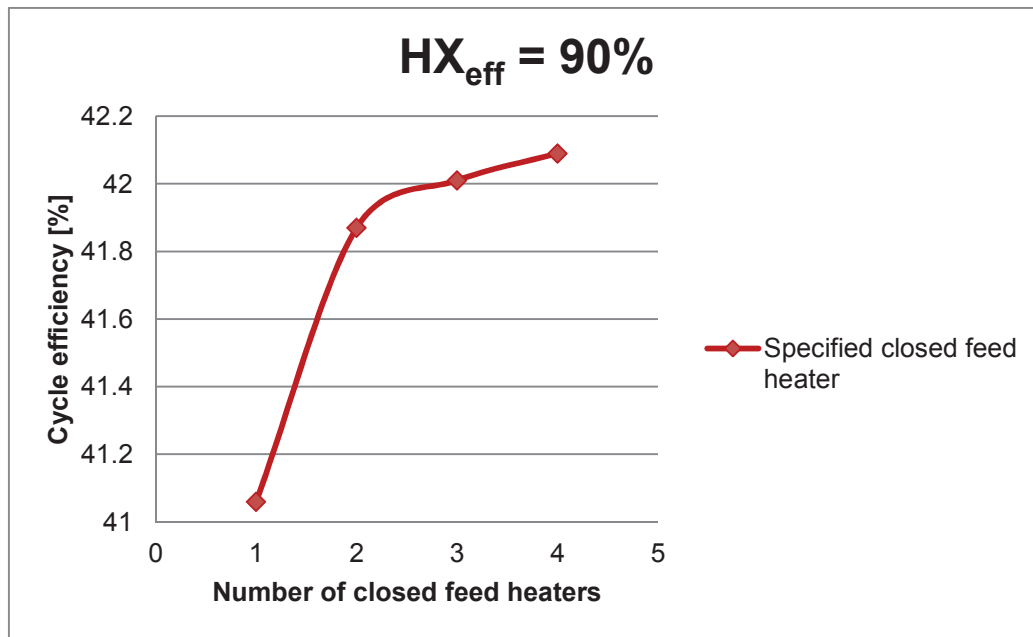


Figure 36 - HX_{eff} = 90%; dct; η_R vs. number of closed feed heaters

Figure 36 is adapted from the simulation model results. These results are calculated when the parameters as determined in Chapters 5 and 6 in combination with a dry cooling tower and a heat exchanger with 90% effectiveness is implemented.

As the amount of closed feed heaters is increased from one to four, the corresponding cycle efficiency is shown in Figure 36. In each configuration, one de-aerator is applied. Reheating and steam turbine driven feed pumps are not incorporated due to techno-economic considerations.

For this cooling tower and heat exchanger combination, two closed feed heaters and a specified de-aerator is the optimum cycle configuration.

8 CHAPTER 8: OPTIMUM CYCLE CONFIGURATION

8.1 INTRODUCTION

In Chapter 7, the optimum cycle configuration for each heat exchanger effectiveness and cooling tower combination is identified. All of the identified optimum cycle configurations consist of one de-aerator and two closed feed heaters.

The optimum cycle configuration for each of these scenarios is discussed in this chapter.

Further energy losses due to generator; transformer and transmission losses are also introduced to calculate the electric energy delivered by each optimum configuration.

8.2 $HX_{EFF} (E) = 80\%$

8.2.1 WET COOLING TOWER

It was determined from section 7.4.1 that the optimum cycle configuration for heat exchanger effectiveness of 80% consists of one specified de-aerator and two closed feed heaters.

Table 22 displays various critical outputs and values of limitation criteria for this optimized cycle configuration. The maximum HPT inlet pressure is optimized at 17.6 MPa as it is limited by the LPT outlet steam quality (x_{crit}) of 88%

Steam flows through the Rankine cycle with a mass flow rate of 32.44 kg/s, as it is enforced by the conditions of the helium and the heat exchanger effectiveness. The polytropic turbine efficiencies are acceptably within the bounds as specified in section 7.2.

Table 22 - $HX_{eff} = 80\%$; wct; Optimum cycle configuration results

	Variable	Value	Unit
Energy Balance	E_b	0	MW
Cycle efficiency	η_R	40.83	%
Net work	W_{net}	40.825	MW
Turbine work	W_{turb}	41.757	MW
Pump work	W_{pumps}	0.932	MW
Heat input	Q_{in}	100	MW
Heat rejected	Q_{out}	59.175	MW
Total mass flow	\dot{m}_{tot}	32.44	kg/s
De-aerator mass flow	$\dot{m}[1]$	2.352	kg/s
HP feed heater mass flow	$\dot{m}[2]$	0.9762	kg/s
LP feed heater mass flow	$\dot{m}[3]$	0.9636	kg/s
Minimum Temperature	T_{min}	322.5	K
Maximum HPT Pressure	P_{max}	17.6	MPa
LPT outlet quality	x_{crit}	88	%
HX water inlet temperature	$T_{HX,i}$	398.2	K
HX water outlet temperature	T_{max}	898	K
Polytropic HPT efficiency	$\eta_{h,\infty}$	88.89	%
Polytropic LPT efficiency	$\eta_{l,\infty}$	79.4	%

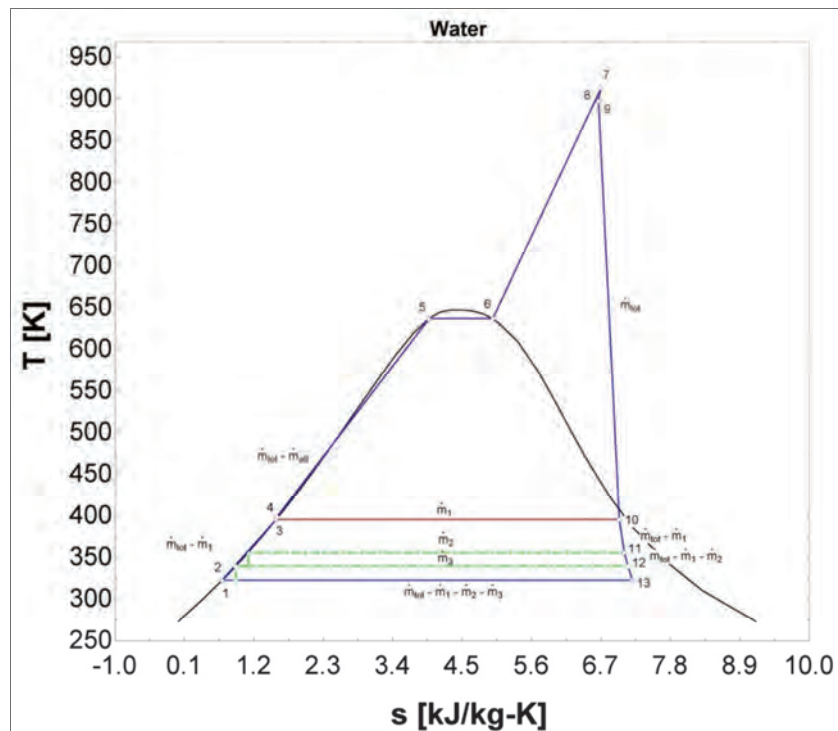


Figure 37 – $Hx_{eff} = 80\%$; wct; Optimum cycle configuration; T-s diagram

Figure 37 shows a T-s diagram for a Rankine steam cycle with the de-aerator as the specified feed heater. The maximum cycle efficiency of this configuration is optimized to be 40.83%, with the net work maximised at 40.825 MW.

Table 23 – $Hx_{eff} = 80\%$; wct; Optimum bleed points

	Description	Specified	Fraction		Pressure	
			Value	Unit	Value	Unit
r_{de}	De-aerator	X	0.005499	-	0.104481	MPa
$r_{bs,1}$	Closed feed heater	✓	0.01274	-	0.24206	MPa
$r_{bs,2}$	Closed feed heater	X	0.001904	-	0.036176	MPa

Optimized bleed point fractions and pressures for the various feed heaters, specified and otherwise, are shown in Table 23. The fractions shown are relative to the HPT inlet pressure.

8.2.2 DRY COOLING TOWER

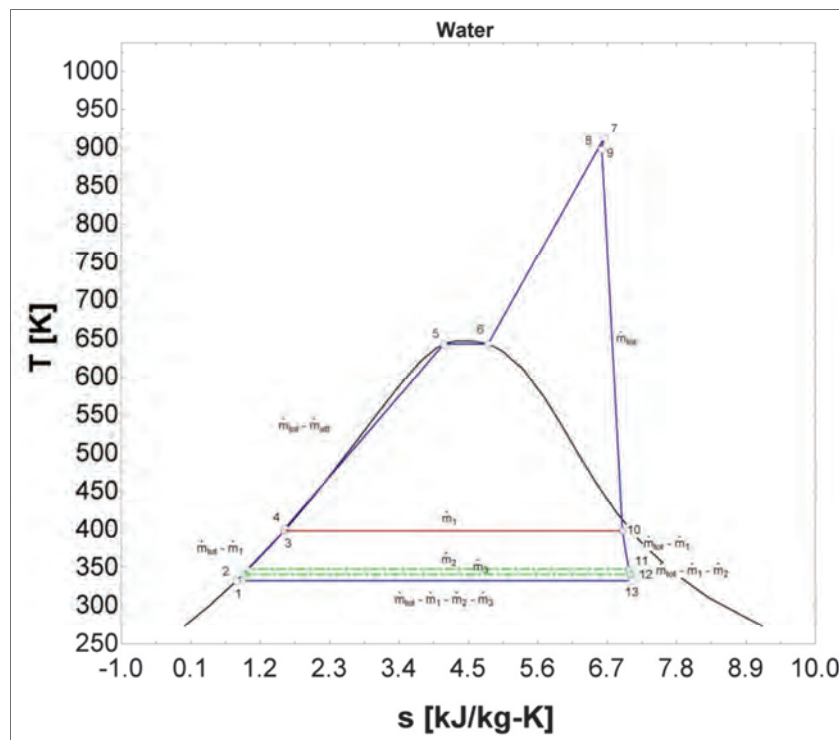


Figure 38 – $Hx_{eff} = 80\%$; dct; Optimum cycle configuration; T-s diagram

Figure 38 shows a T-s diagram for a Rankine steam cycle with the de-aerator as the specified feed heater. The maximum cycle efficiency of this configuration is optimized to be 39.78%, with the net work maximised at 39.775 MW.

Table 24 - $HX_{eff} = 80\%$; dct; Optimum cycle configuration results

	Variable	Value	Unit
Energy Balance	E_b	0	MW
Cycle efficiency	η_R	39.78	%
Net work	W_{net}	39.775	MW
Turbine work	W_{turb}	10.791	MW
Pump work	W_{pumps}	1.016	MW
Heat input	Q_{in}	100	MW
Heat rejected	Q_{out}	60.225	MW
Total mass flow	\dot{m}_{tot}	32.7	kg/s
De-aerator mass flow	$\dot{m}[1]$	3.195	kg/s
HP feed heater mass flow	$\dot{m}[2]$	0.136	kg/s
LP feed heater mass flow	$\dot{m}[3]$	0.4887	kg/s
Minimum Temperature	T_{min}	332.6	K
Maximum HPT Pressure	P_{max}	19	MPa
LPT outlet quality	x_{crit}	88.37	%
HX water inlet temperature	$T_{HX,i}$	398.2	K
HX water outlet temperature	T_{max}	898	K
Polytropic HPT efficiency	$\eta_{h,\infty}$	89.14	%
Polytropic LPT efficiency	$\eta_{l,\infty}$	79.09	%

Table 24 shows a summary of the crucial results as calculated by the simulation model. Note that the results of the maximum HPT inlet pressure and the LPT outlet quality are within the set bounds. Heat input into the cycle remains constant at 100 MW due to the capacity of the reactor.

Table 25 – $HX_{eff} = 80\%$; dct; Optimum bleed points

	Description	Specified	Fraction		Pressure	
			Value	Unit	Value	Unit
r_{de}	De-aerator	✓	0.01224	-	0.2311	MPa
$r_{bs,1}$	Closed feed heater	X	0.001658	-	0.03131	MPa
$r_{bs,2}$	Closed feed heater	X	0.0015	-	0.02832	MPa

The optimised bleed points as fractions of HPT inlet pressure is shown in Table 25. The corresponding bleed pressures are also shown.

8.3 $HX_{EFF} (E) = 85\%$

8.3.1 WET COOLING TOWER

8.3.1.1 OPTIMUM CYCLE CONFIGURATION

The optimum cycle configuration for a heat exchanger with 85% effectiveness, determined from section 7.4.2, consist of one de-aerator and two closed feed heaters with one of these closed feed heaters specified.

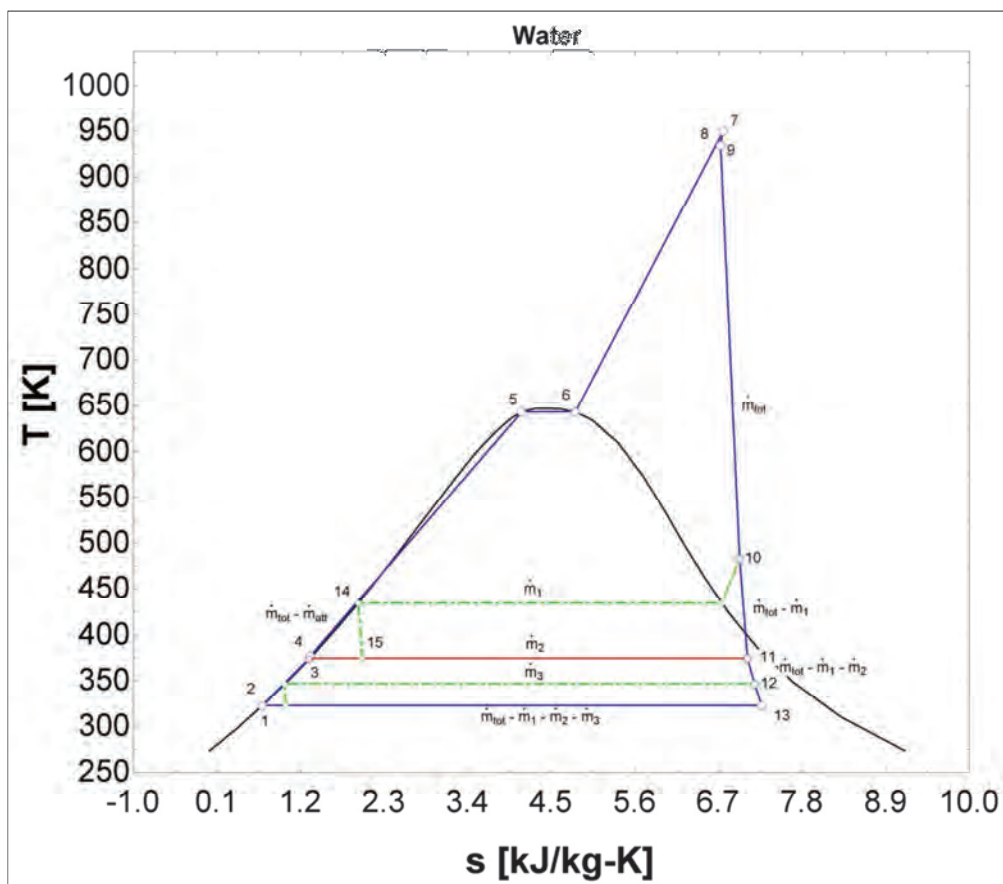


Figure 39 - $HX_{eff} = 85\%$; wct; Optimum cycle configuration; T-s diagram

Figure 39 shows a T-s diagram for a Rankine steam cycle with a closed feed heater specified at the heat exchanger water side inlet temperature. The maximum cycle efficiency of this configuration is optimized to be 42.38%, with the net work maximised at 42.376 MW.

Table 26 - $HX_{eff} = 85\%$; wct; Optimum cycle configuration results

	Variable	Value	Unit
Energy Balance	E_b	0	MW
Cycle efficiency	η_R	42.38	%
Net work	W_{net}	42.376	MW
Turbine work	W_{turb}	43.382	MW
Pump work	W_{pumps}	1.006	MW
Heat input	Q_{in}	100	MW
Heat rejected	Q_{out}	57.624	MW
Total mass flow	\dot{m}_{tot}	32.99	kg/s
HP feed heater mass flow	$\dot{m}[1]$	3.416	kg/s
De-aerator mass flow	$\dot{m}[2]$	1.134	kg/s
LP feed heater mass flow	$\dot{m}[3]$	1.313	kg/s
Minimum Temperature	T_{min}	322.6	K
Maximum HPT Pressure	P_{max}	19	MPa
LPT outlet quality	x_{crit}	88.94	%
HX water inlet temperature	$T_{HX,i}$	435	K
HX water outlet temperature	T_{max}	934.8	K
Polytropic HPT efficiency	$\eta_{h,\infty}$	89.44	%
Polytropic LPT efficiency	$\eta_{l,\infty}$	80.58	%

Table 26 delivers various critical outputs and values of the limitation criteria set for this optimized cycle configuration. The maximum HPT inlet pressure is optimised at 19 MPa. It is not limited by the LPT steam outlet quality ($x_{crit} > 0.88$) but by the critical pressure of water (22.06 MPa) due to the increased maximum cycle temperature.

Steam flows through the Rankine cycle with a mass flow rate of 32.99 kg/s, as it is enforced by the conditions of the helium and the heat exchanger effectiveness. The polytropic turbine efficiencies are acceptably within the bounds as specified in section 7.2.

Optimized bleed point fractions and pressures for the various feed heaters, specified and otherwise, are shown in Table 27. These fractions are relative to the HPT inlet pressure.

Table 27 - $HX_{eff} = 85\%$; wct; Optimum bleed points

	Description	Specified	Fraction		Pressure	
			Value	Unit	Value	Unit
r_{de}	De-aerator	X	0.00555	-	0.10545	MPa
$r_{bs,1}$	Closed feed heater	✓	0.03405	-	0.64695	MPa
$r_{bs,2}$	Closed feed heater	X	0.001884	-	0.035796	MPa

8.3.2 DRY COOLING TOWER

Figure 40 shows a T-s diagram for a Rankine steam cycle with the de-aerator as the specified feed heater. The maximum cycle efficiency of this configuration is optimized to be 41.29% with the net work consequently maximised at 41.287 MW.

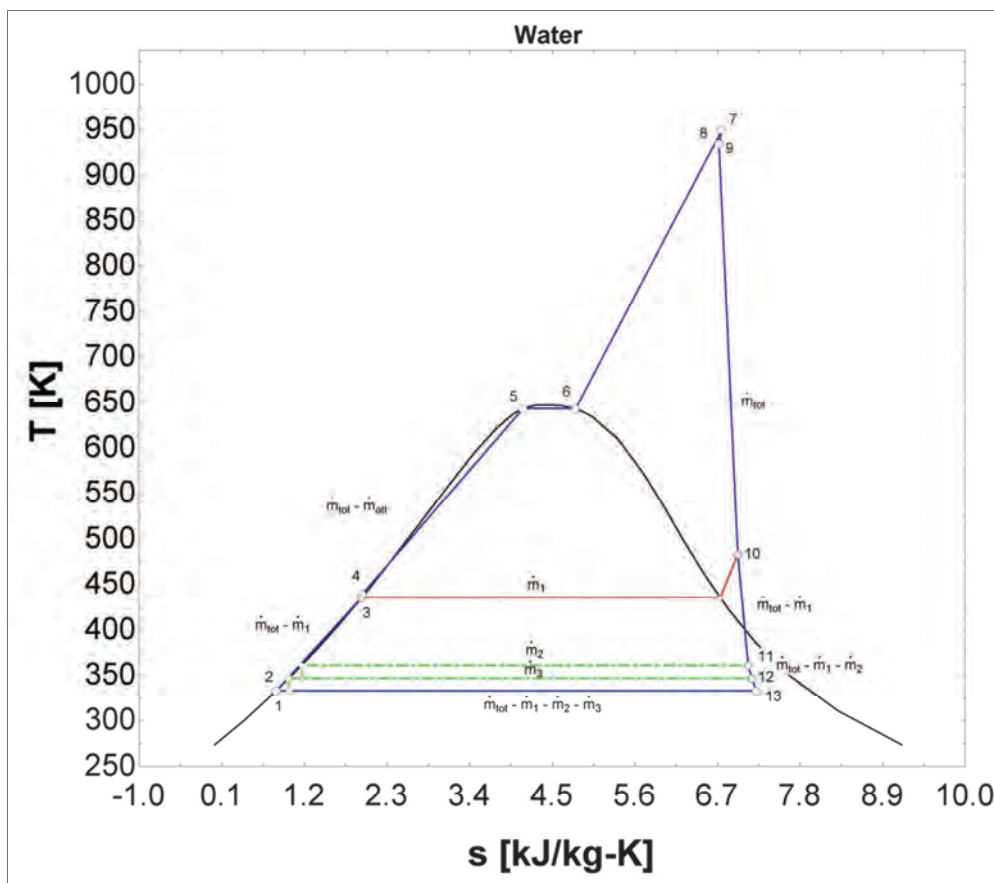


Figure 40 – $H_{x,eff} = 85\%$; dct; Optimum cycle configuration; T-s diagram

Table 28 displays various critical results of this optimised cycle configuration. The cycle is kept sub-critical while the LPT outlet steam quality and polytropic efficiencies remain within the set bounds.

Water flows through the Rankine cycle at 33.36 kg/s. This mass flow is a function of the heat exchanger effectiveness.

Table 28 - $HX_{eff} = 85\%$; dct; Optimum cycle configuration results

	Variable	Value	Unit
Energy Balance	E_b	0	MW
Cycle efficiency	η_R	41.29	%
Net work	W_{net}	41.287	MW
Turbine work	W_{turb}	42.356	MW
Pump work	W_{pumps}	1.069	MW
Heat input	Q_{in}	100	MW
Heat rejected	Q_{out}	58.713	MW
Total mass flow	\dot{m}_{tot}	33.36	kg/s
De-aerator mass flow	$\dot{m}[1]$	4.21	kg/s
HP feed heater mass flow	$\dot{m}[2]$	0.8182	kg/s
LP feed heater mass flow	$\dot{m}[3]$	0.7563	kg/s
Minimum Temperature	T_{min}	332.6	K
Maximum HPT Pressure	P_{max}	19	MPa
LPT outlet quality	x_{crit}	90.11	%
HX water inlet temperature	$T_{HX,i}$	435	K
HX water outlet temperature	T_{max}	934.8	K
Polytropic HPT efficiency	$\eta_{h,\infty}$	89.58	%
Polytropic LPT efficiency	$\eta_{l,\infty}$	79.33	%

Table 29 displays the optimised feed heater bleed point fractions and the corresponding pressures. These bleed point fractions deliver maximised cycle efficiency and therefore a maximised net work output.

Table 29 – $HX_{eff} = 85\%$; dct; Optimum bleed points

	Description	Specified	Fraction		Pressure	
			Value	Unit	Value	Unit
r_{de}	De-aerator	✓	0.03405	-	0.6429	MPa
$r_{bs,1}$	Closed feed heater	X	0.00339	-	0.064	MPa
$r_{bs,2}$	Closed ed heater	X	0.001899	-	0.03586	MPa

8.4 $HX_{EFF} (E) = 87.5\%$

8.4.1 WET COOLING TOWER

8.4.1.1 OPTIMUM CYCLE CONFIGURATION

For a heat exchanger with 87.5% effectiveness, the optimum cycle configuration obtained from section 7.4.3, consist of one de-aerator (specified) and two closed feed heaters.

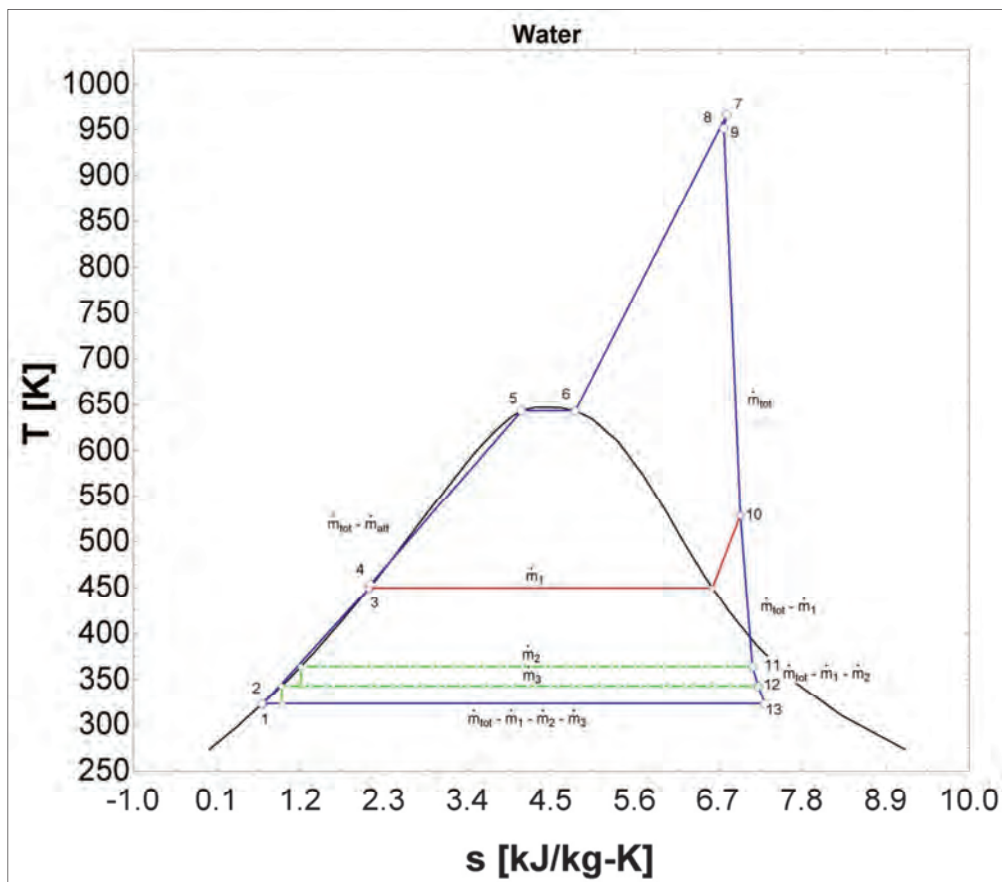


Figure 41 – $HX_{eff} = 87.5\%$; wct; Optimum cycle configuration; T-s diagram

Figure 41 shows a T-s diagram for a Rankine steam cycle with the de-aerator as the specified feed heater. The maximum cycle efficiency of this optimum configuration is optimised at 43.22%, with the net work maximised at 43.216 MW.

Table 30 - $HX_{eff} = 87.5\%$; wct; Optimum cycle configuration results

	Variable	Value	Unit
Energy Balance	E_b	0	MW
Cycle efficiency	η_R	43.22	%
Net work	W_{net}	43.216	MW
Turbine work	W_{turb}	44.307	MW
Pump work	W_{pumps}	1.091	MW
Heat input	Q_{in}	100	MW
Heat rejected	Q_{out}	56.784	MW
Total mass flow	\dot{m}_{tot}	33.59	kg/s
De-aerator mass flow	$\dot{m}[1]$	4.788	kg/s
HP feed heater mass flow	$\dot{m}[2]$	1.19	kg/s
LP feed heater mass flow	$\dot{m}[3]$	1.06	kg/s
Minimum Temperature	T_{min}	322.6	K
Maximum HPT Pressure	P_{max}	19	MPa
LPT outlet quality	x_{crit}	89.43	%
HX water inlet temperature	$T_{HX,i}$	451.8	K
HX water outlet temperature	T_{max}	951.6	K
Polytropic HPT efficiency	$\eta_{h,\infty}$	89.87	%
Polytropic LPT efficiency	$\eta_{l,\infty}$	79.49	%

Table 30 delivers various critical outputs and values of the limitation criteria set for this optimized cycle configuration. The maximum HPT inlet pressure is optimised at 19 MPa for maximum cycle efficiency. Maximum HPT inlet pressure is not limited by the LPT outlet steam quality ($x_{crit} > 0.88$) it is however limited by the critical pressure of water (22.06 MPa).

Steam flows through the Rankine cycle with a mass flow rate of 33.59 kg/s, as it is enforced by the conditions of the helium and the heat exchanger effectiveness. The polytropic turbine efficiencies are acceptably within the bounds as specified in section 7.2.

Table 31 – $HX_{eff} = 87.5\%$; wct; Optimum bleed points

	Description	Specified	Fraction		Pressure	
			Value	Unit	Value	Unit
r_{de}	De-aerator	✓	0.04878	-	0.92682	MPa
$r_{bs,1}$	Closed feed heater	X	0.003824	-	0.072656	MPa
$r_{bs,2}$	Closed feed heater	X	0.001616	-	0.030704	MPa

Optimized bleed point fractions and pressures for the various feed heaters, specified and otherwise (Table 31). These fractions are relative to the HPT inlet pressure. The de-aerator bleed point pressure is at an acceptable pressure ($P_{de} = 921$ kPa).

8.4.2 DRY COOLING TOWER

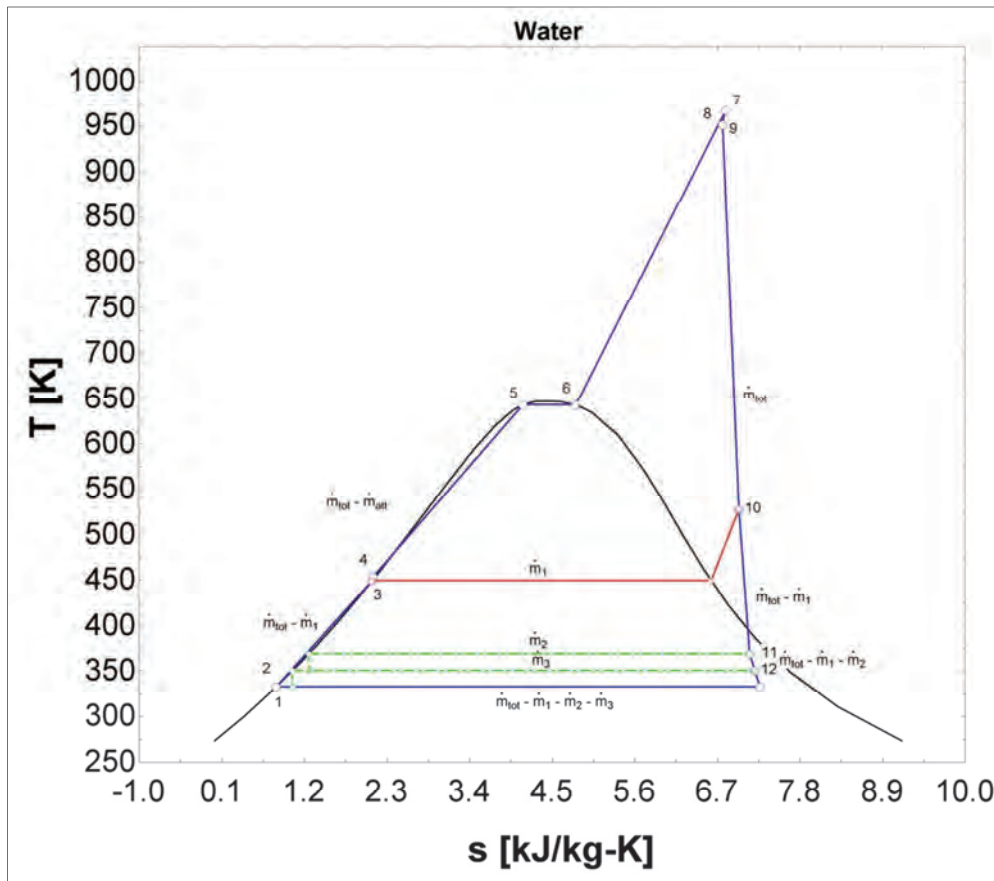


Figure 42 – $Hx_{eff} = 87.5\%$; dct; Optimum cycle configuration; T-s diagram

Figure 42 shows a T-s diagram for a Rankine steam cycle with the de-aerator as the specified feed heater. The maximum cycle efficiency of this configuration is optimized to be 41.9% with the net work maximised at 41.904 MW.

The critical Rankine cycle results are shown in Table 32. Limitations set for various variables, such as LPT outlet steam quality and polytropic efficiencies, have been satisfied.

Table 32 - $HX_{eff} = 87.5\%$; dct; Optimum cycle configuration results

	Variable	Value	Unit
Energy Balance	E_b	0	MW
Cycle efficiency	η_R	41.9	%
Net work	W_{net}	41.904	MW
Turbine work	W_{turb}	42.996	MW
Pump work	W_{pumps}	1.091	MW
Heat input	Q_{in}	100	MW
Heat rejected	Q_{out}	58.096	MW
Total mass flow	\dot{m}_{tot}	33.59	kg/s
HP feed heater mass flow	$\dot{m}[1]$	4.545	kg/s
De-aerator mass flow	$\dot{m}[2]$	1.052	kg/s
LP feed heater mass flow	$\dot{m}[3]$	0.95	kg/s
Minimum Temperature	T_{min}	332.6	K
Maximum HPT Pressure	P_{max}	19	MPa
LPT outlet quality	x_{crit}	90.83	%
HX water inlet temperature	$T_{HX,i}$	451.8	K
HX water outlet temperature	T_{max}	951.6	K
Polytropic HPT efficiency	$\eta_{h,\infty}$	89.94	%
Polytropic LPT efficiency	$\eta_{l,\infty}$	79.42	%

Table 33 displays the optimum bleed fractions and corresponding pressures for the feed heaters of this configuration.

Table 33 – $HX_{eff} = 87.5\%$; dct; Optimum bleed points

	Description	Specified	Fraction		Pressure	
			Value	Unit	Value	Unit
r_{de}	De-aerator	✓	0.04878	-	0.921	MPa
$r_{bs,1}$	Closed feed heater	X	0.004627	-	0.08737	MPa
$r_{bs,2}$	Closed feed heater	X	0.002241	-	0.04231	MPa

8.5 $HX_{EFF} (E) = 90\%$

8.5.1 WET COOLING TOWER

8.5.1.1 OPTIMUM CYCLE CONFIGURATION

In section 7.4.4, it was determined that the optimum cycle configuration for heat exchanger effectiveness of 90%, consist of one de-aerator and two closed feed heaters (one specified).

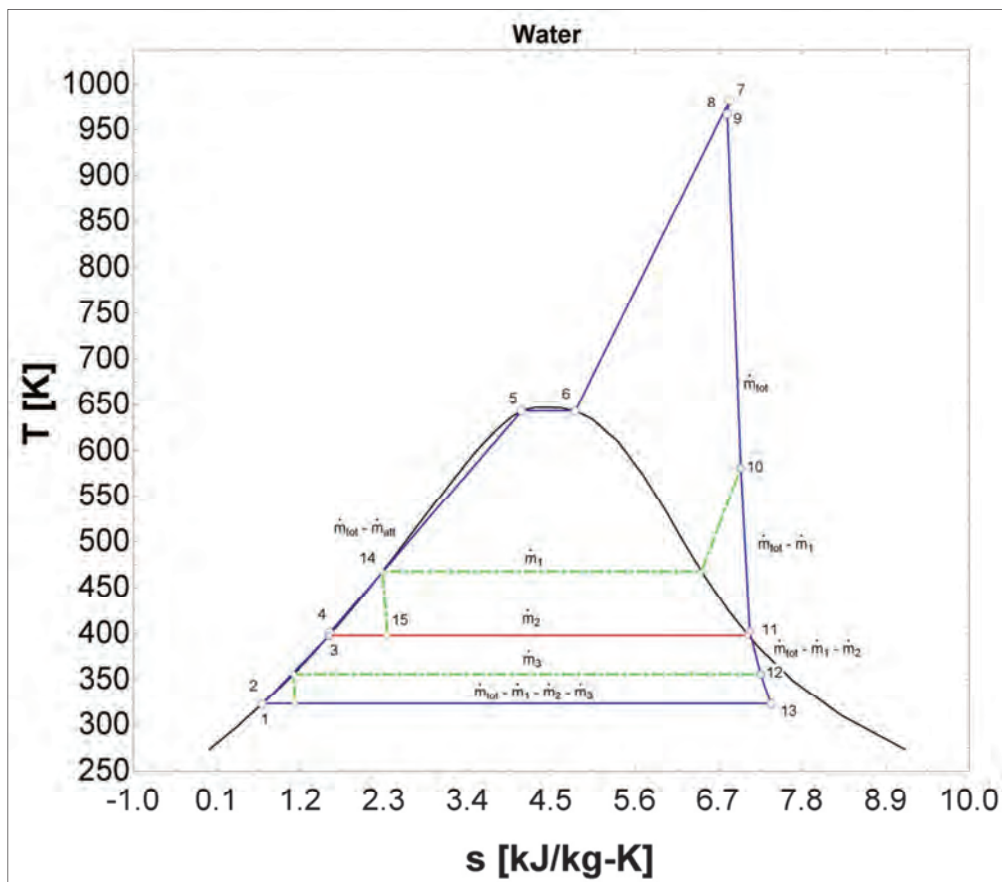


Figure 43 - $HX_{eff} = 90\%$; wct; Optimum cycle configuration; T-s diagram

Figure 43 shows a T-s diagram for a Rankine steam cycle with the de-aerator as the specified feed heater. The maximum cycle efficiency of this configuration is optimized to be 43.39%, with the net work maximised at 43.393 MW.

Table 34 - $HX_{eff} = 90\%$; wct; Optimum cycle configuration results

	Variable	Value	Unit
Energy Balance	E_b	0	MW
Cycle efficiency	η_R	43.39	%
Net work	W_{net}	43.393	MW
Turbine work	W_{turb}	44.436	MW
Pump work	W_{pumps}	1.043	MW
Heat input	Q_{in}	100	MW
Heat rejected	Q_{out}	56.607	MW
Total mass flow	\dot{m}_{tot}	33.63	kg/s
HP feed heater mass flow	$\dot{m}[1]$	4.069	kg/s
De-aerator mass flow	$\dot{m}[2]$	1.67	kg/s
LP feed heater mass flow	$\dot{m}[3]$	1.772	kg/s
Minimum Temperature	T_{min}	322.6	K
Maximum HPT Pressure	P_{max}	19	MPa
LPT outlet quality	x_{crit}	90.56	%
HX water inlet temperature	$T_{HX,i}$	467.7	K
HX water outlet temperature	T_{max}	967.5	K
Polytropic HPT efficiency	$\eta_{h,\infty}$	90.14	%
Polytropic LPT efficiency	$\eta_{l,\infty}$	79.83	%

Table 34 delivers various critical outputs and values of the limitation criteria set for this optimized cycle configuration. The maximum HPT inlet pressure is optimized at 19 MPa for maximum cycle efficiency. Due to the increased maximum cycle temperature, the maximum HPT inlet pressure (P_{\max}) is limited by the critical pressure of water (22.06) rather than the LPT outlet steam quality ($x_{\text{crit}} > 0.88$).

Steam flows through the Rankine cycle with a mass flow rate of 33.63 kg/s, as it is enforced by the conditions of the helium and the heat exchanger effectiveness. The polytropic turbine efficiencies are acceptably within the bounds as specified in section 7.2.

Table 35 - $HX_{\text{eff}} = 90\%$; wct; Optimum bleed points

	Description	Specified	Fraction		Pressure	
			Value	Unit	Value	Unit
r_{de}	De-aerator	X	0.01205	-	0.22895	MPa
$r_{\text{bs},1}$	Closed feed heater	✓	0.07279	-	1.38301	MPa
$r_{\text{bs},2}$	Closed feed heater	X	0.002794	-	0.053086	MPa

Optimized bleed point fractions and pressures for the various feed heaters, specified and otherwise, are shown in Table 35. These fractions are relative to the HPT inlet pressure. The specified feed heater is at 1.38301 MPa which is above the limitation set for de-aeration purposes.

8.5.2 DRY COOLING TOWER

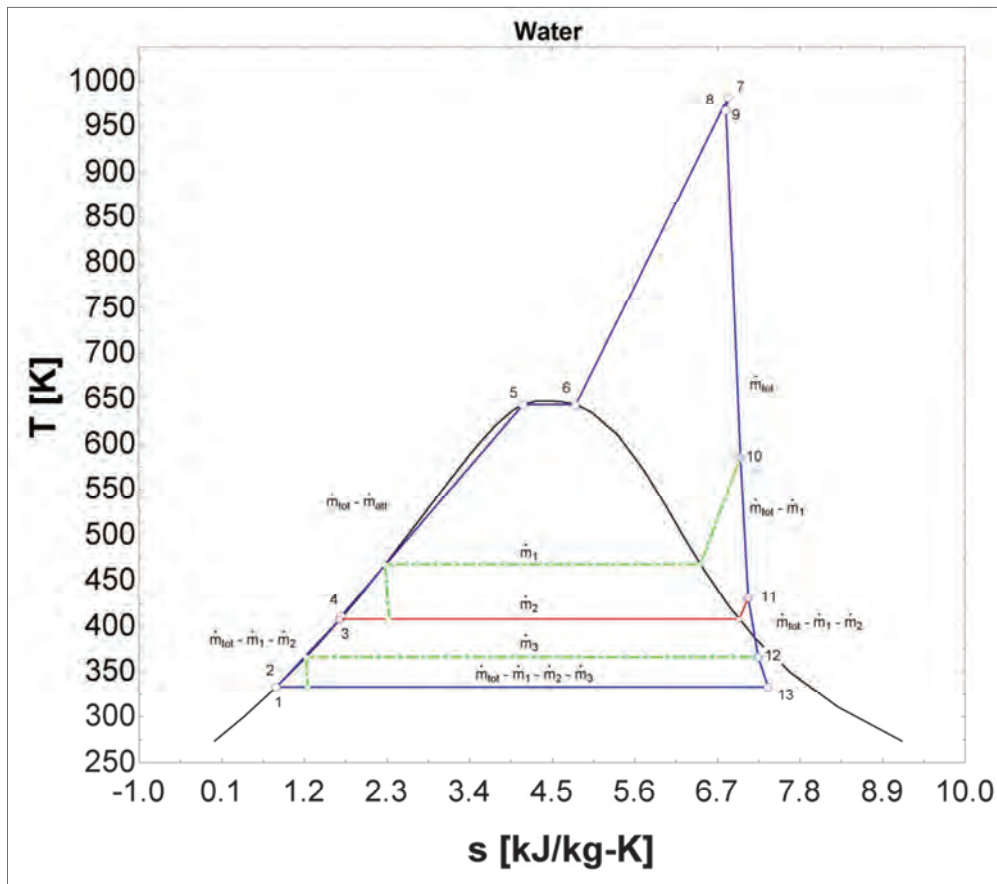


Figure 44 – $Hx_{eff} = 90\%$; dct; Optimum cycle configuration; T-s diagram

Figure 44 shows a T-s diagram for a Rankine steam cycle with the de-aerator as the specified feed heater. The maximum cycle efficiency of this configuration is optimized to be 41.87% with the net work maximised at 41.871 MW.

Various critical results of this optimised configuration are displayed in

Table 36. Water flows through the Rankine cycle at 33.63 kg/s and is a function of the heat exchanger effectiveness.

Limitations set for various variables, such as polytropic efficiencies and the LPT outlet steam quality, have been satisfied. The pressure limitation forced a sub-critical Rankine cycle.

Table 36 - $HX_{eff} = 90\%$; dct; Optimum cycle configuration results

	Variable	Value	Unit
Energy Balance	E_b	0	MW
Cycle efficiency	η_R	41.87	%
Net work	W_{net}	41.871	MW
Turbine work	W_{turb}	42.922	MW
Pump work	W_{pumps}	1.052	MW
Heat input	Q_{in}	100	MW
Heat rejected	Q_{out}	58.129	MW
Total mass flow	\dot{m}_{tot}	33.63	kg/s
HP feed heater mass flow	$\dot{m}[1]$	3.445	kg/s
De-aerator mass flow	$\dot{m}[2]$	1.831	kg/s
LP feed heater mass flow	$\dot{m}[3]$	1.79	kg/s
Minimum Temperature	T_{min}	332.6	K
Maximum HPT Pressure	P_{max}	19	MPa
LPT outlet quality	x_{crit}	92.36	%
HX water inlet temperature	$T_{HX,i}$	467.7	K
HX water outlet temperature	T_{max}	967.5	K
Polytropic HPT efficiency	$\eta_{h,\infty}$	89.27	%
Polytropic LPT efficiency	$\eta_{l,\infty}$	79.81	%

The optimum bleed point fractions and the corresponding bleed pressures for maximised cycle efficiency is shown in Table 37. These optimised bleed points also deliver a maximised net work output since the heat input into the cycle remain constant.

Table 37 – $HX_{eff} = 90\%$; dct; Optimum bleed points

	Description	Specified	Fraction		Pressure	
			Value	Unit	Value	Unit
r_{de}	De-aerator	X	0.01606	-	1.374	MPa
$r_{bs,1}$	Closed feed heater	✓	0.07279	-	0.3032	MPa
$r_{bs,2}$	Closed feed heater	X	0.004109	-	0.07759	MPa

8.6 HEAT EXCHANGER COMPARISON

To make an informative decision, the results of both the wet and dry cooling tower configurations need to be presented as a whole. Cycle efficiency and net work is the main optimising criteria.

Figure 45 is constructed to summarise the results of the various heat exchangers. Since the net work is in direct correlation to the cycle efficiency, it is not necessary to be included. The maximised cycle efficiency is shown for each heat exchanger effectiveness value.

The configurations where more effective heat exchangers than 85% are applied deliver greater cycle efficiency. If cost is not considered, the 87.5% heat exchanger effectiveness configuration would be preferred.

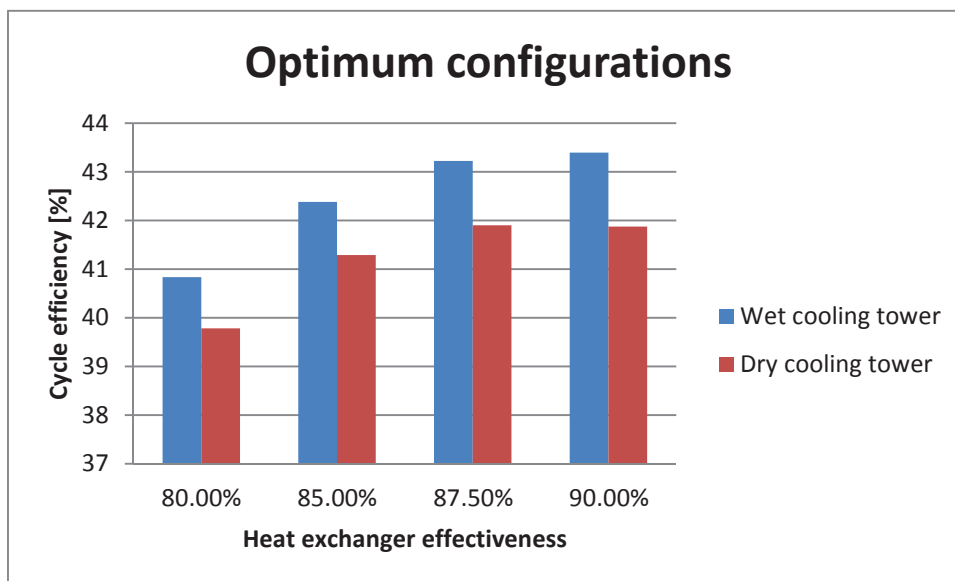


Figure 45 – Optimised configurations; η_R vs. HX_{eff}

With techno-economic constraints taken into account, the heat exchanger effectiveness of 85% is considered to be the optimum cycle configuration.

To confirm that these results are accurate, 85% heat exchanger configuration in combination with a wet cooling tower will be verified using alternative software modelling.

8.7 ELECTRICITY PRODUCTION

Although net work delivered by each cycle configuration is computed and illustrated as results, there are some losses that have not yet been accounted for, such as generator, transformer and transmission efficiencies.

- $\eta_{\text{Generator}} = 0.96$ [-]
- $\eta_{\text{Transformer}} = 0.98$ [-]
- $\eta_{\text{Transmission}} = 1$ [-]

The efficiency of the transmission is set to one due to the on-site construction of the thorium reactor and the PCU.

Table 38 – Optimum cycle configurations; Electric energy produced

	Units Generated	Units Sent Out
HX_{eff} (ε)	W_{net}	W_{electric}
[%]	[MW]	[MW _e]
Wet Cooling Tower		
80	40.825	38.408
85	42.376	39.867
87.5	43.216	40.658
90	43.393	40.824
Dry cooling tower		
80	39.775	37.420
85	41.287	38.843
87.5	41.904	39.423
90	41.871	39.392

Table 38 shows the electric energy delivered by the IPP after the efficiencies of the generator; transformer and transmission lines are incorporated. It is clear that all the optimum cycle configurations produce more electric energy than required by the cement production plant.

9 CHAPTER 9: MODEL VERIFICATION

9.1 INTRODUCTION

Results delivered by the simulation model must be verified. This verification process consists of two parts.

The primary objective is to prove that the Rankine cycle construction done in EES is accurate and credible. To prove this, a FlowNex simulation model is constructed. Temperature and enthalpy values as well as net work and cycle efficiency calculated by Flownex are used to verify the validity of the EES simulation model.

The secondary objective is to prove that the simulation model constructed in EES, delivers the optimised PCU. Excel in combination with its Xsteam macro is used for the construction of the alternative simulation model.

The optimised model for each heat exchanger configuration is verified using the Excel constructed simulation model. Heat exchangers with various effectiveness values are implemented as illustrated in Chapter 8 and available in APPENDIX 12.2.

Due to the models operating at higher than normal HPT inlet temperatures, the Rankine cycle can operate at maximum heat exchanger outlet pressure (19 MPa) without exceeding the LPT outlet quality limit (Section 0). Some limitations still need to be considered, such as the bleed pressure boundaries set for the de-aerator ($0.1 \text{ MPa} < r_{\text{De-aerator}} < 1 \text{ MPa}$).

It is also important that the temperature of the helium re-entering the reactor be 250 °C or higher, to avoid thermal shocks. For an increased maximum cycle temperature, it is necessary to increase the temperature of the Rankine working fluid by implementing feed heaters.

A maximum temperature limitation must be set for the feed heater with the highest bleed pressure. This enables the reactor working fluid to be cooled to 250 °C.

9.2 WET COOLING TOWER

The higher efficiency of the wet cooling tower decreases the minimum cycle temperature. Cycle efficiency is increased when wet cooling towers are implemented due to the increased difference between the minimum and maximum cycle temperatures.

The verification of the EES simulation model will only be done for the implementation of a wet cooling tower. The Rankine cycle results for the 85% heat exchanger will first be verified using a FlowNex simulation model. The optimum bleed point pressures for the feed heaters (from EES) will be verified using Excel (X-Steam).

9.2.1 $HX_{EFF}(E) = 85\%$

9.2.1.1 FLOWNEX

To construct the FlowNex simulation model various nodes need to be specified with pressure, temperature or quality values. The FlowNex simulation model is constructed from pipe; pump; turbine and heat transfer elements.

The FlowNex designer is implemented to calculate the various mass flow values, pressure drops and feed heater energy transfers. The FlowNex simulation model is available on the attached CD and an illustration can be seen in APPENDIX 12.4

Due to the specification of values at some nodes, enthalpy values will be verified. Pump work, turbine work delivered, heat input and heat rejected will all be used to measure the EES simulation model accuracy.

Table 39 displays the enthalpy values at the various nodes of the FlowNex model along with the corresponding EES variables. The difference between the EES and FlowNex enthalpies are listed in the last column.

Table 39 - HXeff = 85%; wct; Enthalpy verification; EES - FlowNex

	FlowNex Node	EES Variable	Unit	EES	FlowNex	Deviation
				Value		%
Enthalpy	1	h[1]	kJ/kg	207	206.831	0.08
	2	h[2]	kJ/kg	207.1	218.123	5.32
	3	h[3]	kJ/kg	423	423.055	0.01
	4	h[4]	kJ/kg	453.4	453.735	0.07
	5	h[5]	kJ/kg	1889	-	-
	6	h[6]	kJ/kg	2341	2339.21	0.08
	7	h[7]	kJ/kg	3751	-	-
	8	h[8]	kJ/kg	3711	3711.58	0.02
	9	h[9]	kJ/kg	3711	3710.45	0.01
	10	h[10]	kJ/kg	2868	2869.11	0.04
	11	h[11]	kJ/kg	2578	2579.68	0.07
	12	h[12]	kJ/kg	2447	2444.52	0.10
	13	h[13]	kJ/kg	2327	2324.95	0.09
	14	h _{bs,f} [1]	kJ/kg	682.5	682.781	0.04
	15	h _{bs,f} [2]	kJ/kg	306.1	307.876	0.58

The deviation column shows that all the FlowNex calculated values, excluding the extraction pump outlet (2), are within an acceptable deviation range. These deviations can be accredited to the variation in the steam tables or the pump and turbine charts used.

The FlowNex node 2 enthalpy is well beyond that calculated by the EES simulation model. This deviation (5.32%) can however be attributed to the graphs assigned to the extraction pump.

Although the FlowNex node 2 enthalpy has a deviation (11.023 kJ/kg) with respect to the EES value, the overall results are more comprehensive (Table 40).

The 150 kW additional pump work calculated (15.31%) is caused by the extraction pump graph. The increased enthalpy value of the extraction pump outlet in Table 39 is inaccurate and is the cause of the increased pump work.

Table 40 - HXeff = 85%; wct; Parameter verification; EES - FlowNex

			EES	FlowNex	Deviation
	Variable	Unit	Value		%
Energy Balance	E_b	MW	0	0.156	0.156
Cycle efficiency	η_R	%	42.38	42.19	0.45
Net work	W_{net}	MW	42.376	42.185	0.45
Turbine work	W_{turb}	MW	43.382	43.345	0.09
Pump work	W_{pumps}	MW	1.006	1.16	15.31
Heat input	Q_{in}	MW	100	100.012	0.01
Heat rejected	Q_{out}	MW	57.624	57.67	0.08
Total mass flow	\dot{m}_{tot}	kg/s	32.99	32.99	-
HP feed heater mass flow	$\dot{m}[1]$	kg/s	3.416	3.416	0.00
De-aerator mass flow	$\dot{m}[2]$	kg/s	1.134	1.134	0.00
LP feed heater mass flow	$\dot{m}[3]$	kg/s	1.313	1.353	3.05
Minimum Temperature	T_{min}	K	322.6	322.6	-
Maximum HPT Pressure	P_{max}	MPa	19	19	-
LPT outlet quality	x_{crit}	%	88.94	88.89	0.06
HX water inlet temperature	$T_{HX,i}$	K	435	431.471	0.81
HX water outlet temperature	T_{max}	K	934.8	934.065	0.08

When the pump work deviation is evaluated with relation to the overall cycle energy, the influence thereof is less than 0.154%. The inaccurate pump work is considered irrelevant for verifying the EES simulation model.

With the inaccurate pump work brought into calculation, the cycle efficiency and net work deviates with less than 0.5%. Heat added to the cycle and the turbine work output is accurate within 0.1%.

9.2.1.2 EXCEL (X-STEAM)

Excel (X-Steam) was used to determine the credibility of the optimised EES results. From Table 48 the bleed point values can be found as delivered by EES. According to the EES simulation model, these bleed points (fractions of the HP turbine inlet pressure) deliver maximum cycle efficiency and therefore maximum net work.

Table 41 - HXeff = 85%; wct; OPTIMUM verification; EES - Excel

			EES	Excel	Deviation
	Variable	Unit	Value		%
Energy Balance	E_b	MW	0	0	-
Cycle efficiency	η_R	%	42.38	42.39	0.02
Net work	W_{net}	MW	42.376	42.428	0.12
Turbine work	W_{turb}	MW	43.382	43.433	0.12
Pump work	W_{pumps}	MW	1.006	1.005	0.10
Heat input	Q_{in}	MW	100	100.09	0.09
Heat rejected	Q_{out}	MW	57.624	57.662	0.07
Total mass flow	\dot{m}_{tot}	kg/s	32.99	32.98	0.03
HP feed heater mass flow	$\dot{m}[1]$	kg/s	3.416	3.41	0.18
De-aerator mass flow	$\dot{m}[2]$	kg/s	1.134	1.134	0.00
LP feed heater mass flow	$\dot{m}[3]$	kg/s	1.313	1.314	0.08
Minimum Temperature	T_{min}	K	322.6	322.6	-
Maximum HPT Pressure	P_{max}	MPa	19	19	-
LPT outlet quality	x_{crit}	%	88.94	88.99	0.06
HX water inlet temperature	$T_{HX,i}$	K	435	434.91	0.02
HX water outlet temperature	T_{max}	K	934.8	934.91	0.01
HP closed feed heater	$r_{bs}[1]$	-	0.03405	?	-
De-aerator	r_{de}	-	0.00555	?	-
LP closed feed heater	$r_{bs}[2]$	-	0.001884	?	-

Figure 46 shows the change in Rankine cycle efficiency as the bleed point fraction of the HP closed feed heater is increased from 0.01 to 0.06. The cycle efficiency increases as the bleed pressure is increased.

An upper limit is set for the top most feed heater, as to extract all the energy from the reactor working fluid. This upper temperature limit is represented by the **blue line**. The optimum bleed fraction for the HP closed feed heater is therefore approximately $r_{bs}[1] = 0.034$. This bleed fraction delivers maximum cycle efficiency and therefore maximum net work.

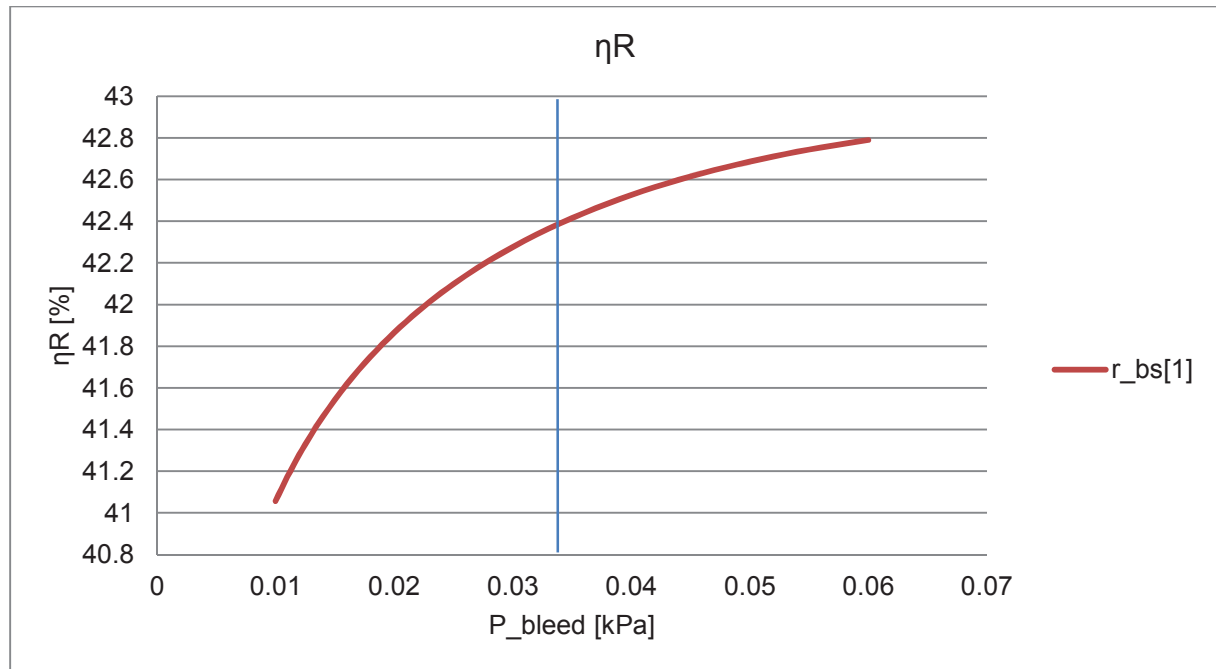


Figure 46 - HXeff = 85%; wct; HP closed feed heater; Verification

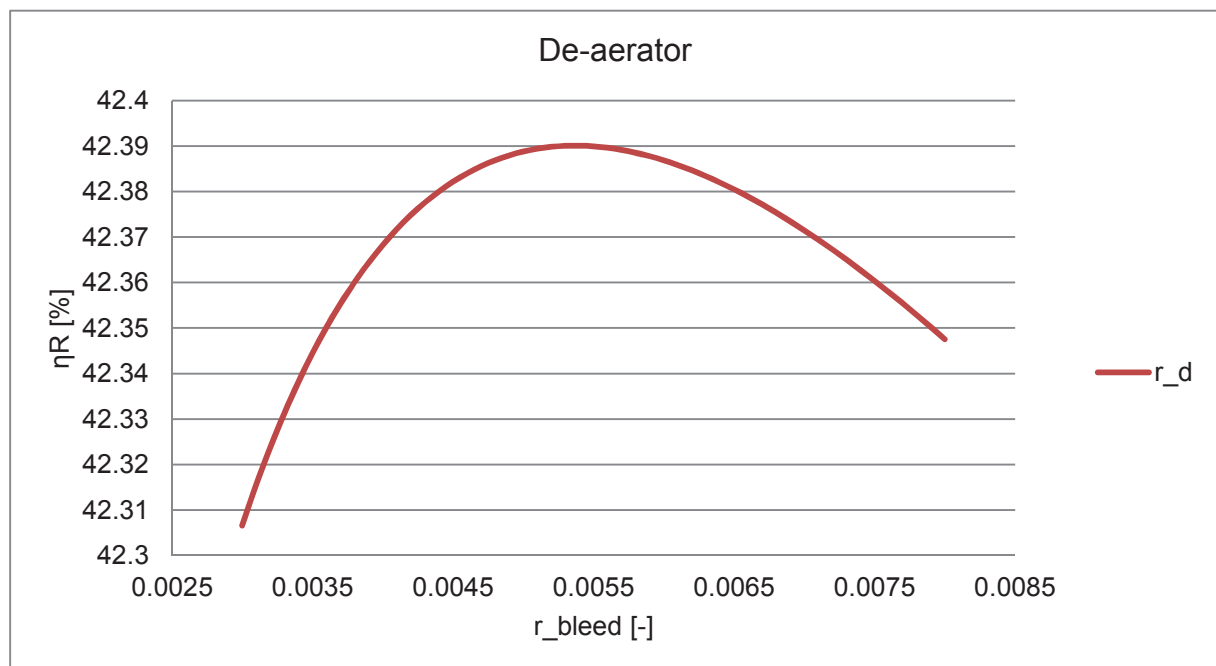


Figure 47 - HXeff = 85%; wct; De-aerator; Verification

Change in cycle efficiency is shown as a function of the increasing de-aerator bleed point fraction in Figure 47. This fraction is relative to the HPT inlet pressure. The secondary function of the de-aerator is eradicating non-dissolved gasses from the Rankine working fluid.

Limits are therefore set for the de-aerator bleed point at 100 kPa and 1 MPa. These limits are however not required in this case due to the optimum bleed fraction being indicated by the graph. Cycle efficiency and net work is maximised at a de-aerator bleed point fraction of 0.0055.

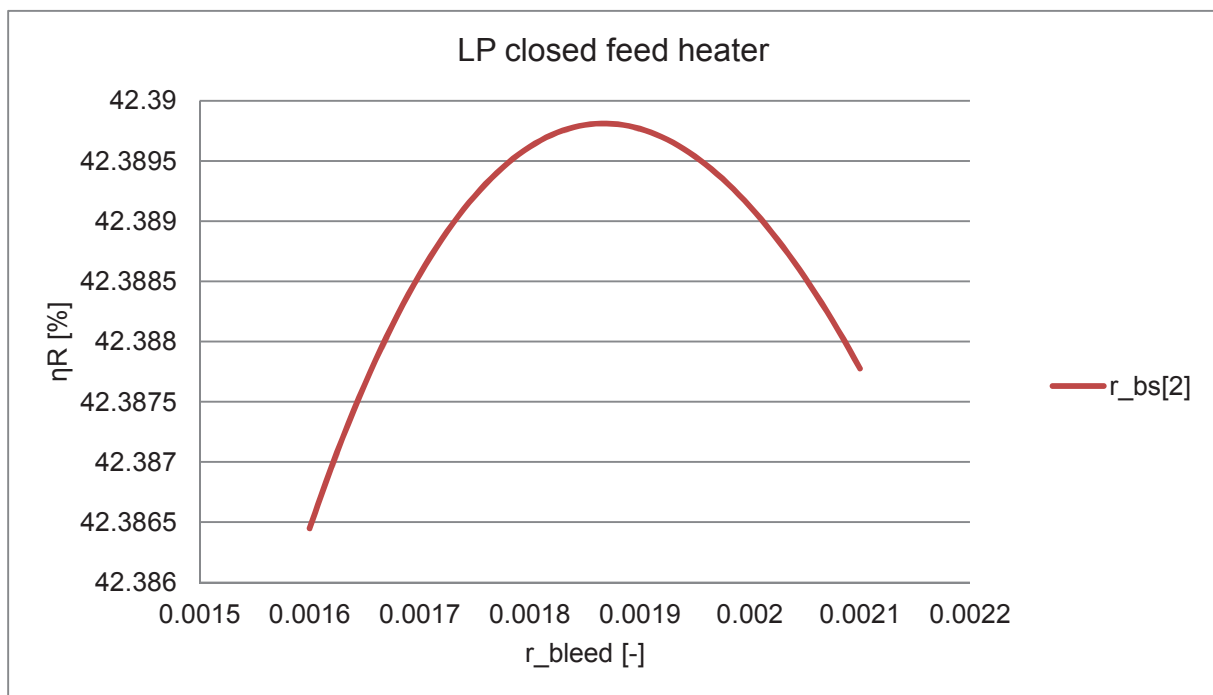


Figure 48 - HXeff = 85%; wct; LP closed feed heater; Verification

Once again the optimum value for the bleed point fraction of the LP closed feed heater is evident in Figure 48. The change in cycle efficiency is shown as the bleed fraction is increased from 0.0016 to 0.0021.

Maximum cycle efficiency and maximum net work is delivered at a LP closed feed heater bleed fraction of approximately $r_{bs} [2] = 0.00185$.

Table 42 – $HX_{eff} = 85\%$; wct; EES versus Excel

	EES	Excel	Accuracy
η_R	42.38	42.39	0.02%
$r_{bs} [1]$	0.03405	0.034	0.15%
r_{de}	0.00555	0.0055	0.90%
$r_{bs} [2]$	0.00188	0.00185	1.80%

10 CHAPTER 10: CONCLUSIONS AND RECOMMENDATIONS

10.1 BACKGROUND

Due to unreliable electric energy supply in India, HOLCIM cement deemed it necessary to investigate the viability of installing an IPP to supply their energy needs. Although coal is abundant in India, the supply thereof is unable to meet the demand due to an insufficient production rate.

Installation of a small thorium HTR is proposed to supply the cement production plant with the required electric energy. The selection of a 100 MW_t thorium HTR is motivated by:

- Cement production consumes 26 MW_e on one of these production plants. Since it is ideal to operate the cement plant independent of external electric energy sources, it is necessary for the PCU to produce more than 26 MW_e.
- The enactment of the Electricity Act 2003 in India, enabled industry owned (IPP) power plants to supply electric energy to the Indian distribution network. It is therefore possible to generate revenue by selling any additional energy to the Indian distribution network.
- The existing structure and processes implemented on these cement production plants are optimised processes. High energy waste heat from the cement production process is recovered and utilised for pre-heating and drying processes. Integration with the IPP for an existing cement production plant is not viable.

Implementation of a Rankine steam cycle is necessary to convert the thermal energy delivered by the reactor to mechanical energy for the production of electricity.

10.2 SUMMARY

- The 100 MW_t thorium HTR (Chapter 5.3):
 - Reactor operates continually at its maximum continuous rating.
 - Reactor working fluid (coolant) - Helium.

Table 43 - Reactor specifications

	Variable	Specification	Unit
Helium mass flow	\dot{m}_r	38.55	kg/s
Reactor outlet temperature	$T_{r_{max}}$	750	°C
Reactor inlet temperature	$T_{r_{min}}$	250	°C
Thermal energy output	Q_r	100	MW

- Coal fired Rankine cycle (section 5.5.1):
 - Maximum cycle temperature (T_{max}) $\leq 540^\circ\text{C}$.
 - Inexpensive materials are used.
 - High heat transfer losses.
- Heat exchanger (Chapter 6):
 - Counter-flow - Helium \leftrightarrow Water/Steam.
 - Effectiveness: 80%, 85%, 87.5% and 90%.
 - $HX_{eff} = 85\%$ is recommended:

Table 44 - Heat exchanger; Rankine working fluid

	Variable	Value	Unit
Rankine total mass flow	\dot{m}_{tot}	32.99	kg/s
Reactor outlet temperature	T_{max}	661.6	°C
Reactor inlet temperature	$T_{HX,i}$	161.8	°C
Thermal energy input	Q_{in}	100	MW

- Super heater tube material (Chapter 0):
 - SAE 436 ferritic stainless steel.
 - High corrosion resistance.
 - Continuous operating temperature $> T_{\max}$ used.
- Rankine cycle component exclusions (Chapter 4):
 - Components are weighed against techno-economic considerations.
 - Reheating - not feasible.
 - Steam turbine driven feed pumps - not feasible.
 - More than one de-aerator - not feasible.
- Cooling tower (sections 4.4.5 and 4.4.6):
 - Multiple construction locations in India.
 - Average ambient temperature across India: 24.4°C.
 - Water availability is unknown.
 - Wet and Dry cooling tower calculations were done.
- Feed heater specification (Section 6.2):
 - Rankine working fluid must be heated to $T_{HX,i}$.
 - $T_{HX,i}$ is a function of the HX_{eff} .
 - Regenerative feed heating must be implemented.
 - The topping (high pressure) feed heater must be specified to the $T_{HX,i}$.

A simulation model was constructed in EES, which allowed the Rankine cycle to be optimised for maximised thermal efficiency and consequently net work. Various Rankine cycle configurations were accommodated and numerous limitations were imposed.

Combinations of de-aerators, closed feed heaters, reheating, attemperation and steam driven feed pumps can all be evaluated in the Rankine cycle simulation models. Out of the norm parameters and limitations such as an increased maximum cycle temperature were accommodated.

- Limitations (Chapter 4.4):
 - Heat exchanger outlet pressure - $P_{\max} \leq 19 \text{ MPa}$.
 - LPT outlet steam quality - $x_{\text{crit}} \geq 88\%$.
 - De-aerator bleed pressure - $0.1 \text{ MPa} \leq P_{\text{de}} \leq 1 \text{ MPa}$.
 - HPT polytropic efficiency - $88\% \leq \eta_{h,\infty} \leq 90\%$
 - LPT polytropic efficiency - $79\% \leq \eta_{l,\infty} \leq 81\%$
- Optimising criteria (Chapter 4.5):
 - Cycle efficiency and net work was maximised (Q_{in} remain constant).
 - Heat exchanger outlet pressure (P_{\max}) was optimised.
 - Feed heater bleed pressure fractions (r) were optimised.

10.3 RECOMMENDATIONS

Following the process as described in the summary of this chapter, various optimum cycle configurations were computed by the simulation model. These optimum cycle configurations are differentiated according to the type of cooling tower implemented.

Independent of the cooling tower type, the heat exchanger configuration with 85% effectiveness is recommended as the optimum cycle configuration. Accounting for techno-economic considerations, justifies the implementation of the 85% effective heat exchanger.

If an adequate water source is available, it is recommended that a wet cooling tower is utilised. The wet cooling tower has an approximate 1% positive influence on the Rankine cycle efficiency, which leads to a 1 MW increase for the units generated (W_{net}).

Results for the optimum cycle configurations are summarised in the sections below:

10.3.1 WET COOLING TOWER

For a wet cooling tower with an ambient temperature of 24.4°C ($T_1 = 30.4$ °C), the minimum cycle temperature was calculated to be 49.4°C ($T_{min} = 322.6$ K). Attenuation of 15°C was applied. Neither reheating nor steam turbine driven feed pumps were utilised for these Rankine cycle designs as neither was considered techno-economic for such a low mass flow Rankine cycle.

Table 45 – Optimised cycle configurations; Wet cooling tower; Summary

HX_{eff} (%)	η_R	W_{net}	x_{crit}	P_{max}	T_{max}	$T_{HX\ c,i}$	P_{de}	\dot{m}_{tot}	FH_{closed}	
[%]	[%]	[MW]	[%]	[MPa]	[K]	[K]	[MPa]	[kg/s]	#	Specified
80	40.83	40.825	88	17.6	898	398.2	0.2141	32.44	2	X
85	42.38	42.376	88.94	19	934.8	435	0.1048	32.99	2	✓
87.5	43.22	43.216	89.97	19	951.6	451.8	0.921	33.59	2	X
90	43.39	43.393	90.56	19	967.5	467.7	0.2274	33.63	2	✓

Table 45 summarises the main parameters of the optimised cycle configurations for the various heat exchangers with a wet cooling tower implemented.

10.3.2 DRY COOLING TOWER

The cooling water at the condenser inlet was $T_1 = 40.4^\circ\text{C}$, for an ambient temperature of 24.4°C . This delivered a minimum cycle temperature of 59.4°C ($T_{\min} = 332.6 \text{ K}$). Attenuation of 15°C was incorporated for control purposes. Neither reheating nor steam turbine driven feed pumps were utilised for these Rankine cycle designs as neither was considered techno-economic for such a low mass flow Rankine cycle.

Table 46 – Optimised cycle configurations; Dry cooling tower; Summary

HX_{eff} (%)	η_R	W_{net}	x_{crit}	P_{max}	T_{max}	$T_{HX \text{ c,i}}$	P_{de}	\dot{m}_{tot}	FH_{closed}	
[%]	[%]	[MW]	[%]	[MPa]	[K]	[K]	[MPa]	[kg/s]	#	Specified
80	39.78	39.775	88.37	19	898	398.2	0.2311	32.7	2	X
85	41.29	41.287	90.11	19	934.8	435	0.6429	33.36	2	X
87.5	41.9	41.904	90.83	19	951.6	451.8	0.921	33.59	2	X
90	41.87	41.871	92.36	19	967.5	467.7	0.3032	33.63	2	✓

10.4 CONCLUSIONS

The (100 MW_t) thorium HTR requires a PCU to convert the thermal energy delivered by the reactor to kinetic and therefore electric energy. Designing and optimising the Rankine steam cycle for this application allows for out of the norm operating parameters (T_{max}).

Depending on the effectiveness of the heat exchanger and the type of cooling tower implemented, optimum cycle configurations were determined using the EES simulation model. The units sent out of every optimum configuration are shown to be greater than 37 MW (Table 47).

Table 47 – Optimum cycle configurations; Electric energy produced

	Units Generated	Units Sent Out
HX _{eff} (ε)	W _{net}	W _{electric}
[%]	[MW]	[MW _e]
Wet Cooling Tower		
80	40.825	38.408
85	42.376	39.867
87.5	43.216	40.658
90	43.393	40.824
Dry cooling tower		
80	39.775	37.420
85	41.287	38.843
87.5	41.904	39.423
90	41.871	39.392

Implementing a wet cooling tower in combination with a heat exchanger with 85% effectiveness is the recommended Rankine cycle configuration.

The Rankine steam cycle powered by the thorium HTR is a suitable solution for the HOLCIM energy crisis in India. This IPP not only produces the energy required for the cement production plant, but produces additional energy that can be sold to the Indian distribution network.

10.5 FUTURE STUDY

Detailed design for the Rankine cycle components are not in the scope of this dissertation. The main focus of this dissertation was to design, simulate and optimise a Rankine steam cycle power by a thorium HTR.

As such, detailed turbine design for the higher temperature conditions needs to be developed. More detailed design for the condenser – cooling tower combination is also required.

The critical role of the heat exchanger interfacing the thorium HTR and the Rankine steam cycle requires further design and material selection. This is due to the multi-phase on the Rankine working fluid and the higher temperature than in fossil fired applications.

11 REFERENCES

1. ALI, M.F. 2011. Chapter 6: Generation III Advanced Nuclear Reactors – Part 1. <http://intuitech.biz/chapter-6-generation-iii-advanced-nuclear-reactors-%e2%80%93-part-1/> Date of use: 21 June 2012.
2. ANONOMOUS. 2012. Small Nuclear Power Reactors. <http://www.world-nuclear.org/info/inf33.html>. Date of use: 22 June 2012.
3. CEMEX. 2011. How we produce cement. http://www.cemexbangladesh.com/ce/ce_cb_pf.html. Date of use: 06 July 2012.
4. ELDER, R. & ALLEN, R. 2009. Nuclear heat for hydrogen production: Coupling a very high/high temperature reactor to a hydrogen production plant. Progress in Nuclear Energy. Vol: 51. p. 500 – 525.
5. ENERGYEFFICIENCYASIA. 2010. http://www.energyefficiencyasia.org/docs/IndustrySectorsCement_draftMay05.pdf. Date of use: 19 June 2012.
6. GESCHWINDT, J.R., LOMMERS, L.J., SOUTHWORTH, F.H. & SHAHROKHI, F. 2011. Performance and optimization of an HTR cogeneration system. Nuclear Engineering and Design. p. 297 - 301.
7. HOLCIM. 2010. Annual Report 2010 Holcim Ltd. http://www.holcim.com/fileadmin/templates/CORP/doc/e-reports/AR_2010/. Date of use: 19 March 2012.
8. HOLCIM. 2012. How we make cement. <http://www.holcim.com/en/products-and-solutions/processes/how-we-make-cement.html>. Date of use: 19 March 2012.
9. INCROPERA, F.P., DEWITT, D.P., BERGMAN, T.L. & LAVINE, A.S. 2007. Fundamentals of Heat and Mass transfer. 6th ed. John Wiley & Sons. p. 678 – 690.
10. JACOTT, M., COMUNES, F., REED, C., TAYLOR, A. & WINFIELD, M. 2003. Commission for Environmental Cooperation 2nd North American Symposium on Assessing the Environmental Effects of Trade. Energy Use in the Cement

- Industry in North America: Emissions, Waste Generation and Pollution Control, 1990-2001. p. 12-14.
11. JANKOVIC, A., VALERY, W. & DAVIS, E. 2004. Minerals Engineering. Cement Grinding Optimisation. p.1075 – 1081.
12. JEONG-SEONG, I. 2012. POSCO Research Institute. Worsening power shortages in India due to coal production disruption. p. 1-7.
13. KUGELER, K. 2009. HTR technology. Potchefstroom: North-West University. (Study guide.)
14. LAMARSH, J.R. & BARATTA, A.J. 2001. Introduction to Nuclear Engineering. 3rd ed. Prentice Hall. p. 137-161, 252.
15. LIOR, N. 1997. Advanced energy conversion to power. Energy Conversion Magazine. Mgm. Vol. 38. p. 941 - 955.
16. MULDER, E. 2012. Steenkampskraal Thorium Ltd. CEO. India HOLCIM cement project initiator, concept design.
17. REMME, U. & TRUDEAU, N. 2011. International Energy Agency Informational Paper. Technology Development Prospects for the India Power Sector. p. 1-88.
18. SASSDA. 2013. Moly Ferritic Stainless steels – Technical brochure. Date of use: 17 August 2013.
19. STEINWARZ, W. 1987. Modular high-temperature reactor launched. *Modern power systems*. 7(8): 45 - 53.
20. STORM, C.P. & KLOPPERS, C.P. 2013. Thermo-fluid systems design. Potchefstroom: North-West University. (Study guide.)
21. SUGISITA, H., MORI, H. & UEMATSU, K. 1998. A Study of thermodynamic cycle and system configurations of hydrogen combustion turbines. International Journal of Hydrogen Energy. Vol. 23. p.705 - 712.
22. WEATHERBASE. 2013. INDIA – Weather averages. <http://www.weatherbase.com/weather/city.php3?c=IN&countryname=India>[http://www](http://www.weatherbase.com/weather/city.php3?c=IN&countryname=India)

www.holcim.com/fileadmin/templates/CORP/doc/e-reports/AR_2010/. Date of use: 15 August 2013.

23. WNA (World Nuclear Association). 2012. Small Nuclear Power Reactors. <http://www.world-nuclear.org/info/inf33.html> Date of use: 22 June 2012.
24. WNA (World Nuclear Association). 2012 [2]. Supply of Uranium. <http://www.world-nuclear.org/info/Nuclear-Fuel-Cycle/Uranium-Resources/Supply-of-Uranium/>. Date of use: 30 January 2014.
25. WNA (World Nuclear Association). 2013. Thorium. <http://www.world-nuclear.org/info/Current-and-Future-Generation/Thorium/>. Date of use: 30 January 2014.
26. YEP, E. 2012. Wall Street Journal. Power Problems Threaten Growth in India. <http://online.wsj.com/article/SB10001424052970203550304577136283175793516.html> Date of use: 20 June 2012.
-

12 APPENDICES

12.1 EES

12.1.1 SIMULATION MODEL

Since a PCU is required for the thorium HTR, the construction of an adequate simulation model is necessary to simulate and optimise the criteria of the Rankine steam cycle. Due to the small nature of the thorium HTR, the Rankine cycle design has specific parameters and limitations such as the economic feasibility of steam-turbine driven feed pumps, the amount of feed heaters, etc.

To determine the optimum configuration for the Rankine steam cycle various simulation models need to be constructed and optimised. Due to the timely and arduous nature of such a project, it was decided not to compare various simulation models with each other, but rather compile one simulation model that can meet the terms of all the various configuration possibilities for the Rankine steam cycle design.

Chapter 4: Rankine cycle development, demonstrates the effect of various component additions to the Rankine cycle. These configuration possibilities include the incorporation of attemperation, amount of contact and closed feed heaters, reheat, steam turbine driven feed pumps, etc. The simulation model also accommodates the possibility of out of the norm Rankine cycle parameters.

Using the limitation parameters as specified in Chapter 5: Design Considerations, a simulation model is constructed. Various input parameters and configuration options are integrated into the simulation model, allowing the model to adapt to various requirements. Due to economic, viability and feasibility considerations, the ability to compare various design possibilities are vital to obtain the optimum configuration.

12.1.2 PROCEDURE

12.1.2.1 INPUT PARAMETERS

Figure 49 represents the parameter input window of the simulation model. Inputs for this window include the limitations of the Rankine cycle as discussed in section 0 as well as efficiency losses of the actual Rankine cycle. Crucial additional inputs such as the mass flow of the PCU and attemperation ΔT are also included.

The screenshot shows a window titled "INPUT Variables" with the following parameters and values:

- $T_{atm} = 293.2$ [K]
- $T_r = 20$ [C]
- $T_c = 3$ [C]
- $TTD = 2$ [C]
- $T_{max} = 813.2$ [K]
- $\Delta T_{att} = 15$ [C]
- $m_{tot} = 32$ [kg/s]
- $\eta_p = 0.83$ [-]
- $\eta_{hp,t} = 0.91$
- $\eta_{lp,t} = 0.88$ [-]
- $\eta_{SFP} = 0.88$ [-]

Figure 49 - Parameter INPUT window

Section 4.4.4 shows that the minimum temperature of the Rankine cycle is a function of T_{atm} , T_r , T_c and TTD

$$T_{min} = T_{atmosphere} + T_r + T_c + TTD \quad (11)$$

All efficiency inputs (η) are polytropic. The input parameters only allow for high and low pressure turbine efficiencies, as intermediate pressure turbine efficiency is assumed to equal that of the high pressure turbine.

Efficiency of steam turbine driven feed pumps (η_{SFP}) are only used for the simulation, if the design specifies the implementation thereof.

12.1.2.2 CONFIGURATION

To incorporate steam turbine driven feed pumps, the radio button of the specific pump has to be changed to “yes” in Figure 50. FTP_{inlet} allows the user to specify the inlet pressure for the steam turbines driving the feed pumps. FTP_{inlet} is specified by the slider. The slider value refers to the pressure of a bleed point for a feed heater (closed or contact), starting at the highest pressure and descending.

Figure 50 - Steam turbine driven feed pump INPUT window

Starting at the pump delivering the highest pressure, the order of the radio buttons descend according to pressure delivered by the specific pump. Figure 50 allows for 5 pumps not including the extraction pump, as the simulation model allows for a maximum of 5 de-aerators (contact feed heaters).

Figure 51 - Feed heater and Reheat INPUT window

Figure 51 shows the input window for the configuration of the cycle. The amount of de-aerators determines the number of feed pumps. These inputs therefore specify the amount of feed pumps and whether or not the steam is reheated after the high pressure turbine

expansion. The amount of closed feed heaters must also be specified in this window. The amount of closed feed heaters is limited to 10.

Once all the above parameters are specified, the Rankine cycle can be simulated. To determine the optimum cycle efficiency, various variables are not specified as each contributes to the optimum cycle efficiency. These variables are optimisation parameters, as the cycle efficiency is a function thereof.

12.1.2.3 OPTIMISING PARAMETERS

Maximum cycle pressure (P_{\max}) is dependent of the steam quality at the low pressure turbine outlet as explained in section 4.4.3. Low pressure turbine outlet steam quality is a function of the amount of feed heaters; the pressure fraction at which each is bled from and whether or not a reheat is part of the cycle configuration.

Minimising heat energy injected into the cycle relative to maximum net work is critical to maximise cycle efficiency. Heat energy added to the cycle is constant since the thorium reactor continually runs at its maximum continuous rating (section 4.5). For efficiency to be maximised, net work needs to be at a maximum. Which in turn implies that the work delivered by the turbine combination needs to be maximised.

Feed heating requires a fraction of the working fluid to be bled from the turbine. Reducing the mass flow through the turbine decreases the work delivered by the turbine. It is therefore crucial that the various pressure fractions, at which steam is bled from the turbine, are optimised for maximum cycle efficiency.

Subsequently, the maximum cycle pressure is dependent on the various pressure fractions at which steam is bled from the turbine, as well as the amount of feed heaters throughout the cycle. It then follows that, as the various pressure fractions need to be optimised, so too must maximum cycle pressure be optimised for maximum cycle efficiency. It is crucial that these variables be optimised simultaneously to avoid an endless loop situation as the bleed points are fractions of turbine inlet pressure (reheat = IPT, else HPT).

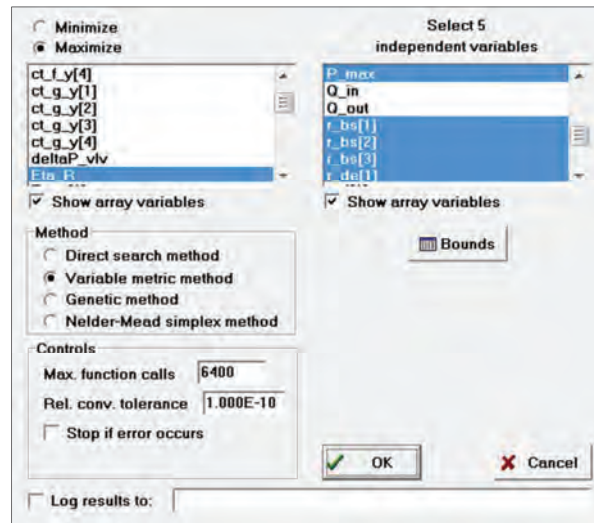


Figure 52 - Optimisation criteria vs. parameters

Figure 52 refers to the min/max function window of EES. Maximum cycle pressure and the amount of feed heaters selected for the specific configuration need to be selected as independent variables. These independent variables require bounds (limits) to specify the values for which each is defined. As the pressure fractions of the bleed points are fractions of turbine inlet pressure (reheat = IPT, else HPT), $0.0001 < r < 0.9999$. Maximum cycle pressure is limited by the critical pressure of water as discussed in section 4.4.2.

To compute the maximum cycle efficiency, the optimising process must be able to alternate the order of the closed and contact feed heaters. Such that the highest bleed point pressure can either be a de-aerator or a closed feed heater. Cycle efficiency (η_R) will therefore be maximized by computing the optimum bleed points and configuration combination of the selected independent variables.

12.1.2.4 RESULTS WINDOW

After the optimum configuration combination with regards to maximum cycle efficiency is determined, the relevant results need to be shown as output values. An energy balance is done to verify the validity and accurateness of the specific simulation.

As seen in Figure 53, various critical values (η_R , E_b , P_{max} , x_{crit}) are shown as well as work and heat energy in and out of the system. These values are shown, as they are critical for comparison to other cycle configurations and economic or requirement satisfaction.

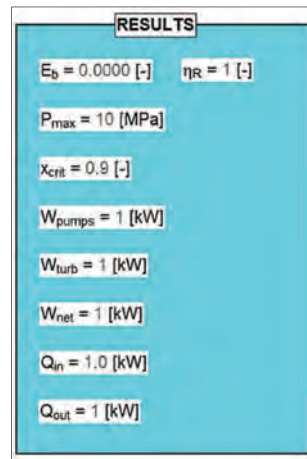


Figure 53 - Simulation model result OUTPUT window

Parameters shown as results do however not entirely illustrate the optimum cycle configuration. To find the optimum configuration it is important to specify the computed bleed point pressure fractions. These pressure fractions can be seen in Figure 54.

Optimised fractions are fractions of turbine inlet pressure (reheat = IPT, else HPT). Closed feed heater fractions are represented by r_{bs} and de-aerator fractions are represented by r_{de} .

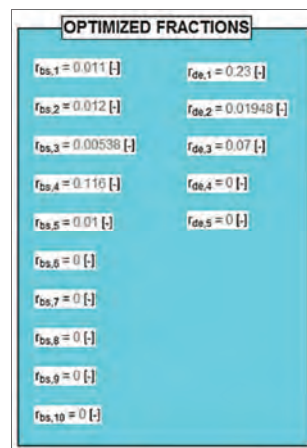


Figure 54 - Simulation model Optimised fraction window

12.2 EES OPTIMISED RESULTS

The full spectrum of results is available in the Appendices on the attached CD.

12.2.1 WET COOLING TOWER

12.2.1.1 $HX_{EFF} = 80\%$

RESULTS	
$E_b = 0.0000$ [kW]	$\eta_R = 0.4083$ [-]
$W_{net} = 40825$ [kW]	$\dot{m}_{tot} = 32.44$ [kg/s]
$W_{turb} = 41757$ [kW]	$P_{max} = 17.6$ [MPa]
$W_{pumps} = 932$ [kW]	$T_{max} = 898$ [K]
$Q_{in} = 100000.0$ [kW]	$T_{HX,i} = 398.2$ [K]
$Q_{out} = 59175$ [kW]	$P_{de} = 0.2141$ [MPa]
$\dot{m}_r = 38.55$ [kg/s]	$\eta_{h, infinity} = 0.8889$ [-]
$x_{crit} = 0.88$ [-]	$\eta_{l, infinity} = 0.794$ [-]

Figure 55 - $HX_{eff} = 80\%$; wct; Results

12.2.1.2 $HX_{EFF} = 85\%$

RESULTS	
$E_b = 0.0000$ [-]	$\eta_R = 0.4238$ [-]
$W_{net} = 42376$ [kW]	$\dot{m}_{tot} = 32.99$ [kg/s]
$W_{turb} = 43382$ [kW]	$P_{max} = 19$ [MPa]
$W_{pumps} = 1006$ [kW]	$T_{max} = 934.8$ [K]
$Q_{in} = 100000.0$ [kW]	$T_{HX,i} = 435$ [K]
$Q_{out} = 57624$ [kW]	$P_{de} = 0.1048$ [MPa]
$\dot{m}_r = 38.55$ [kg/s]	$\eta_{h, infinity} = 0.8944$ [-]
$x_{crit} = 0.8894$ [-]	$\eta_{l, infinity} = 0.8058$ [-]

Figure 56 - $HX_{eff} = 85\%$; wct; Results

12.2.1.3 $HX_{EFF} = 87.5\%$

RESULTS	
$E_b = 0.0000 [-]$	$\eta_R = 0.4322 [-]$
$W_{net} = 43216 \text{ [kW]}$	$\dot{m}_{tot} = 33.59 \text{ [kg/s]}$
$W_{turb} = 44307 \text{ [kW]}$	$P_{max} = 19 \text{ [MPa]}$
$W_{pumps} = 1091 \text{ [kW]}$	$T_{max} = 951.6 \text{ [K]}$
$Q_{in} = 100000.0 \text{ [kW]}$	$T_{HX,i} = 451.8 \text{ [K]}$
$Q_{out} = 56784 \text{ [kW]}$	$P_{de} = 0.921 \text{ [MPa]}$
$\dot{m}_r = 38.55 \text{ [kg/s]}$	$\eta_{h, infinity} = 0.8997 [-]$
$x_{crit} = 0.8943 [-]$	$\eta_{l, infinity} = 0.7949 [-]$

Figure 57 - $HX_{eff} = 87.5\%$; wct; Results

12.2.1.4 $HX_{EFF} = 90\%$

RESULTS	
$E_b = 0.0000 [-]$	$\eta_R = 0.4339 [-]$
$W_{net} = 43393 \text{ [kW]}$	$\dot{m}_{tot} = 33.63 \text{ [kg/s]}$
$W_{turb} = 44436 \text{ [kW]}$	$P_{max} = 19 \text{ [MPa]}$
$W_{pumps} = 1043 \text{ [kW]}$	$T_{max} = 967.5 \text{ [K]}$
$Q_{in} = 100000.0 \text{ [kW]}$	$T_{HX,i} = 467.7 \text{ [K]}$
$Q_{out} = 56607 \text{ [kW]}$	$P_{de} = 0.2274 \text{ [MPa]}$
$\dot{m}_r = 38.55 \text{ [kg/s]}$	$\eta_{h, infinity} = 0.9014 [-]$
$x_{crit} = 0.9056 [-]$	$\eta_{l, infinity} = 0.7983 [-]$

Figure 58 - $HX_{eff} = 90\%$; wct; Results

12.2.2 DRY COOLING TOWER

12.2.2.1 $HX_{EFF} = 80\%$

RESULTS	
$E_b = 0.0000$ [kW]	$\eta_R = 0.3978$ [-]
$W_{net} = 39775$ [kW]	$\dot{m}_{tot} = 32.7$ [kg/s]
$W_{turb} = 40791$ [kW]	$P_{max} = 19$ [MPa]
$W_{pumps} = 1016$ [kW]	$T_{max} = 898$ [K]
$Q_{in} = 100000.0$ [kW]	$T_{HX,i} = 398.2$ [K]
$Q_{out} = 60225$ [kW]	$P_{de} = 0.2311$ [MPa]
$\dot{m}_r = 38.55$ [kg/s]	$\eta_{h, infinity} = 0.8914$ [-]
$x_{crit} = 0.8837$ [-]	$\eta_{l, infinity} = 0.7909$ [-]

Figure 59 - $HX_{eff} = 80\%$; dct; Results

12.2.2.2 $HX_{EFF} = 85\%$

RESULTS	
$E_b = 0.0000$ [-]	$\eta_R = 0.4129$ [-]
$W_{net} = 41287$ [kW]	$\dot{m}_{tot} = 33.36$ [kg/s]
$W_{turb} = 42356$ [kW]	$P_{max} = 19$ [MPa]
$W_{pumps} = 1069$ [kW]	$T_{max} = 934.8$ [K]
$Q_{in} = 100000.0$ [kW]	$T_{HX,i} = 435$ [K]
$Q_{out} = 58713$ [kW]	$P_{de} = 0.6429$ [MPa]
$\dot{m}_r = 38.55$ [kg/s]	$\eta_{h, infinity} = 0.8958$ [-]
$x_{crit} = 0.9011$ [-]	$\eta_{l, infinity} = 0.7933$ [-]

Figure 60 - $HX_{eff} = 85\%$; dct; Results

12.2.2.3 $HX_{EFF} = 87.5\%$

RESULTS	
$E_b = 0.0000 [-]$	$\eta_R = 0.419 [-]$
$W_{net} = 41904 [kW]$	$\dot{m}_{tot} = 33.59 [kg/s]$
$W_{turb} = 42996 [kW]$	$P_{max} = 19 [MPa]$
$W_{pumps} = 1091 [kW]$	$T_{max} = 951.6 [K]$
$Q_{in} = 100000.0 [kW]$	$T_{HX,i} = 451.8 [K]$
$Q_{out} = 58096 [kW]$	$P_{de} = 0.921 [MPa]$
$\dot{m}_r = 38.55 [kg/s]$	$\eta_{h, infinity} = 0.8994 [-]$
$x_{crit} = 0.9083 [-]$	$\eta_{l, infinity} = 0.7942 [-]$

Figure 61 - $HX_{eff} = 87.5\%$; dct; Results

12.2.2.4 $HX_{EFF} = 90\%$

RESULTS	
$E_b = 0.0000 [-]$	$\eta_R = 0.4187 [-]$
$W_{net} = 41871 [kW]$	$\dot{m}_{tot} = 33.63 [kg/s]$
$W_{turb} = 42922 [kW]$	$P_{max} = 19 [MPa]$
$W_{pumps} = 1052 [kW]$	$T_{max} = 967.5 [K]$
$Q_{in} = 100000.0 [kW]$	$T_{HX,i} = 467.7 [K]$
$Q_{out} = 58129 [kW]$	$P_{de} = 0.3032 [MPa]$
$\dot{m}_r = 38.55 [kg/s]$	$\eta_{h, infinity} = 0.8927 [-]$
$x_{crit} = 0.9236 [-]$	$\eta_{l, infinity} = 0.7981 [-]$

Figure 62 - $HX_{eff} = 90\%$; dct; Results

12.3 EXCEL (X-STEAM)

12.3.1 $HX_{EFF} = 80\%$

Table 48 - $HX_{eff} = 80\%$; wct; Optimised cycle configuration; EES results

	Variable	Unit	EES	Excel	Accuracy
			Value		%
Energy Balance	E_b	MW	0	0	-
Cycle efficiency	η_R	%	40.83	40.84	0.02%
Net work	W_{net}	MW	40.825	40.837	0.03%
Turbine work	W_{turb}	MW	41.757	41.769	0.03%
Pump work	W_{pumps}	MW	0.932	0.9307	-0.14%
Heat input	Q_{in}	MW	100	100	0.00%
Heat rejected	Q_{out}	MW	59.175	59.162	-0.02%
Total mass flow	\dot{m}_{tot}	kg/s	32.44	32.41	-0.09%
De-aerator mass flow	$\dot{m}[1]$	kg/s	2.352	2.347	-0.21%
HP feed heater mass flow	$\dot{m}[2]$	kg/s	0.9762	0.9752	-0.10%
LP feed heater mass flow	$\dot{m}[3]$	kg/s	0.9636	0.964	0.04%
Minimum Temperature	T_{min}	K	322.6	322.6	-
Maximum HPT Pressure	P_{max}	MPa	17.6	17.6	-
LPT outlet quality	x_{crit}	%	88	88	0.00%
HX water inlet temperature	$T_{HX,i}$	K	398.2	398.56	0.09%
HX water outlet temperature	T_{max}	K	898	898.2	0.02%
De-aerator	r_{de}	-	0.01224	0.01224	-
HP closed feed heater	$r_{bs}[1]$	-	0.003009	0.003009	-
LP closed feed heater	$r_{bs}[2]$	-	0.001509	0.001509	-

Excel (X-Steam) was used to determine the credibility of the optimised EES results. From Table 48 the bleed point values can be found as delivered by EES. According to the EES simulation model, these bleed points (fractions of the HP turbine inlet pressure) deliver maximum cycle efficiency and therefore maximum net work.

Each feed heater bleed point is inspected individually. While the other bleed point fractions remain constant, each bleed point fraction is varied. Cycle efficiency is then shown for each corresponding bleed point fraction.

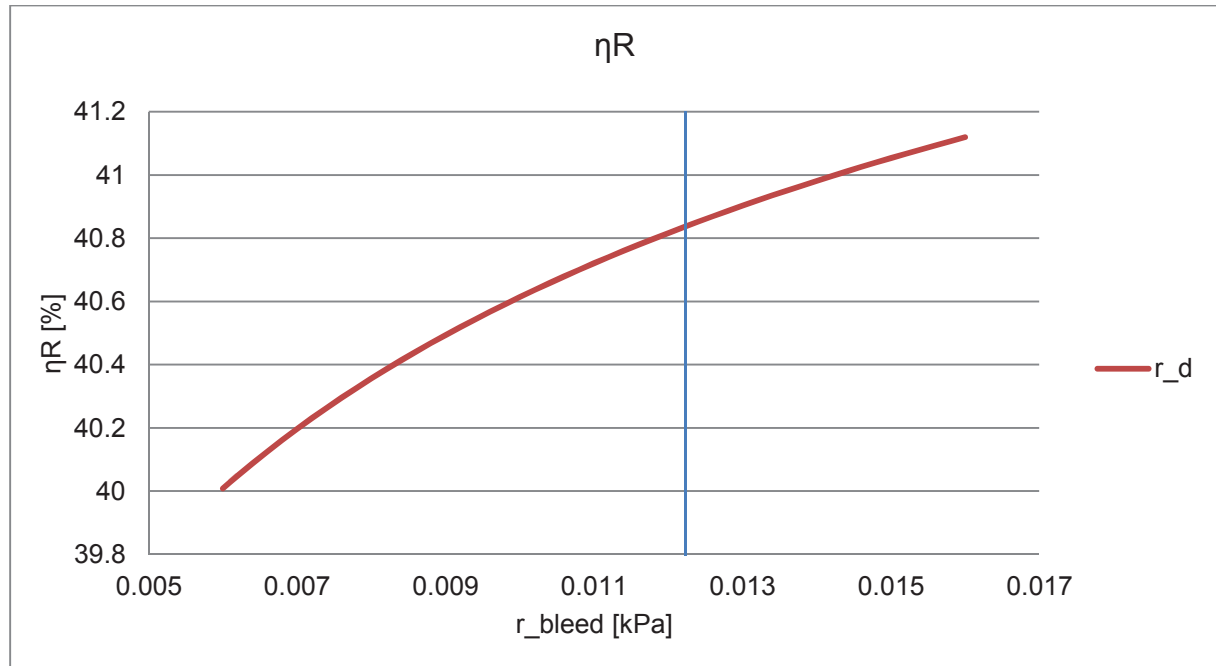


Figure 63 - HXeff = 80%; wct; De-aerator; Verification

Figure 63 shows the change in cycle efficiency as the bleed point fraction of the de-aerator is changed from $0.006 < r_{\text{de}} < 0.016$. Cycle efficiency is increased as the bleed point fraction is increased. The heat input into the cycle is being decreased due to the raising temperature delivered by the top most feed heater.

Since it is necessary to extract all the energy delivered by the reactor, the Helium needs to be cooled to 250°C . The top most feed heater is therefore limited by the effectiveness of the heat exchanger. This bleed point fraction limitation (feed heater upper temperature limit) is represented by the blue line in Figure 63.

The optimum bleed point fraction as determined by the Excel simulation model is therefore at the specified limit ($r_{\text{de}} = 0.0122$).

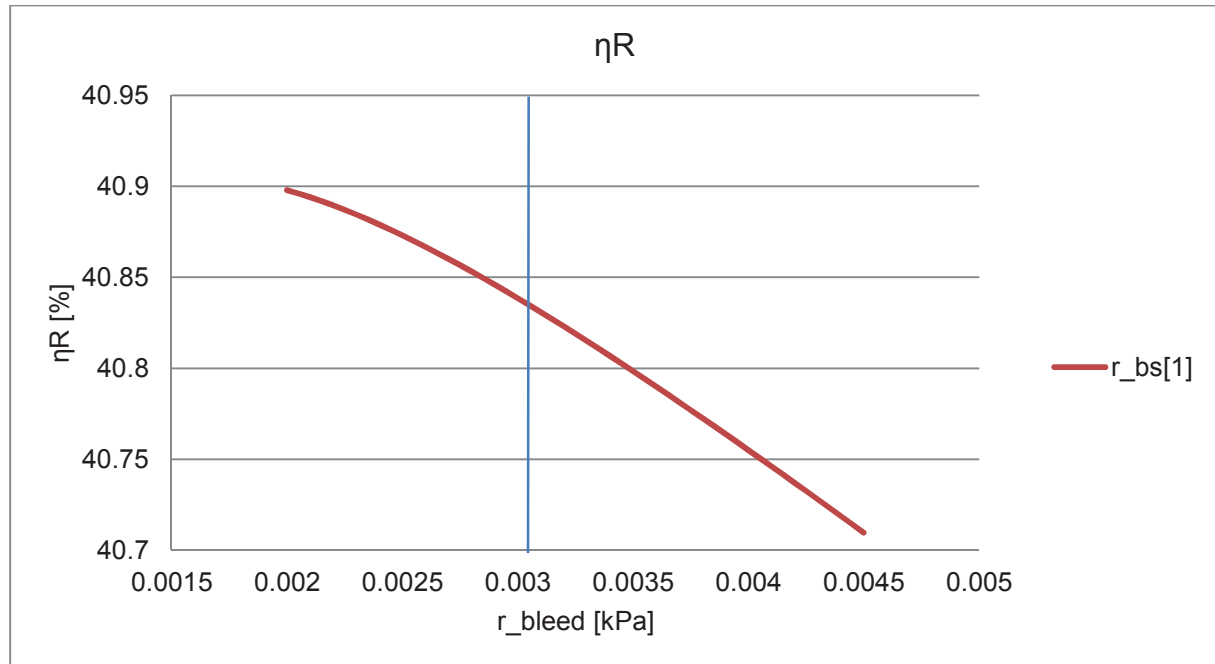


Figure 64 - $HX_{eff} = 80\%$; wct; HP closed feed heater; Verification

The corresponding cycle efficiency is shown in Figure 64 as the bleed fraction of the HP closed feed heater is increased from 0.002 to 0.0045. Cycle efficiency is decreased as the bleed point fraction is increased. The decreasing cycle efficiency is as a consequence of a decreasing turbine mass flow.

The LPT outlet steam quality limit (88%) is set to prevent corrosion on the turbine blades. The blue line in Figure 64 represents the lower LPT outlet steam quality limit. It is therefore necessary for the bleed point fraction to be equal to or greater than 0.003.

According to Excel, the optimum bleed point fraction for the HP closed feed heater, while adhering to the set limitations, is therefore $r_{bs} [1] = 0.003$.

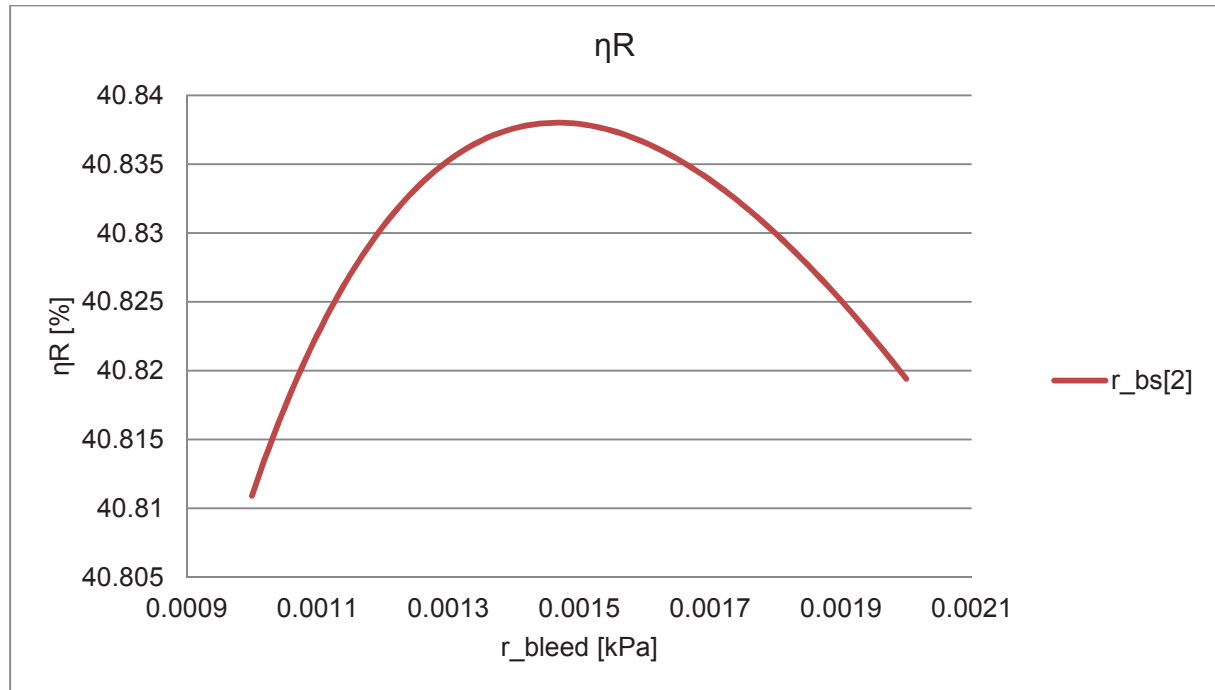


Figure 65 - $HX_{eff} = 80\%$; wct; LP closed feed heater; Verification

Figure 65 shows cycle efficiency as the LP closed feed bleed fraction is increased ($0.001 < r_{bs} [2] < 0.002$). This graph clearly shows an optimum bleed fraction for maximum cycle efficiency and therefore maximum net work delivered by the cycle. The turning point on the graph is the optimum bleed fraction at approximately $r_{bs} [2] = 0.00149$.

Table 49 – $HX_{eff} = 80\%$; wct; EES versus Excel

	EES	Excel	Accuracy
η_R	40.83	40.84	0.02%
$r_{bs} [1]$	0.01224	0.0122	-0.33%
r_{de}	0.003009	0.003	-0.30%
$r_{bs} [2]$	0.001509	0.00149	1.26%

12.3.2 $HX_{EFF} = 87.5\%$

Table 50 - $HX_{eff} = 87.5\%$; wct; Optimised cycle configuration; EES results

			EES	Excel	Accuracy
	Variable	Unit	Value		%
Energy Balance	E_b	MW	0	0	-
Cycle efficiency	η_R	%	43.22	43.23	0.02%
Net work	W_{net}	MW	43.216	43.228	0.03%
Turbine work	W_{turb}	MW	44.307	44.317	0.02%
Pump work	W_{pumps}	MW	1.091	1.089	-0.18%
Heat input	Q_{in}	MW	100	100	0.00%
Heat rejected	Q_{out}	MW	56.784	56.772	-0.02%
Total mass flow	\dot{m}_{tot}	kg/s	33.59	33.56	-0.09%
HP feed heater mass flow	$\dot{m}[1]$	kg/s	1.19	1.187	-0.25%
De-aerator mass flow	$\dot{m}[2]$	kg/s	4.788	4.778	-0.21%
LP feed heater mass flow	$\dot{m}[3]$	kg/s	1.06	1.061	0.09%
Minimum Temperature	T_{min}	K	322.6	322.6	-
Maximum HPT Pressure	P_{max}	MPa	19	19	-
LPT outlet quality	x_{crit}	%	89.43	90.61	1.32%
HX water inlet temperature	$T_{HX,i}$	K	451.8	451.72	-0.02%
HX water outlet temperature	T_{max}	K	951.6	951.72	0.01%
HP closed feed heater	$r_{bs}[1]$	-	0.003824	0.003824	-
De-aerator	r_{de}	-	0.04878	0.04878	-
LP closed feed heater	$r_{bs}[2]$	-	0.001616	0.001616	-

Excel (X-Steam) was used to determine the credibility of the optimised EES results. From Table 48 the bleed point values can be found as delivered by EES. According to the EES simulation model, these bleed points (fractions of the HP turbine inlet pressure) deliver maximum cycle efficiency and therefore maximum net work.

As seen in Figure 66, the bleed fraction of the de-aerator is limited due to the energy extraction limitation of the reactor working fluid. Maximum cycle efficiency and net work therefore has a de-aerator bleed point fraction of $r_{de} = 0.05$.

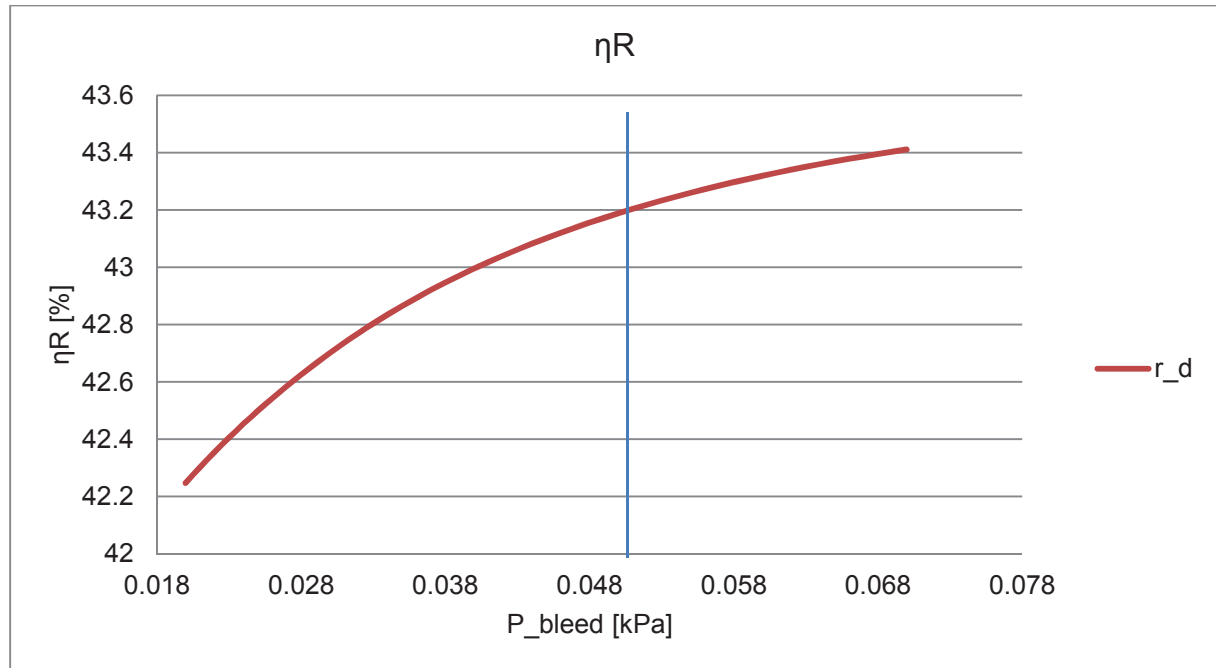


Figure 66 - HXeff = 87.5%; wct; De-aerator; Verification

It is evident from Figure 67 that the optimum HP closed feed heater bleed fraction for maximised Rankine efficiency is $r_{bs} [1] = 0.0038$.

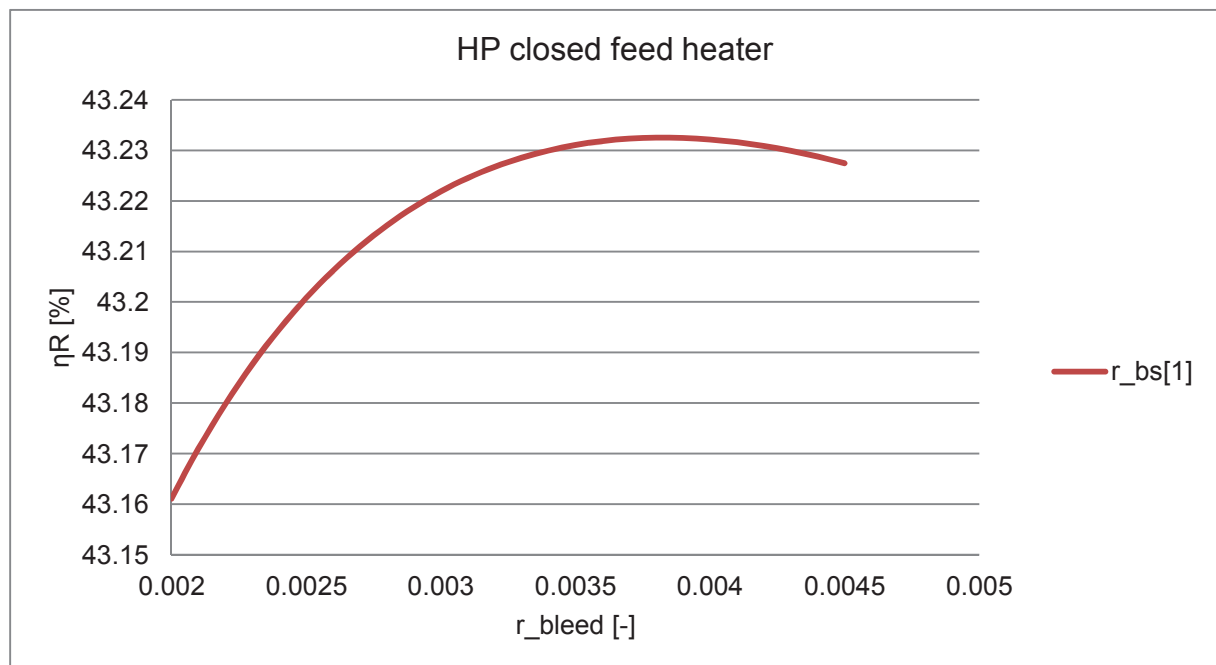


Figure 67 - HXeff = 87.5%; wct; HP closed feed heater; Verification

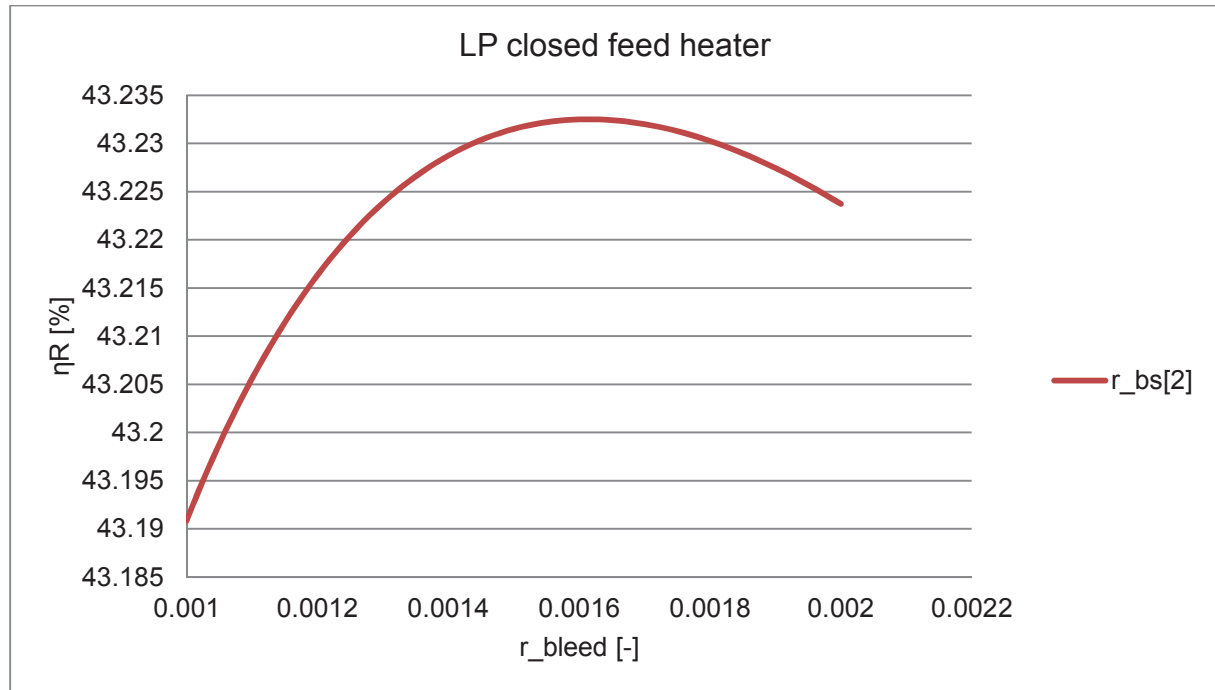


Figure 68 - $HX_{eff} = 87.5\%$; wct; LP closed feed heater; Verification

It is evident from Figure 68 that the optimum LP closed feed heater bleed fraction for maximised Rankine efficiency is $r_{bs} [2] = 0.0016$.

Table 51 – $HX_{eff} = 87.5\%$; wct; EES versus Excel

	EES	Excel	Accuracy
η_R	43.22	43.23	0.02%
$r_{bs} [1]$	0.00382	0.0038	0.63%
r_{de}	0.04878	0.05	2.5%
$r_{bs} [2]$	0.00162	0.0016	0.99%

12.3.3 $HX_{EFF} (E) = 90\%$

Table 52 - $HX_{eff} = 90\%$; wct; Optimised cycle configuration; EES results

			EES	Excel	Accuracy
	Variable	Unit	Value		%
Energy Balance	E_b	MW	0	0	-
Cycle efficiency	η_R	%	43.39	43.40	0.03%
Net work	W_{net}	MW	43.393	43.451	0.13%
Turbine work	W_{turb}	MW	44.436	44.495	0.13%
Pump work	W_{pumps}	MW	1.043	1.043	0.00%
Heat input	Q_{in}	MW	100	100.11	0.11%
Heat rejected	Q_{out}	MW	56.607	56.657	0.09%
Total mass flow	\dot{m}_{tot}	kg/s	33.63	33.63	0.00%
HP feed heater mass flow	$\dot{m}[1]$	kg/s	4.069	4.064	-0.12%
De-aerator mass flow	$\dot{m}[2]$	kg/s	1.67	1.67	0.00%
LP feed heater mass flow	$\dot{m}[3]$	kg/s	1.772	1.773	0.06%
Minimum Temperature	T_{min}	K	322.6	322.6	-
Maximum HPT Pressure	P_{max}	MPa	19	19	-
LPT outlet quality	x_{crit}	%	90.56	90.61	0.06%
HX water inlet temperature	$T_{HX,i}$	K	467.7	467.59	-0.02%
HX water outlet temperature	T_{max}	K	967.5	967.59	0.01%
HP closed feed heater	$r_{bs}[1]$	-	0.07279	0.07279	-
De-aerator	r_{de}	-	0.01205	0.01205	-
LP closed feed heater	$r_{bs}[2]$	-	0.002794	0.002794	-

Excel (X-Steam) was used to determine the credibility of the optimised EES results. From Table 48 the bleed point values can be found as delivered by EES. According to the EES simulation model, these bleed points (fractions of the HP turbine inlet pressure) deliver maximum cycle efficiency and therefore maximum net work.

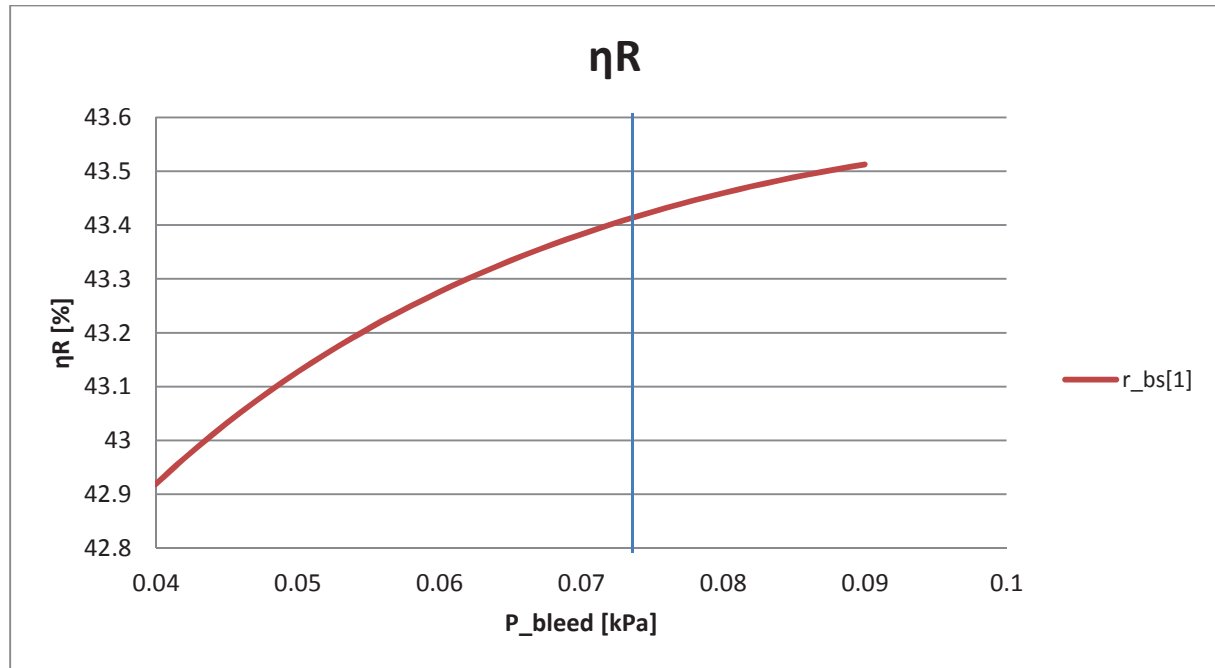


Figure 69 - HXeff = 90%; wct; HP closed feed heater; Verification

The bleed fraction of the top most feed heater is limited by the heat exchanger outlet temperature of the reactor working fluid. This limitation is represented by the [blue line](#). Maximum cycle efficiency is thus achieved by implementing a closed feed heater at the limitation set ($r_{bs} [1] = 0.073$).

It is evident from Figure 70 that the optimum de-aerator bleed fraction for maximised Rankine efficiency is $r_{de} = 0.0118$. Since the heat input into the cycle remains constant, net work is maximised when cycle efficiency is maximised.

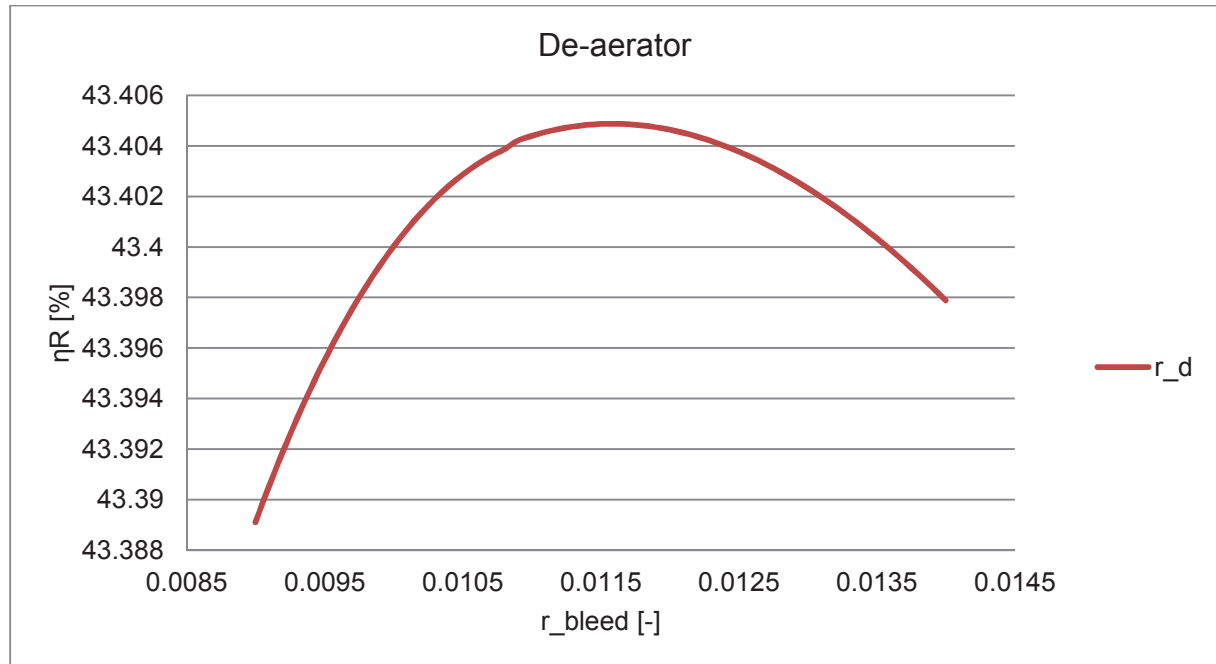


Figure 70 - HXeff = 90%; wct; De-aerator; Verification

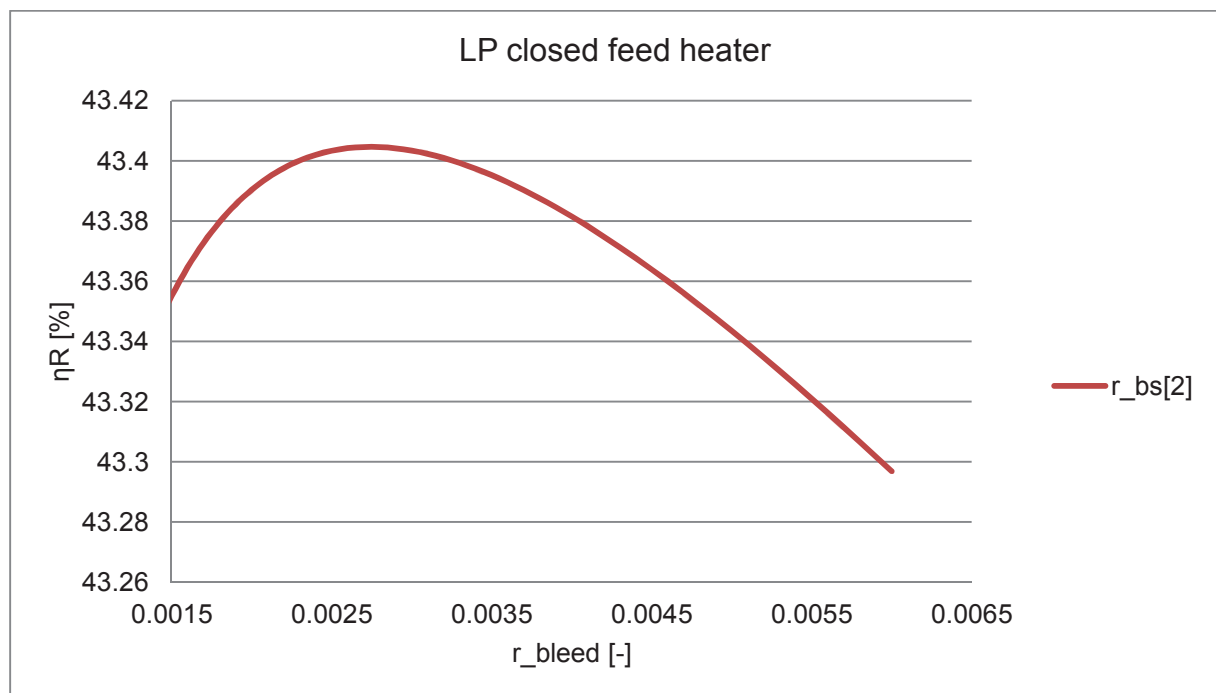


Figure 71 - HXeff = 90%; wct; LP closed feed heater; Verification

It is evident from Figure 71 that the optimum LP closed feed heater bleed fraction for maximised Rankine efficiency is $r_{bs} [2] = 0.00275$.

Table 53 – $HX_{\text{eff}} = 90\%$; wct; EES versus Excel

	EES	Excel	Accuracy
η_R	43.39	43.40	0.03%
$r_{bs} [1]$	0.07279	0.073	0.29%
r_{de}	0.01205	0.0118	2.07%
$r_{bs} [2]$	0.00279	0.00275	1.57%

12.4 FLOWNEX SIMULATION MODEL

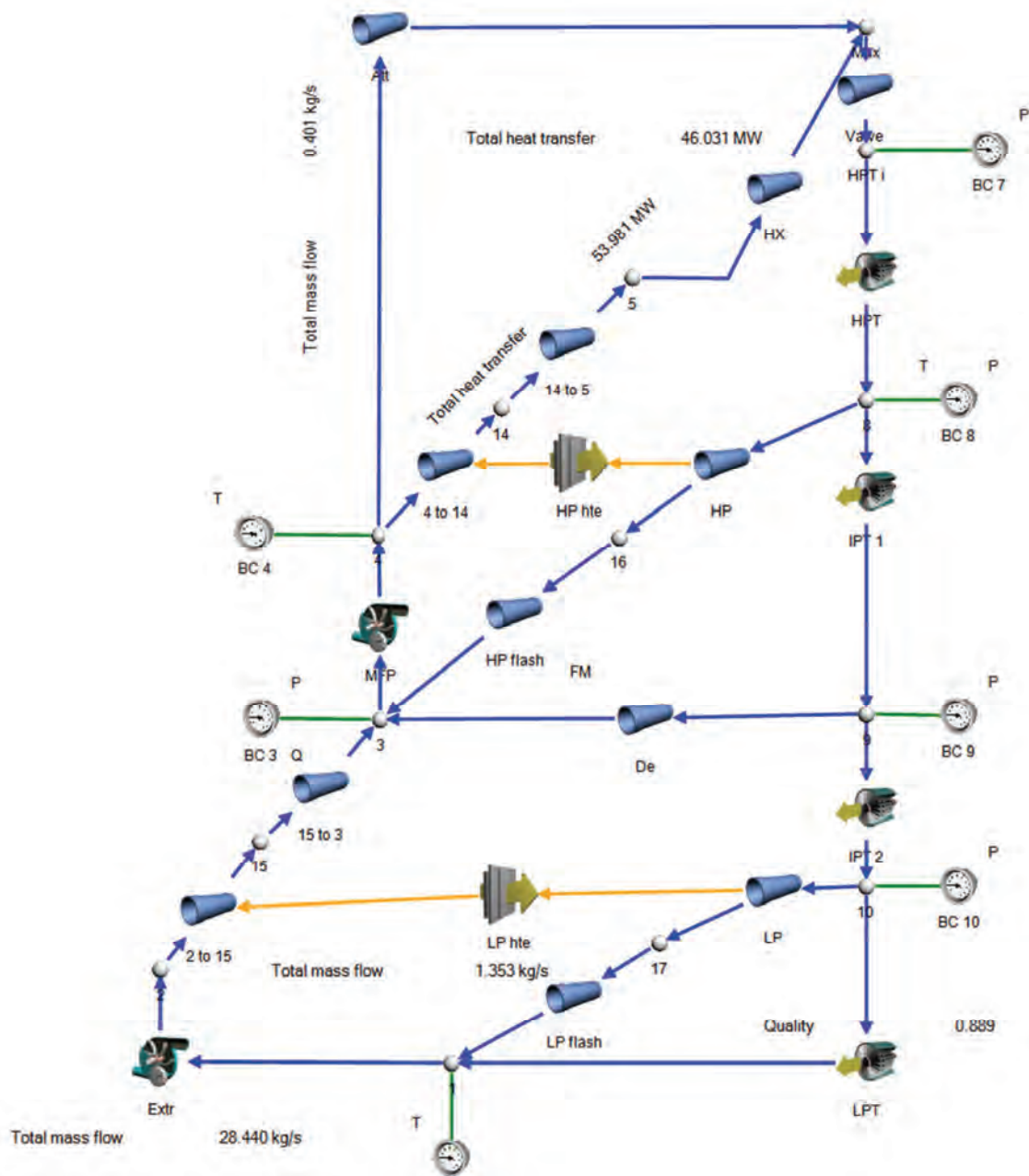


Figure 72 – FlowNex Simulation model; $HX_{eff} = 85\%$; wct

12.5 INFLUENCE OF MINIMUM AND MAXIMUM TEMPERATURES

The law of Carnot in equation (3), can be written as:

$$\eta_c = 1 - \frac{T_2}{T_1}$$

To find the maximum cycle efficiency, the equation must be differentiated.

$$d\eta_c = \frac{T_2}{T_1^2} dT_1 - \frac{1}{T_1} dT_2$$

Suppose that the minimum cycle temperature T_2 is kept constant and the maximum cycle temperature be changed, then $dT_2 = 0$.

$$\delta\eta_c \propto \frac{1}{T_1^2}$$

Should the maximum cycle temperature T_2 be kept constant and the minimum cycle temperature be changed, then $dT_1 = 0$.

$$\delta\eta_c \propto \frac{1}{T_1}$$

For $T_1 > 1$, change in minimum cycle temperature will always have a greater influence on cycle efficiency than the maximum temperature, due to $\frac{1}{T_1} > \frac{1}{T_1^2}$.

(STORM: 2013)

12.6 CD